LOUGHBOROUGH
UNIVERSITY OF TECHNOLOGY
LIBRARY

AUTHOR/FILING TITLE

HOBLEY, J.

ACCESSION/COPY NO.

040116931

VOL. NO. | CLASS MARK

LOAN
COPY

0401169316

BADMINTON PRESS
LEICESTER
ENGLAND

PHOTOCHROMISM OF NAPHTHOXAZINE-SPIRO-INDOLINES.

By

Jonathan Hobley B.Sc.

A Doctoral thesis submitted in partial fulfilment of the requirements for the award of

Doctor of Philosophy of Loughborough University of Technology

28th February 1995

(c) Jonathan Hobley 1995.

Loughborough University
of Technology Library
Date Dec 91
Class
Acc. No. 040116931

03091859

To Julie for being my most inspirational, best and at times, my only friend without whose advice and help this work would never have been achieved. I'll never forget the help you've given to me over the last and the best six years of my life, hold on in there chuck.

Acknowledgements.

I wish to thank Professor Wilkinson for giving me the chance to carry out photochemistry research in his group.

Jeff Williams, Martin Rickwood, Anna, Mary and the rest of the staff in the polymers technology group at the Pilkington Glass research centre at Lathom for their advice and help with this work.

Pilkington Glass PLC for providing the photochromic materials and for their financial assistance during my time at Loughborough University.

Mira Naftaly and Igor Kmellinskii for their assistance with the work on B-form extinction coefficients.

David Worrall, David Mc Garvey, Garry Sturley, Waseem Shaikh, Andrew Langley, Andrew Goodwin and Mira for their assistance with the picosecond studies.

I would also like to thank Darren Greenhall, David Mandley and Sian Williams for their moral support and advice.

Finally I would like to thank the SERC for funding this research.

Abstract.

Naphthoxazine-spiro-indolines (NOSI's) can exist in a colourless and a coloured form. These compounds can interconvert between these two forms either photochemically or thermally and are resilient to degradation even after repeated cycles of colouration and bleaching. Absorption spectra of both the stable colourless form and the energetically less stable coloured form have been measured.

Several NOSI compounds have been shown to photoconvert to the coloured form with an efficiency of between 0.06-0.74, depending upon the compound conditions under which the conversion is brought about. The factors which have been varied in this work are; the basicity of the 6'-substituent, the size of the N-alkyl group within these compounds and the nature solvent or matrix in which the reaction occurs. Electron donation from the 6'-group has been shown to increase the quantum yield of the forward reaction whereas solvent polarity increases have been shown to reduce the quantum yield.

Picosecond spectroscopic methods monitoring both transient absorption changes and time resolved resonance Raman spectra have established the presence of several intermediates in the photochemical formation of the coloured form and further that these transients are sensitive to both solvent changes and changes in the 6'-substituent. The size of the N-alkyl group has been shown to have no effect on the photochemical isomerisation but to influence the thermally activated isomerisation along the ground state potential energy surface.

It has been demonstrated that the lowest triplet state of the colourless form of NOSI compounds have an energy of ~200 $kJ.mol^{-1}$ and that production of this state via energy transfer leads to the formation of the coloured form with unit efficiency.

On the basis of these results mechanisms are proposed for both the photochemical colouration reaction and the thermal fade reaction.

Contents.

CHAPTER 1

INTRODUCTION.

Chapter 1 Introduction.

1.1. Photochemical principles.

1.1.1. Photochemical reactions.

Photochemical reactions are different to thermally activated processes in that the activation energy is provided by a photon of energy rather than by heat. As a consequence of the reaction proceeding via an electronically excited state, which will have very different electronic and nuclear properties to the ground state, the products may be very different to those obtained from thermally activated processes. The energy input from a photon is generally greatly in excess of that achievable from heat input and several processes with high activation energies become possible, however a photochemical reaction is only possible when certain conditions are met. Only light which is absorbed by a molecule can be effective at producing a photochemical change in a molecule.
A single quantum of radiation is required to be absorbed to promote a single molecule into an excited state and this may enable that molecule to undergo photochemistry. These two statements are based upon the Grotthus-Draper law and the Stark-Einstein laws respectively and although not strictly true nowadays with the availability of the high photon fluxes from laser excitation making possible multiphoton excitation, they are historically the basic principles of photochemistry and are described, along with many of the photochemical principles mentioned in this chapter, in several textbooks [1,2,3,4].

1.1.2. The absorption of radiation by a molecule.

The absorption of light by a molecule is a resonance process, that is to say that if a molecule is to absorb a quantum of radiation then the radiation must have an energy corresponding to a transition which can occur within that molecule. The energy of that quanta cannot be split. In photochemistry we normally deal with photon energies capable of bringing about electronic transitions.
The molar excitation energy corresponding to a transition within a molecule is given by:

$$\Delta E = N h \nu = \frac{N h C}{\lambda} \qquad 1.1$$

Where N is Avogadro's constant, h is Planck's constant, C is the speed of light in a vacuum, ν is the frequency of the light and λ is the wavelength of the light.

The relationship between the concentration of a dispersion of molecules and the fraction of light which it will absorb is given by the Beer-Lambert law;

$$A = \log_{10}\frac{I_0}{I_T} = \epsilon.c.l \qquad 1.2$$

Where A is the absorbance, ϵ is the molar decadic absorption coefficient, c is the concentration of absorbing species and l is the optical pathlength.

The quantum efficiency or quantum yield of a photochemical reaction can be defined as follows;

$$\Phi = \frac{N°\,of\,molecules\,of\,photoproduct\,formed}{N°\,of\,quanta\,of\,energy\,absorbed} \qquad 1.3$$

$$\Phi = \frac{rate\,of\,production\,of\,photoproduct}{rate\,of\,absorption\,of\,quanta} \qquad 1.4$$

Equation 1.3 defines the quantum efficiency as a ratio of the number of molecules reacted over the number of photons absorbed and equation 1.4 defines it as a ratio of the rates of the processes involved. If there are no processes competing with the photoproduct formation then the efficiency of the reaction should be unity. If other processes are in competition then the efficiency will be determined by the relative rates of the competing processes.

1.1.3. Electronic energy levels.

The position that an electron occupies within a molecule can be described using its molecular orbitals and their wavefunctions. The wavefunction of an orbital can be envisaged as the square root of the probability function of the electrons position in space. Molecular orbitals are the result of the combination of the wavefunctions of the individual atoms that form the molecule. In other words they are the result of the combination of the atomic orbitals. Molecular orbitals are described as being either σ, Π, or n (non-bonding), depending upon their symmetry. In the case of a simple diatomic molecule σ orbitals have a wavefunction for which the sign is unchanged with respect to rotation about the bond axis, Π orbitals undergo a sign reversal upon rotation about the molecular axis of 180°. Molecular orbitals can be either bonding, non-bonding or antibonding orbitals. The anti-bonding orbitals are differentiated from the bonding orbitals by being superscripted with a "*". For example an anti-bonding Π orbital is referred to as a Π^* orbital.
The electronic states of molecules possess a fundamental property called "the spin multiplicity", which is given the symbol M. M has a value which is given by; $M = 2S + 1$, where S is the total spin angular momentum quantum number which results from the vector addition applied to the spin quantum numbers "s" of the individual electrons in a molecule.

The value of s can be $\pm 1/2$ depending on the "direction" of the electrons spin. If all of the electrons in a molecule are spin paired, i.e. they are diamagnetic, the value of S is zero and the value of M is therefore 1. This state is said to have a multiplicity of 1 and is referred to as a singlet state. If two electrons in the molecule have parallel spins then S=1 and M=3, in this case the molecule is described as a triplet state. Singlet and triplet multiplicities are the most common of those encountered by the organic photochemist.

Pauli's exclusion principle states that two electrons cannot posses exactly the same set of quantum numbers, it follows from this that the two unpaired electrons of a triplet state must occupy different molecular orbitals.

Hunds rule states that:
(a) Electrons will occupy different degenerate molecular orbitals whenever it is energetically possible to do so.
(b) Two electrons in different degenerate orbitals will have parallel spins in their lowest energy state.

It is predicted from this that the triplet state will be lower in energy than the corresponding singlet state.

1.1.4. Electronic transitions.

An electromagnetic wave can be described as an electric and magnetic field sinusoidally oscillating at right angles to each other and at right angles to the direction of propagation of the wave. The absorption of a photon of light can be thought of as occurring as a result of the interaction of the electrons in the molecule with the electric field component of the photon. There are certain selection rules which apply to electronic transitions:
(a) Radiative transitions take place with no change in the total spin angular momentum, in other words $\Delta S = 0$. This means that singlet-triplet and triplet-singlet transitions are spin forbidden.
(b) Good spatial overlap must exist between the orbitals involved in the transition. This rule forbids transitions of the type $n \rightarrow \Pi^*$.
These selection rules can be and are frequently broken and forbidden transitions do occur in practice albeit weakly.

For most organic molecules the $\sigma \rightarrow \sigma^*$ transitions are the highest in energy followed by the $\Pi \rightarrow \Pi^*$ with the lowest energy being the $n \rightarrow \Pi^*$transition. The energy of the $\sigma \rightarrow \sigma^*$ transition are generally such that they correspond to the absorption of photons having

wavelengths of less than 200nm and these are only transmitted through a vacuum. Hence for most frequently studied photochemical processes the initial step is the excitation into an n->Π^* or a Π->Π^* transition.

One can represent electronic transitions as vertical lines on a diagram showing the potential energy of the molecule as a function of the internuclear distances plotted for both the initial and the final states. This type of representation is shown below in figure 1.1.

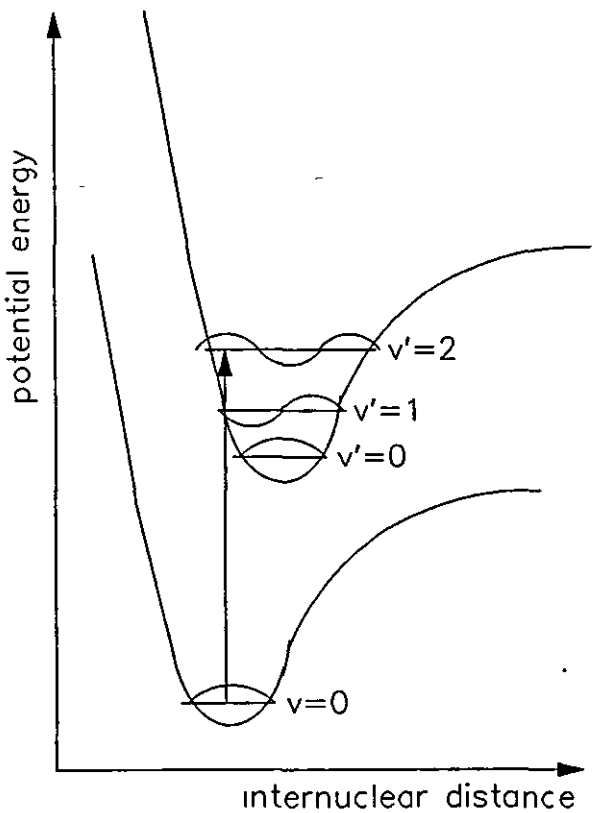

Figure 1.1. Potential energy as a function of internuclear distance.

The energy distribution of molecules is such that the majority of molecules in the lowest electronic energy state are in the lowest vibrational energy level of that state (v=0). It is from this state that most electronic transitions arise. Since electronic transitions are much faster than the nuclear motions that occur during a molecular vibration the most favourable electronic transitions occur when the structures final and initial states are similar to each other. This is the basis of the Franck-Condon principle, which effectively says that on the potential energy diagram shown above, the electronic transitions are drawn perpendicularly upwards or downwards because the molecular separation has no time to alter during the transition.

The probability of an electronic transition occurring is dependant upon the vibrational

wavefunctions of the vibrational energy levels of the states between which the transition is occurring. These wavefunctions are shown in figure 1.1 as a wave having different numbers of nodes for the different vibrational levels. A simple rule determines the number of nodes for the probability function which is basically this; for a given level v, there are v+1 nodes that occur between the maxima in the vibrational wavefunction. The strongest transitions are most likely to occur from a position of high probability to another position of high probability. It is fairly obvious that the relative intensity of an absorption or an emission from the different vibrational levels will depend on these probability functions this coupled with the rotational energy levels within each vibrational level leads to the broad nature of typically observed electronic absorption spectra of complex organic molecules.

1.1.5. Forbidden and allowed transitions between states.

The extent to which photochemical processes occur will depend on the relative rates for the processes involved. Such processes are pictorially represented by the Jablonski diagram below in figure 1.2.

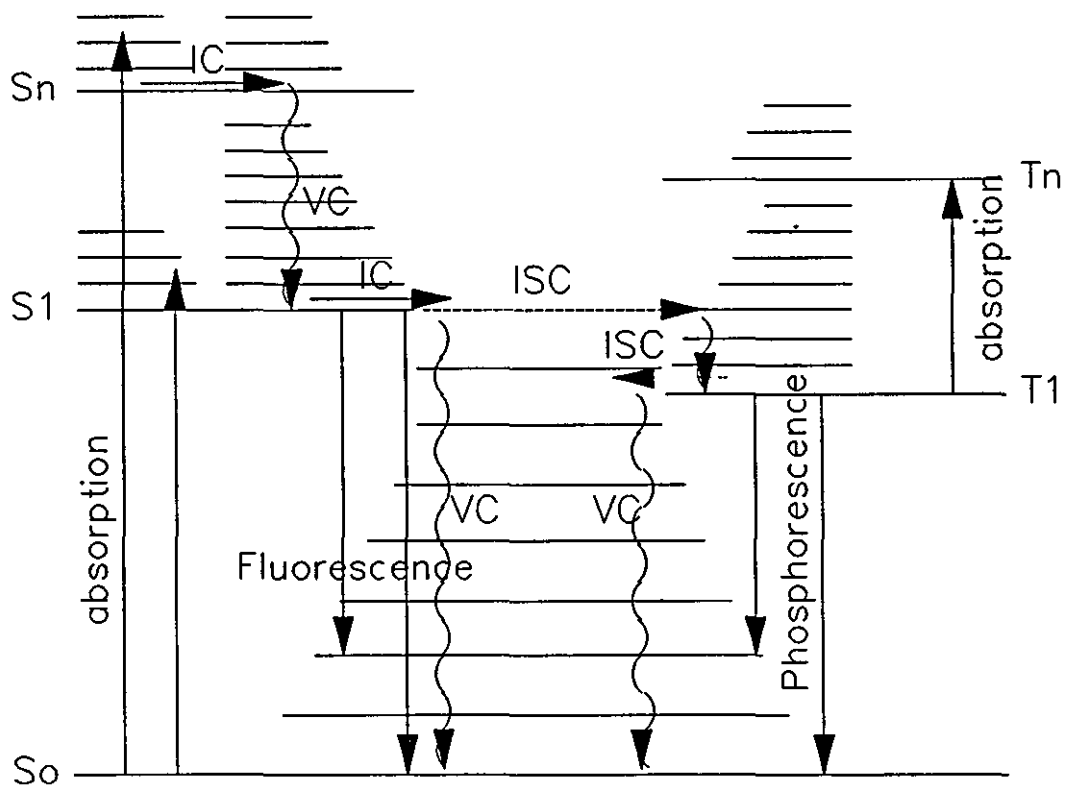

Figure 1.2. A Jablonski diagram for a complex molecule.

The absorption of a photon of light results in the promotion of an electron into a higher energy electronic state, often with excess vibrational energy. The absorption of a photon and the corresponding transition between electronic states generally takes place on femtosecond timescales. The excess vibrational energy is rapidly dissipated after the rapid non radiative internal conversion process (I.C.). This is the allowed transition between states having the same spin. The rate constant for internal conversion, k_{ic}, is often large with a value $\sim 10^{13}\ s^{-1}$. Such transitions are in practice limited by an isoenergetic Franck-Condon factor, f_v, since they sometimes involve large changes in the nuclear positions, and the overlap of the vibrational wavefunctions may be small due to an increase in the number of oscillations in the Franck-Condon factors upon a change from V_0 to V_n. Internal conversion is rapidly followed by the faster process of vibrational cascade to the V_0 level in the new electronic state.

An equation which gives an approximation for k_{ic} is given below (5) in equation 1.5.

$$k_{ic} \sim 10^{13} f_v \qquad 1.5$$

The value of f_v is sensitive to the energy gap ΔE, between the initial and final vibrational levels, often the bigger the energy gap the less overlap of the vibrational wavefunctions. The following equation has been given (5);

$$k_{ic} = 10^{13} e^{-\alpha \Delta E} \qquad 1.6$$

where α is a proportionality constant.

The value of ΔE for the $S_1 \rightarrow S_0$ transition is often large enough that the rate of internal conversion is low compared with the rate of fluorescence. Fluorescence is the radiative transition between states having the same spin multiplicity and as such is a spin allowed process. Even weak $S_1 \rightarrow S_0$ transitions show fluorescence with a value of $k_f > 10^5\ s^{-1}$, whereas k_{ic} is generally $\sim 10^8$-10^5 for the same transitions. Therefore I.C. and I.S.C, (inter system crossing, see later) can compete with fluorescence as a mechanism for depopulating the S_1 level. The energy gaps for the $S_n \rightarrow S_1$ transition, where $n > 1$, tend to be much smaller and the isoenergetic Franck-Condon overlap much better than for the $S_1 \rightarrow S_0$ transitions. The resulting k_{ic} is therefore usually much bigger, ranging from 10^{11}-$10^{13}\ s^{-1}$ for most organic molecules. This means the S_1 state will tend to be populated from the S_n states via internal conversion before any other processes, such as fluorescence, can occur. This

is the basis of Kasha's rule which basically says that photochemical reactions only arise from the lowest excited state of any multiplicity so only the S_1 or the T_1 states are likely to lead to further photochemistry.

As mentioned above the selection rules for transitions between states are sometimes broken. For example a singlet state may intersystem cross to form a triplet state. The mechanism by which this process occurs depends upon a process called "spin-orbit coupling." This process can be pictured in the following way:
Electrons are moving charges which can generate magnetic fields. These fields can act locally with another electron. The magnetic torque so generated is capable of flipping the spin of the electron thereby leading to a change in the total spin angular momentum of the system. The change in spin angular momentum is compensated for by a change in the orbital angular momentum which helps to conserve the total angular momentum of the system. This spin orbit coupling allows intersystem crossing (I.S.C.) to occur. Apart from spin the main factor governing $S_1 -> T_1$ efficiency is the energy gap between the two states. If the energy gap is small then the transition will be more favourable. The presence of heavy atoms enhances the probability of S<->T transitions also via the spin orbit coupling mechanism. Generally the rate constant for intersystem crossing from $S_1 -> T_1$ has a value, $k_{isc} > 10^6\ s^{-1}$.

Phosphorescence is the radiative transition between electronic states of different spin multiplicities for example from the T_1 to the S_0 state. These transitions are forbidden and tend to be much slower than fluorescence. The rate of phosphorescence is slow enough for this process to be in competition with collisional energy transfer to solvent molecules which is why it is more readily observed in rigid media where diffusion of the molecules cannot occur.
As a result of spin-orbit coupling pure singlet and pure triplet states do not really exist, each state will contain some degree of character from the other. Spin-orbit perturbation occurs between states having different configurations for example a $\Pi - \Pi^*$ triplet state can borrow a degree of singlet character from an $n\text{-}\Pi^*$ singlet state, but cannot do the same as efficiently from a $\Pi - \Pi^*$ singlet state, the converse is also true. Since a $\Pi - \Pi^*$ singlet state going to S_0 is a fully allowed transition it then follows that an $n\text{-}\Pi^*$ triplet state going to S_0 is more spin allowed than the $\Pi - \Pi^*$ triplet state going to S_0. Hence the rate of phosphorescence from a $\Pi - \Pi^*$ triplet such as naphthalene is much slower than the rate of phosphorescence from an $n\text{-}\Pi^*$ triplet state such as benzophenone. So far we have looked at the transitions which can occur for a single molecule, however the energy of an excited state can be transferred to other molecules.

1.1.6. Intermolecular energy transfer.

This is a process whereby energy from an excited state donor molecule can be transferred to an acceptor molecule usually in its ground state.

$$D^* + A \rightarrow D + A^* \qquad 1.7$$

Energy transfer reactions can be classified according to the spin multiplicity of the donor molecule. For example if the donor is an excited triplet state then the process is termed as a triplet-triplet energy transfer reaction. The mechanisms by which such reactions proceed is discussed below:

(a) Radiative energy transfer.

For this mechanism the donor molecule produces a quanta of energy which then excites the acceptor molecule. This quanta of energy is reabsorbed.

$$D^* \rightarrow D + h\nu \qquad 1.8$$

$$h\nu + A \rightarrow A^* \qquad 1.9$$

This mechanism requires that the donor emits a photon which the acceptor molecule can absorb. That is to say that the absorption spectrum of A must overlap the emission spectrum of D^* to some extent. The efficiency of such reactions will depend on the degree of overlap of these spectra and the strength of the transitions.

(b) Collisional or exchange mechanism.

This mechanism involves the exchange of electrons between the donor and the acceptor molecular orbitals. In this mechanism an electron jumps from the HOMO of the donor molecular orbital into the LUMO of the acceptor molecular orbital at the same time as an electron from the acceptor HOMO jumps into the donor molecular orbital. This process is represented below in figure 1.3.

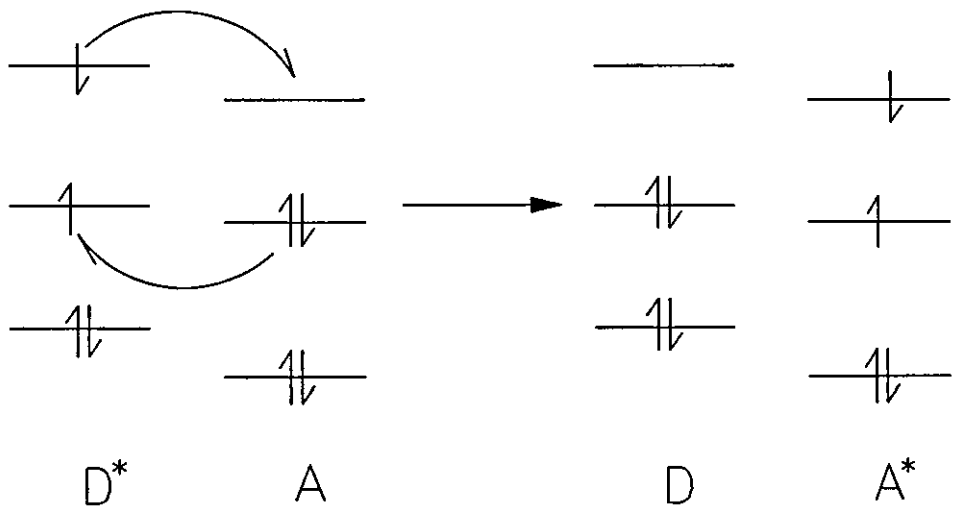

Figure 1.3. The collisional energy transfer mechanism.

This process requires the donor and acceptor molecules to approach one another to within a distance whereby their molecular orbitals can overlap.

(c) Coulombic or induced dipole mechanism.

In this mechanism it is the long range Coulombic interactions experienced by the donor and the acceptor electron clouds which facilitate the transfer of energy. In this case the oscillations in the electric field generated by an electron from say the donor molecule may cause an electron in the acceptor molecule to become more energetic. If the acceptor electron becomes sufficiently energetic then it may be promoted to a higher energy orbital at the same time as the donor electron initially causing the perturbation relaxes into a lower energy orbital. This mechanism can occur over much greater distances than the Van der Vaals radii of the donor and acceptor molecules. The Coulombic mechanism is analogous to the electronic excitation caused by the perturbations from the electric component of an electromagnetic wave and as such the rate constant for this process is determined by the overlap and the intensity of the donor emission spectrum and the acceptor absorption spectrum. The more overlap that exists between these spectra the greater the probability that the process will occur.

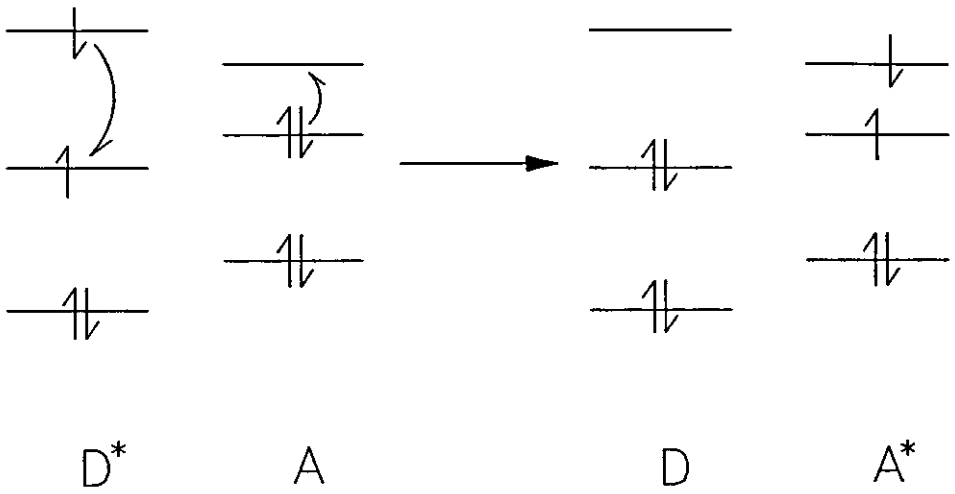

Figure 1.4. The coulombic energy transfer mechanism.

The triplet-triplet energy transfer process is perhaps the most common type of energy transfer encountered by the organic photochemist but the question arises as to which mechanism it proceeds by.

$$D^{3*} + A^{1} \rightarrow D^{1} + A^{3*} \qquad 1.10$$

The radiative and the Coulombic mechanisms both require good spectral overlap and must be highly allowed for the emission and absorption spectra of the donor and triplet molecules respectively. This does not occur in the case of triplet-triplet energy transfer and this process proceeds via a collisional mechanism which is spin allowed. The collisional mechanism requires diffusion of the donor and acceptor molecules to within the Van der Vaals radii of the two molecules. The limit on the rate of this process is the rate of diffusion of the molecules through the solution. The diffusion controlled rate constant in a solution is given by the Smoluchowski-Stokes-Einstein expression below (6).

$$k_{diff} = \frac{8RT}{3\eta} \qquad 1.11$$

Where k_{diff} is the diffusion controlled rate constant, R is the gas constant T is the temperature and η is the solvent viscosity.

1.2. Photochromic compounds.

1.2.1. Photochromism.

Photochromism is a term which is used to describe photochemical processes which result in a reversible change in the absorption spectra of the molecule or in some cases molecules which are involved in the reaction. The reversibility of the reaction can be thermally or photochemically induced. The absorption changes occurring during a typical solution phase photochromic reaction will result in a change in the colour of the solution. Most reactions that are described as photochromic are unimolecular and many involve isomerisations (7,8,9).

Photochromism was a term which was suggested by Hirshberg (10) in 1950 to describe the wide range of reactions which fit the above description. It must be noted that the systems which undergo photochromic transformations are linked to one another only by the fact that they are in general unimolecular photochemical processes which give colour changes during the course of the reaction. These reactions are not necessarily different to other unimolecular reversible processes nor similar in mechanism to other photochromic reactions.

1.2.2. Photochromics in technology.

Photochromic materials have been put forward as candidates for a number of technological applications: They have been suggested for use in binary optical switching elements which can photoconvert to one form after irradiation with one laser and then be "switched" back using a different laser to irradiate the initial photoproduct (11). Variable optical filters can be produced which are based on the principle that a typical photochromic material will change colour to an extent that is governed to some extent by the intensity of the exciting radiation. Hence one component of a continuum excitation source, such as the ultra violet radiation from sun or from the flash produced by a nuclear explosion, can photoconvert the photochromic enough that the resulting colour change blocks out the rest of the light. This property has been used in various products from protective antiflash visors for military personnel (12) to photochromic ophthalmic lenses (13).

Optical image storage is possible using photochromic materials, which when irradiated by a laser with a suitable wavelength, can create high resolution micrographic images. With the right photochromic this image could be continuously updated using two lasers, one to bring about the photochromic reaction and the other to reverse it. This process has been applied to the production of holographic gratings which can be continuously and reversibly altered to produce moving three dimensional images (14).

For most technological applications a photochromic compound will ideally have certain characteristic properties the requirements will be different for each different application but the main desirable characteristics are listed below:

(a) The molecule should absorb strongly at the excitation wavelengths.

(b) It should have the ability to exist in two interchangeable forms which have distinct absorption spectra with one or both having strong absorption in the visible.

(c) The two forms of the molecule should have sufficiently long lifetimes that the colour changes upon photoexcitation can be easily observed.

(d) The compound should be stable to repeated colouration cycles without degradation occurring. For example one source states that a photochromic which is to be considered for use in ophthalmic lenses is generally required to decompose by less than 25% over a 2 year period for an average wearer [13].

(e) For some applications such as anti flash visors the photochromic may be required to photocolour rapidly after photoexcitation [12] so that some component in the initial part of a flash will colour the visor and then absorb the light from the rest of the flash. The absorbances required to cut out extremely intense visible light flashes would cause discomfort to the wearer if the visor was coloured continuously.

One series of photochromic compounds which satisfies many of the requirements of the technological applications are the benzopyran spiro indolines and the naphthopyran spiro indolines.

1.2.3. Benzopyran spiro indolines and naphthopyran spiro indolines.

The photochromic reactions of the benzopyran spiro indolines (BPSI's) and naphthopyran spiro indolines (NPSI's) bring about some of the strongest colour changes seen for photochromic compounds [15]. The basic BPSI molecule is shown below in its uncoloured form with the convention of numbering the substituent positions on the molecule also shown.

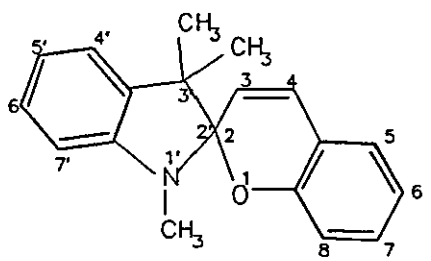

Figure 1.5. The BPSI molecule.

BPSI and NPSI compounds are comprised of two heterocyclic parts which are held at 90° to one another by a spiro link. In this form conjugation occurs on each separate half of the molecule, but does not extend past the spiro carbon. As a result of this limit to the conjugation solutions of these molecules appear colourless. Upon absorbing a U.V. photon the spiro C-O bond can break and the molecule can then isomerise to a more planar form which is more extensively conjugated than before. In the near planar form the molecule absorbs strongly in the visible region of the spectrum. This process is both photochemically and thermally reversible with the coloured form yielding the original colourless form.
BPSI and NPSI compounds have been known to exhibit thermochromic properties since 1921 [11], however their photochromic properties were not realised until 1952 [11]. A few years after this discovery it was suggested that, due to the photochemical reversibility of the reaction, these compounds may be suitable as an optical binary element for use in computers. This notion that the BPSI's and NPSI's could be used for fast optical switching devices has led to a great deal of research into their photochemistry.
One major drawback with these compounds is that they are inherently unstable to repeated photocolouration and fade cycles and as a result are not of much use for most commercial applications. The related naphthoxazine spiro indoline compounds were found to be much more stable to repeated colouration-decolouration cycles and have recently overtaken the BPSI and NPSI compounds in terms of their commercial importance [16].

1.2.4. Naphthoxazine spiro indoline compounds.

Naphthoxazine spiro indoline (NOSI) compounds have a similar photochemistry to the NPSI and BPSI compounds mentioned above. They will photochemically transform from a colourless form to a coloured one and can then thermally reform the colourless form. The basic NOSI molecule is shown below in figure 1.6 with its substituent positions numbered as is the convention.

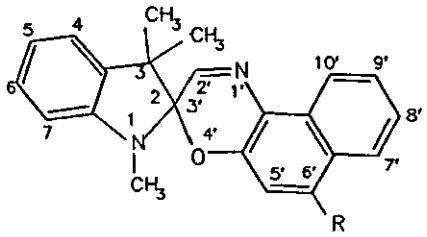

Figure 1.6. The naphthoxazine spiro indoline (NOSI) molecule.

As can be seen the only difference between a NOSI compound and an NPSI compound is that the carbon atom opposite the oxygen on the NPSI molecule has been replaced by a

nitrogen atom. This change albeit slight confers a much greater stability on the NOSI compounds to repeated photochemical colouration and fade cycles.
The photochromic transformation of a typical NOSI compound is shown below

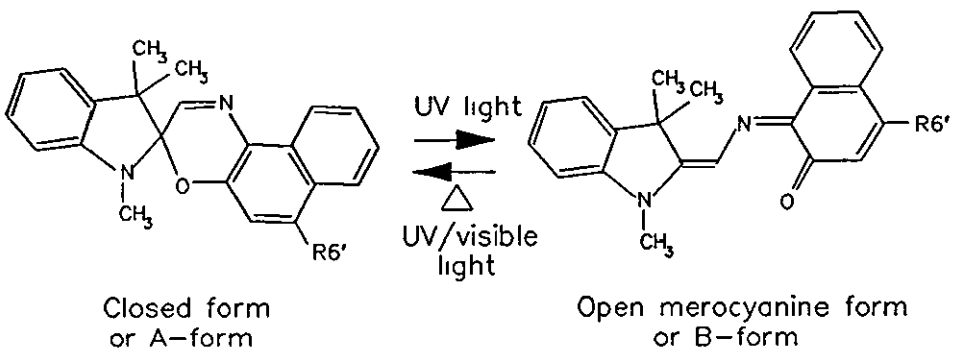

Figure 1.7. The NOSI photochromic reaction.

The closed colourless form of a NOSI compound is often referred to as the A-form of the molecule and the open coloured form is referred to as the B-form.
NOSI compounds have not been as extensively researched as the BPSI's or NPSI's and it is the aim of the present work to elucidate the mechanisms by which the colouration and fade reactions occur. In particular one series of compounds, which have been substituted with an electron donating amine group at the 6'-position on the oxazine ring, have shown very good colouration properties and it is the aim here to evaluate what it is about these compounds which makes them perform better than other NOSI compounds.

The subsituents at the 6'-position for the compounds which have been studied in this thesis are given below in table 1.1.

Table 1.1. The different 6'-substituted NOSI compounds.

6'–substituent	Compound
H	NOSI1
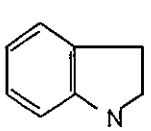	NOSI2
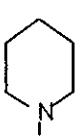	NOSI3
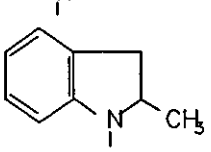	NOSI4

As well as the compounds given in table 1.1, NOSI2 compounds substituted at the main NOSI indoline nitrogen with a propyl or an iso-butyl group have also been studied.
The 6'-substituents vary in their electron donating powers in other words they vary in their basicities with hydrogen being the least basic. Indoline is the least basic of the 6'-amine substituents since the benzene ring on the indoline will tend to mesomerically draw electron density from the nitrogen in competition with the naphthoxazine ring. The next most basic substituent is the methyl indoline group. This is more basic than the indoline because the methyl group will tend to mesomerically push electrons towards the indoline nitrogen. Piperidine is the most basic group because it has no aromatic group in competition with the naphthoxazine for the nitrogen electrons.

Chapter 1 References.

1. N.J. Turro, Modern Molecular Photochemistry, Benjamin Cummings Pub. Co. 1978 ISBN-0-8053-9353-6

2. Calvert and Pitts, Photochemistry, J. Wiley and Sons, 1966, ISBN-65-24288, 19,

3. P.W. Atkins Physical Chemistry 3rd Ed. 1988, ISBN-0-19-855186-X, 1988, p721.

4. J.B. Birks, Organic Molecular Photochemistry, J. Wiley and Sons, 1975, ISBN 0-471-07421-7V2.

5. N.J. Turro, Modern Molecular Photochemistry, Benjamin Cummings Pub. Co. 1978 183.

6. S.L. Murov, I. Carmichael G.L. Hug, Handbook of Photochemistry, 2nd Ed. Marcel Dekker, ISBN-0-8247-7911-8, 1993, 207.

7. J.C. Scaiano, Handbook of Organic Photochemistry, Vol. 2. C.R.C Press ISBN-0-8493-2954X, 1989, 449.

8. H. Durr, H. Bouas-Laurent, Photochromism Molecules and Systems, Elsevier, ISBN-0-444-87432, 1990, 5.

9. C.B. McArdle, Applied Photochromic Polymer Systems, Blackie, ISBN 0-412-02971-5, 1992, 1.

10. Y. Hirshberg, Compt. Rend. 231 1950 903.

11. H. Durr, H. Bouas-Laurent, Photochromism Molecules and Systems, Elsevier, ISBN-0-444-87432, 1990, 314.

12. R.E. Fox, Research Reports and Tests Pertaining to Eye Protection For Air Crew Personnel, Final Rep. Contract, A.F.41(657)-215, April 1961, AD440226.

13. C.B. McArdle, Applied Photochromic Polymer Systems, Blackie, ISBN 0-412-02971-5, 1992, 31.

14. C.B. McArdle, Applied Photochromic Polymer Systems, Blackie, ISBN 0-412-02971-5, 1992, 170.

15. H. Durr, H. Bouas-Laurent, Photochromism Molecules and Systems, Elsevier, ISBN-0-444-87432, 1990, 331.

16. N.Y.C. Chu, Can. J. Chem. 61, 1983, 300.

CHAPTER 2

THE ABSORPTION SPECTRA OF NAPHTHOXAZINE-SPIRO-INDOLINES (NOSI'S).

Chapter 2. The absorption spectra of NOSI compounds (NOSI'S).

2.1 Introduction.

NOSI compounds posses the ability to exist in either of two molecular forms which have absorption spectra that are quite distinct from each other. The two different forms of the molecule are often referred to as the A-form and the B-form. Whilst in its A-form the molecule exists as two conjugated heterocyclic regions which are held at ninety degrees to one another by a tetrahedral spiro link. The A-form cannot extend its conjugation across the spiro link since Π-electron overlap cannot occur when the Π-electron systems are at right angles to each other. This limitation to the extent of Π-electron conjugation means that the energy gap S_1->S_0 is such that the absorption spectrum of the A-form does not extend much into the visible region of the spectrum (1).

When a NOSI compound is in its B-form the spiro C-O bond is broken which allows the two heterocyclic regions of the molecule to rotate about the central C-N bond until they are nearly in the same plane as one another. The fact that in the B-form the two halves of the molecule are nearly planar means that the extent of conjugation can then increase which results in a decrease in the energy of the S_1->S_0 transition. As a consequence of this the B-form absorption spectrum is extended far into the visible region of the spectrum. This effect is clearly demonstrated in figure 2.1.

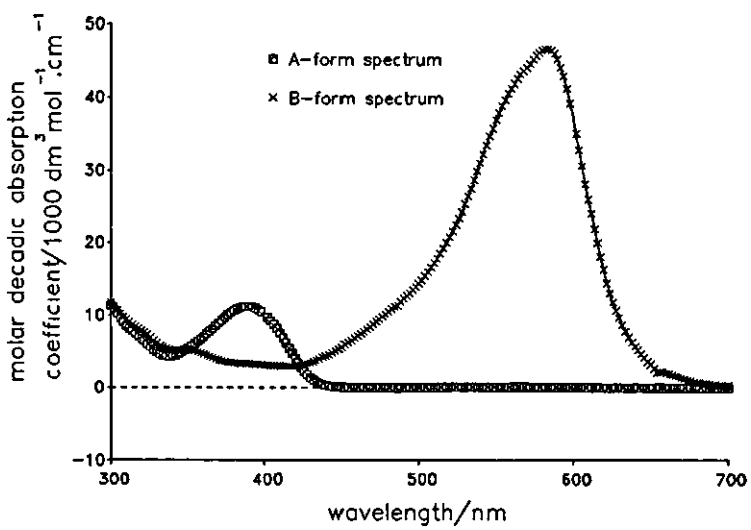

Figure 2.1. The NOSI2 A-form and B-form absorption spectra.

This ability of NOSI molecules to exist in both a colourless and a coloured form has aroused a great deal of interest in these compounds with a view to using them for several of the technological applications that were mentioned in the introduction to this thesis.

2.1.1 The A-form spectrum.

When NOSI compounds are in their A-form they do not generally absorb light very far into the visible region of the spectrum. This is because the two heterocyclic regions of the molecule are electronically isolated from one another. This electronic isolation has been demonstrated for the closely related BPSI and NPSI compounds by Wilkinson *et al* [2] and Becker *et al* [3] who mixed equimolar solutions of suitable model compounds which represented the two halves of the fused BPSI or NPSI molecule. These mixed model compound solutions had absorption spectra which were very similar to the absorption spectra of solutions of the corresponding fused spiro-pyran systems. This result suggests that in the fused system the two halves of the molecule still behave in a manner that is similar to the individual component parts in other words they are essentially electronically isolated from one another. It is unfortunate that as yet similar experiments cannot be carried out on NOSI compounds, this is because, although several indoline derivatives are available, including indoline itself, which can be used as model compounds for the indoline half of the molecule, no derivatives have so far been isolated which can be used to represent the oxazine part of the molecule.

The A-form absorption spectra of most of the NOSI compounds studied in this thesis are not greatly affected by changes in solvent, however the addition of different substituents onto either the oxazine or the indoline regions of the molecule does change both the spectral shape and the positions of peak maxima [4].

2.1.2 The B-form spectrum.

The B-form of a NOSI compound absorbs strongly in the visible as well as in the U.V. region of the spectrum. The absorption in the visible can be photochemically initiated by irradiating the A-form with U.V. photons [5]. This results in the breaking of the C-O bond from the spiro link allowing the two conjugated heterocyclic halves of the molecule to freely rotate and eventually adopt a near planar conformation.

The absorption spectrum of the B-form of a NOSI compound in the visible region is broad and fairly unstructured. The spectral shapes and the positions of the peak maximum absorption for the B-form spectra are greatly affected by changes in the nature of the solvent [4], the reasons for this will be discussed later in this chapter. It has previously been shown that the measured spectrum of an NPSI B-form solution is actually a composite spectrum made up from the individual contributions from the spectra of the several possible merocyanine isomers [6]. The NOSI B-form spectrum may also be comprised, among other things, of the summed spectra of several merocyanine isomers. Unfortunately this is not

easy to establish owing to the broad and featureless nature of the NOSI spectra. This lack of features makes it difficult to assign specific spectral regions to the individual contributions from either the different possible isomers that may make up the B-form or to specific electronic transitions. Although much can be guessed about the B-form spectral origins based on their structural similarity to NPSI and BPSI compounds, very few solid facts have been unambiguously established.

2.2 Experimental

2.2.1 The determination of the A-form spectrum.

A NOSI A-form spectrum can be easily measured using a conventional U.V./Visible spectrometer simply by making up a solution of the compound in the desired solvent placing the solution in an optical cell and scanning the absorbance of the solution over the desired wavelength range. Although some B-form is always present in solution in thermal equilibrium with the A-form, generally the amount constitutes a fraction of a percentage of the total NOSI concentration and the overall contribution of this species to the measured A-form absorption spectrum in the U.V. is negligible. Even at 295K in 1-propanol NOSI2 has a B-form concentration in thermal equilibrium with the A-form which is only 0.32% of the total NOSI2 concentration.
Absorption spectra were measured for NOSI1-4 and for n-iso-butyl NOSI2, also for comparison the absorption spectrum of indoline was also measured. Indoline itself is a good model for the indoline part of the molecule. Spectra were measured in several polar non polar and hydrogen bonding solvents in order to establish any solvent effects upon the observed absorption bands.

2.2.2 Verification of Beer's law for NOSI compounds.

The absorbance of a beam of collimated monochromatic light in an homogeneous medium is proportional to the pathlength of the medium and to the concentration of the absorbing species. This can be shown from Beers law which is described in the introduction.
Beers law can be established for a particular NOSI A-form simply by making up a range of solutions of the particular NOSI compound being investigated to give a suitable range of concentrations. Measuring the absorbance of these solutions at the desired wavelength or wavelength range and plotting the absorbance of the solution against the concentration of the solution should give a straight line if Beers law is obeyed. Figure 2.2 shows such a plot for NOSI2 in toluene.

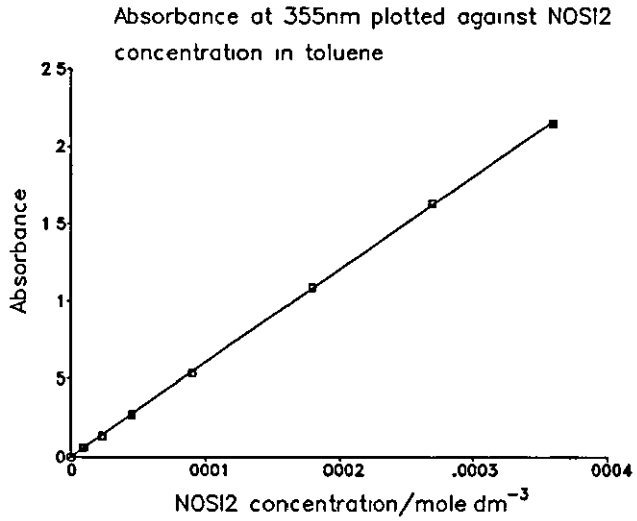

Figure 2.2. Graph showing the obeyance of Beer's law for NOSI2.

Deviation from Beers law could occur for several reasons, including; chemical effects such as dimerisation or cluster formation, or instrument effects such as non linearity of the photomultiplier response. In the case of our experiments the solutions that were made up covered the concentration range from $1x10^{-5}$mol.dm^{-3} to $4.5x10^{-4}$ mol.dm^{-3}. Absorbance measurements were made in a 1cm pathlength cell using a Philips Pu8800 U.V. visible spectrometer at 355nm using a 0.5nm resolution slit width and a ten second integration time. Molar decadic absorption coefficients were measured at the ~390nm peak as well as at 355nm. This latter value was measured mainly for our future convenience since this was the most commonly used wavelength in subsequent studies, it being the U.V. wavelength obtainable by mixing undoubled 1064nm light from an Nd-YAG laser with doubled 532nm light in a KDP mixing crystal. Once it had been established in this way that a typical NOSI system obeyed Beers law values of ϵ_A were measured for several other NOSI compounds in several solvents. Although similar plots were not determined for all of the compounds in all of the solvents used, each value of ϵ_A given was the average of several values measured at different NOSI concentrations. The similarity between the ϵ_A values measured at the different concentrations was taken as confirmation that again the Beer Lambert law was being obeyed for that particular system.

2.2.3 The determination of the B-form spectrum.

The absorption spectrum of a typical NOSI B-form solution cannot easily be obtained using a conventional spectrometer this is because a normal spectrometer scans each individual wavelength separately and in the time that is required to construct a complete spectrum over a significant wavelength range, the concentration of the B-form invariably

has time to deplete due to the thermal reformation of the A-form. This would result in the B-form concentration being greater at one wavelength end of the spectrum than at the other end and the resulting spectrum would be distorted. However, if enough B-form is present in solution due to its thermal equilibrium with the A-form, then the B-form absorption spectrum can be determined, but only in the visible region where the A-form does not absorb. If the thermal reverse reaction can be stopped or sufficiently slowed down by reducing the temperature of the solution, then the photostationary equilibrium B-form concentration will reach the maximum achievable by photo-excitation, even using a conventional mercury lamp. With this method the input of exciting photons must be enough so that inputting more photons will not result in a greater photostationary concentration of B-form molecules. This method was used by Chu [7] to obtain a complete B-form spectrum that covered both the visible region and also the U.V. region where the A-form of the molecule also absorbs. The temperature reduction required for this method depends upon the incident photon intensity as well as the thermal fade rate of the particular photochromic being studied. Temperature variation can cause NPSI B-form spectra to change [6] and from inspection of Chu's spectra [7] these too appear to show slight temperature dependence. The availability of high photon flux's that are available with many modern lasers means that this saturation of conversion to the B-form with respect to incident photons can be achieved even at room temperature. This means that any temperature effects on the spectral shape and on the intensity of the absorption bands do not need to be considered. Unfortunately even under these conditions one hundred percent conversion to the B-form cannot be guaranteed, because there is always the possibility that a photochemical reverse reaction can be induced by the absorption of U.V. photons by the B-form. This means that using this method the B-form spectrum cannot be unambiguously measured in the region where the A-form also absorbs since full conversion to the B-form cannot be guaranteed in such cases unless it is known that the forward efficiency is much higher than the reverse. If full conversion has not been achieved then obviously the A-form will still be contributing to the spectrum in the U.V.

The B-form spectrum can be determined using flash spectroscopic methods where the B-form absorbance is measured individually at different wavelengths at a set time delay or a series of delays after the initial U.V, flash [8,9], but again full conversion to the B-form is not guaranteed.

The use of a diode array detector allows the B-form spectrum to be measured at each wavelength simultaneously following a U.V. flash. Here again and for the same reasons

mentioned above, full conversion to the B-form cannot be guaranteed under these circumstances, therefore the B-form spectral shape in the U.V. cannot be determined.
A further problem arises due to the fact that it is not possible to determine the residual A-form spectral contribution to the B-form spectrum. This is that the molar decadic absorption coefficients for the B-form ϵ_B cannot be determined with certainty. This problem arises because the B-form absorbs at each wavelength where the A-form does and it is therefore not possible to simply determine the degree of conversion to the B-form, because the depletion of the A-form cannot be found from the measured spectrum in the region where the A-form absorbs.
In the present study three methods have been applied in order to determine B-form spectra and the corresponding values of ϵ_B. The first is a method involving the construction of a B-form spectrum from a mixed A-form and B-form spectrum, by making assumptions about the B-form spectral shape in the region where the A-form absorbs. This method is similar in principle to the methods of triplet extinction coefficient determination used by several other authors [10,11] who also based their determinations on assumptions about the relationship between the two spectra making up the mixed spectrum. The second method is based on the method first applied by Fischer [12] which uses irradiation at two different U.V. wavelengths where both the A-form and the B-form absorb. The third method assumes that total conversion to the B-form is possible after irradiation with the chosen excitation wavelength produced by a krypton ion C.W. laser, in other words the yield of the reverse photochemical reaction is assumed to be insignificant compared with that of the forward reaction. This method was only used when no other methods could be applied.

2.2.3.1 Anticorrelation of A-form and B-form spectra.

This method is not universally applicable and has been used only for NOSI2 and n-iso-butyl NOSI2. The method relies on there being some region in the spectrum of the B-form alone, where the A-form alone would also absorb, which does not peak or trough in concert with the spectrum of the A-form alone. By inspection it was apparent that, for the compounds NOSI2 and n-iso-butyl NOSI2, in the spectral region lying between the isosbestic points of the A-form and B-form spectra which spans from ~345nm to ~420nm, the mixed A-form and B-form spectrum became flatter as more B-form was produced, wheres the A-form spectrum peaks in this region. This implies that, in this region the B-form spectrum does not correlate either positively or negatively with that of the A-form thus satisfying the demands of the method. It must be stressed that this method will only work if such a suitable region is available in the spectra of the two forms of the compound, this is not the case with all NOSI compounds. Fortunately if such a spectral region does not exist then the

correlation that does occur between the spectra is usually easy to see simply by inspection and comparison of the A-form and B-form spectra.

Absorption spectra for solutions of the A-forms were obtained using a Hewlett Packard HP8452A diode array spectrometer having a spectral resolution of 2nm. Mixed absorption spectra for the same solutions partially converted to the B-form were collected on the same piece of apparatus closely following flash excitation with a photographic flash gun.

From these measurements values of ϵ_B were obtained using the following analysis method and assuming the model shown below in figure 2.3.

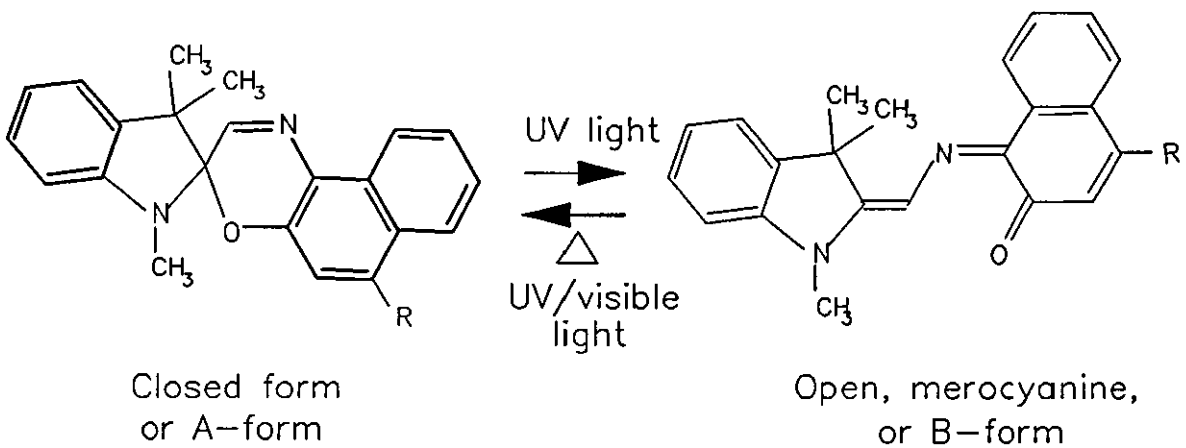

Figure 2.3 The general NOSI isomerisation reaction.

If full conversion to the B-form has not been achieved following flash excitation then the measured absorption spectrum contains elements from both the A-form and the B-form of the particular NOSI compound being studied, i.e.

$$A = A_A(1-x) + A_B x \qquad 2.1$$

Where x is the fraction of A-form converted to the B-form. The value of x is fractional and therefore lies between 0 and 1.

A_A is the absorbance due to the A-form.

A_B is the absorbance due to the B-form.

The above equation can be re-written in terms of A_B

$$A_B = A(1/x) - A_A[(1/x) - 1] \qquad 2.2$$

In order to calculate the spectrum of the B-form, values of x are chosen to give the most likely spectrum of the B-form.

One method of choosing the value of x is to calculate the correlation coefficient, r

between the A-form spectrum and the B-form spectrum across the region between the two isosbestic points for each value of x used.
The correlation coefficient, r, measures the linear correlation between the two spectra and is given by:

$$r = \frac{\int_{\lambda_1}^{\lambda_2} (A_A - \overline{A}_A)(A_B - \overline{A}_B) d\lambda}{\left[\int_{\lambda_1}^{\lambda^2} (A_A - \overline{A}_A) d\lambda \int_{\lambda_1}^{\lambda^2} (A_B - \overline{A}_B) d\lambda \right]^{1/2}} \qquad 2.3$$

Where $\overline{A}_A$ is the average absorption of the A-form over the integral and $\overline{A}_B$ is the average absorption of the B-form over the integral.

If the chosen value of x is too low then the B-form spectrum will tend to follow the A-form spectrum, in other words it will peak and trough at the same places as the A-form spectrum. This will give a correlation coefficient which is positive. If the value of x was too high then the B-form spectrum will tend to the inverse of the A-form spectrum, in other words it will trough where the A-form spectrum peaks and vice-versa. This will give a correlation coefficient which is negative. A correlation coefficient of zero means that the two spectra are totally unrelated to one another in the region for which the function is calculated. Since it has been assumed that the two spectra are unrelated between the isosbestics then the value of x which gives a zero correlation coefficient is determined and it is this value which is then used to construct the B-form spectrum. Figure 2.4 gives examples of derived B-form spectra. Spectrum 1 is oversubtracted because it troughs where the A-form peaks and spectrum 3 which is undersubtracted peaks where A-peaks. Spectrum 2 is correctly subtracted, because it has the minimum correlation to the A-form spectrum, hence the A-form spectrum and the derived B-form spectrum neither peak nor trough in concert.

The method described above is in essence the same as that used by Labhart *et al* [11], who reconstructed triplet-triplet absorption spectra using trial and error by substituting a value of x such that no evidence was seen for peaks or troughs from the original singlet absorption spectrum.

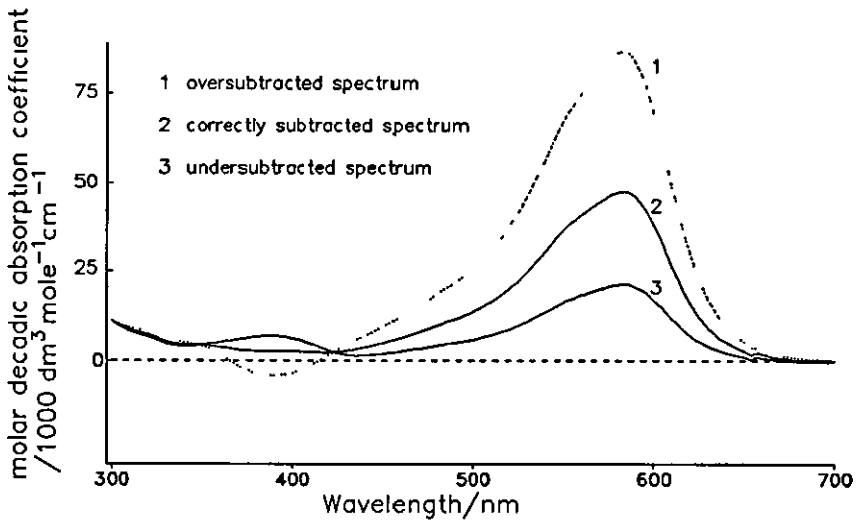

Figure 2.4. NOSI2 B-form spectra generated using the anticorrelation method.

2.2.3.2 Two irradiation wavelengths under conditions of saturation with respect to incident photons.

As mentioned previously it is not possible to guarantee full conversion to the B-form of a NOSI compound simply by irradiating at a sufficiently high laser intensity to saturate the conversion to the B-form with respect to the incident photon flux. This is because the absorption of a U.V. photon by the B-form can initiate a photochemical reverse isomerisation which reforms the A-form. If the efficiency of this process is sufficient to cause a significant reversion to the A-form then full conversion or near to full conversion will never be attained by steady state irradiation. This will only be a problem when a significant reversion to the A-form can brought about photochemically by the same excitation source which is populating the B-form.

In circumstances such as these it is still possible to determine values of ϵ_B by irradiating a solution of a NOSI compound at two excitation wavelengths where both the A-form and the B-form absorb. The irradiation intensity must be sufficient that no more B-form will be produced by increasing the photon flux.

The method used in this case is a modification of the method first applied by Fischer [12]. Measurements were carried out using the apparatus shown in figure 2.5.

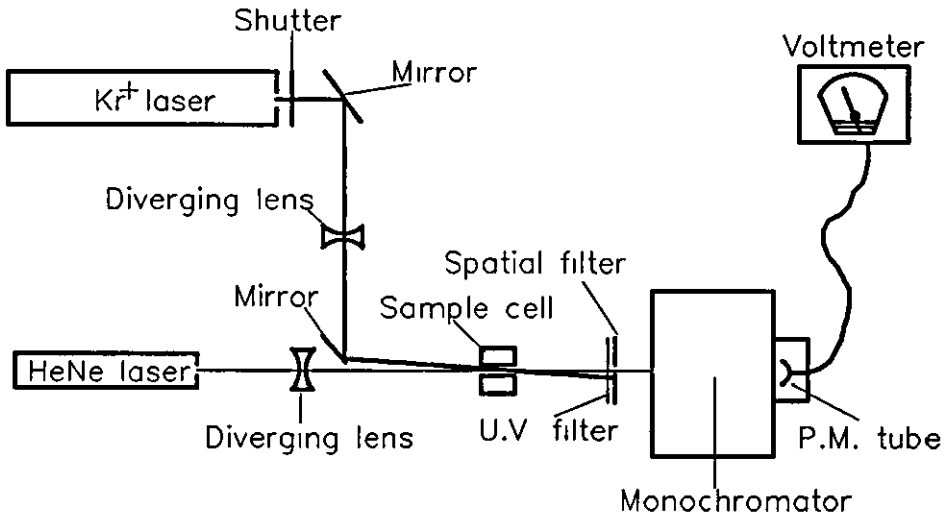

Figure 2.5. The apparatus used in the modification of the method first applied by Fischer to determine ϵ_B and the ratio of Φ_B/Φ_A.

The irradiation source was a krypton ion C.W. Laser producing laser lines at 352nm and 414nm depending upon the choice of reflecting and transmitting mirrors used in the laser. These two wavelengths were alternately employed as the irradiating wavelengths. The probe beam was the 632.8nm line produced by a helium neon laser. The pump and probe beams passed through the sample as near to colinearly as possible but still allowing the excitation beam to be spatially filtered after the sample before the monochromator. The probe beam intensity was measured using a photomultiplier connected to a voltmeter. In order for this method to be effectively applied the following set of conditions must exist: First a region must exist where the B-form of the molecule absorbs but the A-form does not, this condition always applies in the case of NOSI compounds, secondly, as mentioned above, the intensity of the incident irradiating light must be sufficiently high that the thermal reverse reaction is not depleting the B-form significantly compared with the rate of photochemical population of the B-form. This condition was confirmed by establishing that increasing the irradiation intensity did not increase the absorption due the B-form.
The theory behind the method is as follows:
for an unstirred irradiated solution of a photochromic compound the respective concentrations of the A-form and the B-form $a(I,z)$ and $b(I,z)$ photochemically generated at a depth z within the sample by an exciting laser intensity $I(a,b,z)$ are given, according to the kinetic scheme in figure 2.3, by the following differential equations:

$$\frac{\delta a(l,z)}{\delta t} = -2.3I(a,b,z)\Phi_A\epsilon_A^e a(l,z) + [2.3I(a,b,z)\Phi_B\epsilon_b^e + k]b(l,z)$$

$$\frac{\delta b(l,z)}{\delta t} = 2.3I(a,b,z)\Phi_A\epsilon_A^e a(l,z) - [2.3I(a,b,z)\Phi_B\epsilon_b^e + k]b(l,z)$$

$$a(l,z) + b(l,z) = a_o \qquad 2.4$$

Where Φ_A is the quantum efficiency for the formation of the B-form from the A-form and Φ_B the quantum efficiency for the reformation of A-form. a_o is the initial concentration of the NOSI compound in solution, and the superscript e denotes "at the excitation wavelength." Under conditions where the rate of the thermal reverse reaction is no longer significant compared with the rate of population of the B-form, in other words $I\Phi_A\epsilon_A^e \gg k$, then the photostationary concentrations of the A-form and the B-form (the infinite time solutions) in the excited region of the sample are given by equations 2.5.

$$a_s = a_o \frac{\Phi_B\epsilon_B^e}{\Phi_A\epsilon_A^e + \Phi_B\epsilon_B^e}$$

$$b_s = a_o \frac{\Phi_A\epsilon_A^e}{\Phi_A\epsilon_A^e + \Phi_B\epsilon_B^e}$$

$$a_s + b_s = a_o \qquad 2.5$$

Where the subscript s denotes that photostationary conditions prevail. Noticeable from these equations is the fact that the intensity factor has cancelled out and that the concentrations of the A-form and the B-form is now constant across the sample. In other words equation 2.6 applies.

$$A^p = (\epsilon_A^p a_s + \epsilon_B^p b_s)D \qquad 2.6$$

Where the superscript p denotes "at the probe wavelength," and D is the sample thickness. Substituting the concentrations from equation 2.5 and subsequent rearrangement gives equation 2.7.

$$\frac{A^p}{a_o D} = \frac{\epsilon_A^e\epsilon_B^p + r\epsilon_B^e\epsilon_A^p}{\epsilon_A^e + r\epsilon_B^e} \qquad 2.7$$

where; $r = \Phi_B/\Phi_A$

This applies to exciting wavelengths, where both the A- and B-form absorb.

$$\frac{A^{e}}{a_{o}D} = \frac{(1+r)\epsilon_{A}^{e}\epsilon_{B}^{e}}{\epsilon_{A}^{e}+r\epsilon_{B}^{e}} \qquad 2.8$$

or alternatively the same equation can be applied at a wavelength where the A-form does not absorb.

$$\frac{A^{p}}{a_{o}D} = \frac{\epsilon_{A}^{e}\epsilon_{B}^{p}}{\epsilon_{A}^{e}+r\epsilon_{B}^{e}} \qquad 2.9$$

Equations 2.8 and 2.9 can be employed at a different excitation wavelength. In the present case, since the excitation source was a krypton ion CW laser, the two different excitation wavelengths were in fact comprised themselves of two closely lying wavelengths and this had to be taken into account in subsequent calculations by using weighted averages dependant on the intensity of the different component wavelengths.

If it is assumed that the value of Φ_B/Φ_A is independent of the excitation wavelength employed then we have four equations to solve which will give us values for the ratio Φ_B/Φ_A. The result is equation 2.10.

$$r = \Phi_B/\Phi_A = \frac{A_{e1}^{p} - A_{e2}^{p}}{A_{e2}^{p}\left(1-\frac{A_{e1}^{e1}}{A^{e1}}\right) - A_{e1}^{p}\left(1-\frac{A_{e2}^{e2}}{A^{e2}}\right)} \qquad 2.10$$

Where;

A^{e1} is the absorbance at the first excitation wavelength with no excitation.

A^{e2} is the absorbance at the second excitation wavelength with no excitation.

A_{e1}^{e1} is the absorption at the first excitation wavelength while exciting at that wavelength.

A_{e2}^{e2} is the absorption at the second excitation wavelength while exciting at that wavelength.

A_{e1}^{p} is the absorption at the probe wavelength while irradiating at the first excitation wavelength.

A_{e2}^{p} is the absorption at the probe wavelength while irradiating at the second excitation wavelength.

Once the value of Φ_B/Φ_A has been determined then the value of ϵ_B can be calculated using equations 2.8 and 2.9.

If the absorbance value of the coloured form is the same at the probe wavelength for each of the excitation wavelengths employed then, unless $A_{e1}^{e1}/A^{e1} = A_{e2}^{e2}/A^{e2}$, the implication must be that Φ_B is very small in comparison to Φ_A and that total conversion to the coloured form is achievable at both excitation wavelengths. If this is the case then the absorbance at the probe wavelength is simply given by:

$$A^{p} = \epsilon_{B}^{p} a_{o} D \qquad 2.11$$

Absorption measurements at the excitation wavelength are difficult to measure due to scattered light from the krypton ion laser by-passing the cut off filters, spatial filter and the monochromator and entering the photomultiplier tube, the photon intensities produced by the krypton ion were high enough that this became a problem, saturating the photomultiplier response. In order to overcome these problems the absorbance at the probe wavelength were made indirectly. This was achieved by measuring the absorption spectrum of the NOSI compounds being investigated using a Hewlett Packard HP8452A diode array spectrometer after flashing the solution with a photographic flash gun, as well as measuring the absorbance at the probe wavelength during C.W. laser irradiation. The absorbances at the exciting and probe wavelengths are given by the following equations:

Using flashlamp excitation;

$$A_{f}^{e} = [\epsilon_{A}^{e}(1 - x_{f}) + \epsilon_{B}^{e} x_{f}] a_{o} D$$

$$A_{f}^{p} = \epsilon_{B}^{p} x_{f} a_{o} D \qquad 2.12$$

Using laser excitation.

$$A_{l}^{e} = [\epsilon_{A}^{e}(1 - x_{l}) + \epsilon_{B}^{e} x_{l}] a_{o} D$$

$$A_{l}^{p} = \epsilon_{B}^{p} x_{l} a_{o} D \qquad 2.13$$

In these equations:
x is the fraction of A-form converted into the B-form,
subscript f denotes "following flash gun excitation,"
subscript l denotes "during CW laser excitation."

$$A_{l}^{e} = \left(1 - \frac{A_{l}^{p}}{A_{f}^{p}}\right) \epsilon_{A}^{e} a_{o} D + A_{e}^{f} \frac{A_{l}^{p}}{A_{f}^{p}} \qquad 2.14$$

It is therefore possible to calculate values of absorption at each excitation wavelength used, these values being necessary in order to calculate the ratio Φ_{B}/Φ_{A}, and hence the value of the molar decadic absorption coefficient.

2.2.3.3 Total conversion to the B-form.

In certain cases it was not possible to use the modified Fischer method [12] or the anti-correlation method in order to determine values of ϵ_{B}. This was only found to be the case for NOSI1. The NOSI1 B-form does not possess any spectral regions, at wavelengths where the A-form also absorbs, which do not correlate either positively or negatively with the

A-form absorption envelope. The anticorrelation method cannot be applied in this instance since it requires that such non correlating regions do exist. Another problem that arises in the case of NOSI1 is that its A-form absorption spectrum does not extend to high enough wavelengths for it to absorb one of the lines produced by the krypton ion laser. Absorption of the two laser lines by the A-form is necessary for the Fischer method described above to be applied using our apparatus. In the case the NOSI1 a value of ϵ_B was eventually obtained from an absorption value measured in the visible, when the maximum photostationary conversion to the B-form had been achieved. Such conversions can only occur when the laser intensity is sufficiently high that the condition that $I\Phi_A\epsilon_A^\circ \gg k$ is met. The value of ϵ_B was then calculated from the B-form absorption measured under this condition of saturation with the assumption the value of Φ_B/Φ_B for NOSI1 is small enough for the photochemical reverse reaction to be negligible when irradiating at 352nm. This assumption would in fact have been a valid one with all of the NOSI systems for which the ratio Φ_B/Φ_B was actually determined. In these cases the absorbance in the visible produced under the same conditions was the same as would have been expected with total conversion to the B-form. The same experimental set-up was used to determine the value of the NOSI1 ϵ_B as was used for the Fischer method, except in this case only the 352nm line was used to create the photostationary solution. If the concentration of the A-form in solution and the final B-form absorbance at the probe wavelength are both known then, assuming that the condition $\Phi_B \ll \Phi_A$ applies in this case as it did for the NOSI systems for which this ratio was determined, the full spectrum of the NOSI1 coloured form and hence the extinction coefficients can be derived.

2.3 Results and discussion.

2.3.1 The A-form absorption spectrum.

The NOSI A-form spectra show marked spectral differences due to the presence of the different 6'-substituents. This can clearly be seen in figure 2.6 below.

In these toluene solutions the different 6'-substituents shift the A-form spectra towards the red in the following order NOSI2 $\geq$ NOSI4 > NOSI3 > NOSI1. This is as expected in view of the degree to which the different substituents are expected to increase the extent of conjugation.

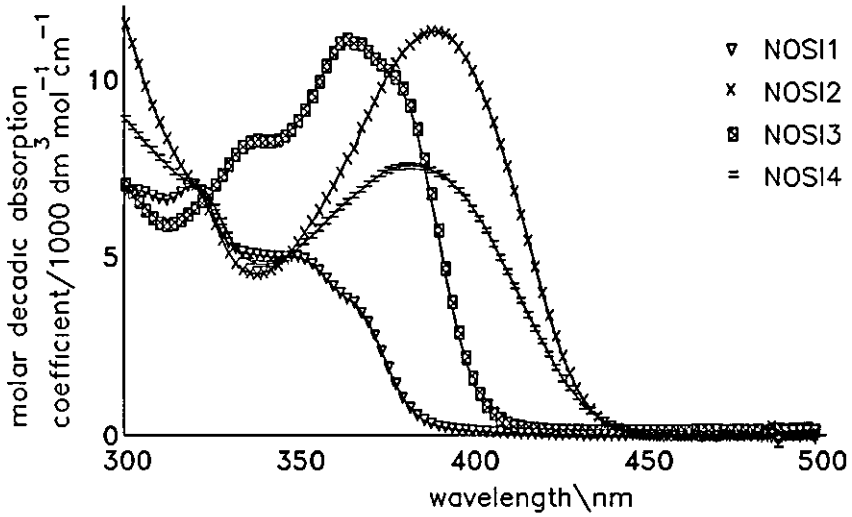

Figure 2.6. The A-form spectra of the compounds NOSI1-4 in toluene.

2.3.1.1 The NOSI1 A-form absorption spectrum.

As mentioned previously it has been shown, using model compounds to represent the two hetrocyclic parts of both BPSI and NPSI molecules [2,3], that the two heterocyclic regions of these molecules are essentially electronically separated from one another. This is due to the sp^3 hybridised spiro link which holds their two ring systems at ninety degrees to one another. This may also occur with NOSI compounds and whilst as yet no suitable model compounds have been synthesized which represent the oxazine ring, indoline itself makes an ideal model compound for the representation of the indoline half of the molecule. For this reason the indoline absorption spectrum was compared with that of NOSI1 in an attempt to find either similarities or differences which may be evident in the different spectra. The absorption spectrum of indoline shows peaks at 205nm, 244nm and 299nm, so if the two halves of the NOSI1 molecule are in fact electronically separated these bands should also appear under its absorption envelope. Figure 2.7 shows the absorption spectra of NOSI1 and indoline in methanol plotted on the same axes. From inspection of figure 2.7 it appears possible that the transitions that occur which give rise to the indoline spectrum may also contribute to the overall NOSI1 spectrum, since features are observed in the NOSI1 spectrum in similar positions to some of the absorption bands seen in the indoline spectrum. These common bands are namely the indoline peaks at 205nm and 299nm. The 235nm band in the NOSI1 spectrum is relatively large and would probably obscure the 244nm band that is seen in the spectrum of indoline alone even if this band is to be found within the NOSI1 spectrum. The similarities between the two spectra supports but by no means proves the theory that the indoline and oxazine rings are also isolated electronically

from each other. If the two halves of the NOSI molecule do absorb light in isolation then the absorption bands occurring at around 320nm and 350nm are then by elimination assignable solely to absorptions by the oxazine region of the molecule. The absorption in the 235nm region of the spectrum would then be due to significant absorption by the indoline but mainly due to absorption by the oxazine ring.

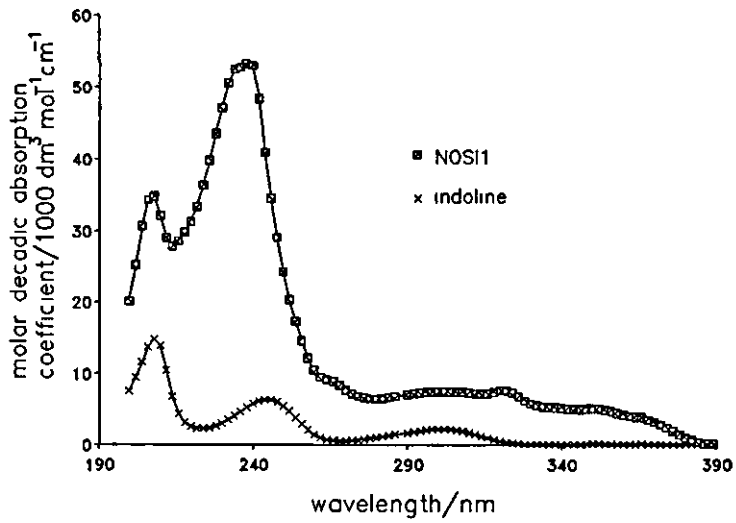

Figure 2.7. The spectra of the NOSI1 A-form in methanol compared to that of indoline in methanol.

As can be seen in figure 2.7 the NOSI1 absorptions are too large to be the result of any forbidden electronic transitions and are therefore assigned here as being $\Pi - \Pi^*$ in nature.

None of the NOSI1 absorption bands significantly altered position or shape upon changing the solvent from toluene to ethanol to cyclohexane to methanol. Absorptions which are $\Pi - \Pi^*$ in nature would be expected to shift, if anywhere, to the red upon changing from a non-polar to a polar solvent, whereas $n - \Pi^*$ transitions would shift to the blue, neither of these effects was seen for NOSI1. This lack of solvent polarity shift gives no reason for changing the previous assignment of the bands to $\Pi - \Pi^*$ transitions. The molar decadic absorption coefficients of NOSI1 have been determined specifically at 355nm in toluene and ethanol, the values obtained are 4800 $dm^3.mol^{-1}cm^{-1}$ and 4600 $dm^3.mol^{-1}cm^{-1}$ respectively. These two values are within five percent of each other which highlights the similarities between the absorption spectra determined in solvents of different polarities. If we take the idea that the two halves of the NOSI1 molecule may be electronically isolated from one another a stage further, then a theoretical oxazine spectrum can be constructed by subtracting the indoline spectrum from the NOSI1 spectrum. This has been done and the resulting spectrum is shown in figure 2.8. This spectrum demonstrates that oxazine

transitions will give an appreciable contribution to the overall NOSI1 absorption across the entire spectrum. This is not so for the indoline transitions and the indoline part of the molecule will effectively stop absorbing at ~315nm and will not give rise to absorption anywhere in the spectrum that the oxazine does not. This result may have implications to the photochemistry of this molecule as well as other NOSI molecules, since it suggests that there is the possibility of exciting electronic transitions on the oxazine ring without directly exciting the indoline ring but not vice-versa. This could be an important consideration, since the suggested electronic isolation of the oxazine and the indoline may hold up energy transfer past the spiro carbon after absorption of a photon by the indoline ring. The C-O bond which breaks prior to isomerisation is located on the oxazine ring.

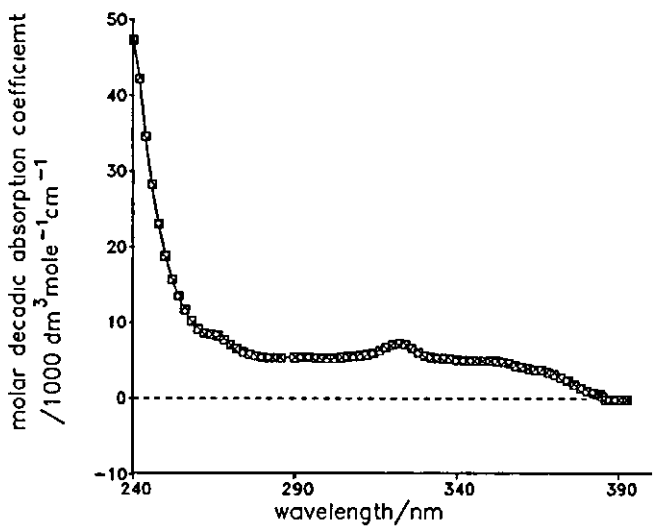

Figure 2.8. The proposed spectrum of the oxazine ring generated by subtracting the indoline spectral contribution to the NOSI1 spectrum in methanol.

2.3.1.2 The NOSI2, n-iso-butyl NOSI2 and NOSI4 A-form absorption spectra.

NOSI2, n-iso-butyl NOSI2 and NOSI4 all absorb further into the visible region than NOSI1. The shift in these spectra compared with that of NOSI1 is no doubt due to the presence of the 6'-indoline or in the case of NOSI4 the 6'-methyl-indoline which increases the extent of the oxazine Π-electron system thereby lowering the energy of the $\Pi - \Pi^*$ transition and resulting in a red shift in the spectrum. Hence solutions of these three compounds continue absorbing until around 450nm. The absorption spectra of NOSI1, NOSI3, NOSI2 and NOSI4 in toluene are shown in figure 2.6, the spectrum of n-iso-butyl NOSI2 is not shown but is similar to that of NOSI2. As can be seen, at these wavelengths the spectra of NOSI2 and NOSI4 are less resolved than the NOSI1 and NOSI3 spectra because they have a broad absorption band at around 390nm which masks other features.

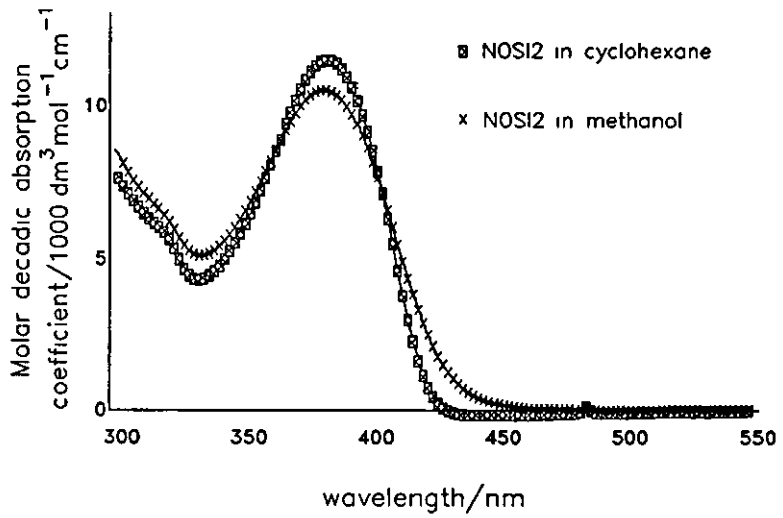

Figure 2.9. The NOSI2 A-form spectra measured in cyclohexane and methanol.

Figure 2.9 shows the absorption spectra obtained for NOSI2 in cyclohexane and methanol. It is evident from this that spectral broadening results as a consequence of changing the solvent from cyclohexane to methanol. This is could be the result of an increase in the extent of solvent solute interactions occurring in methanol which leads to an increase in the number of available vibrational modes. This could be caused by a polarity increase or by hydrogen bonding. This type of spectral broadening is the only solvent effect seen for these compounds and no solvent shifts occur due to polarity changes. It therefore is once again the large molar decadic absorption coefficient of these absorption bands which leads to the assignment of their origin as $\Pi - \Pi^*$ transitions. The positions of peak maxima occurring at around 390nm and values of ϵ_A at the peak maxima and at 355nm in different solvents are given in tables 2.1 and 2.2.

The positions of the peak maxima do not vary much from solvent to solvent, and the differences which are observed here follow no definite trends. The choice of solvent in each case appears to have relatively little effect upon the value of ϵ_A at either the 390nm peak maximum or at 355nm. The ϵ_A values measured here in the different solvents show no obvious pattern. The differences in values of ϵ_A measured here could be due to very slight shifts in the relative positions of the absorption bands which make up the observed absorption envelope, or to spectral broadening as a result of solvent polarity increases. The NOSI4 molar decadic absorption coefficient was determined in toluene and was found to be 5600 $dm^3.mol^{-1}cm^{-1}$ at 355nm this value is similar to that of NOSI2 and n-iso-butyl NOSI2 at 355nm.

Table 2.1. Peak maxima positions and ϵ_A values determined for n-iso-butyl NOSI2 in various solvents.

Solvent	Position of A-form peak maximum/nm	ϵ_A at peak maximum./ $1000.dm^3.mol^{-1}cm^{-1}$	ϵ_A measured at 355nm/ $1000.dm^3.mol^{-1}cm^{-1}$
cyclohexane	384	11.5	6.4
toluene	389	11.3	5.3
benzene	391	12.6	5.6
acetonitrile	386	10.7	6.2
polyurethane	391	12.1	6.9
propanol	387	11.7	6.2
methanol	386	10.7	6.6

Table 2.2. Peak maxima positions and ϵ_A values determined for NOSI2 in various solvents.

Solvent	Position of A-form peak maximum/nm	ϵ_A at peak maximum./ $1000.dm^3.mol^{-1}cm^{-1}$	ϵ_A at 355nm/ $1000.dm^3.mol^{-1}cm^{-1}$
cyclohexane	385	11.8	6.8
toluene	388	11.2	5.9
benzene	390	12.0	6.0
acetonitrile	384	11.8	6.8
polyurethane	388	12.0	6.8
propanol	387	11.3	6.9
methanol	383	10.1	6.8

2.3.1.3 The NOSI3 absorption spectrum.

NOSI3 absorption spectra in toluene are shown in figure 2.6. Figure 2.10 shows NOSI3 spectra measured in acetonitrile and cyclohexane. Evident from these is the increased spectral structure that is seen in the NOSI3 spectra compared with those of the 6'-indoline derivatives. The 6'-piperidine group shifts the A-form absorption further towards the visible

region than the spectrum of the unsubstituted NOSI1, however solutions of NOSI3 still appear colourless and do not absorb as far towards the red as the 6'-indoline substituted NOSI compounds. This is because the 6'-piperidine does not provide as long an extension to the oxazine conjugation as the 6'-indoline.

The molar decadic absorption coefficient has been measured for NOSI3 in toluene at 355nm and was found to be 9200 $dm^3.mol^{-1}cm^{-1}$ which again suggests that the spectrum is due to $\Pi - \Pi^*$ transitions. The same effects are seen for NOSI3 upon changing from polar to non-polar solvent media. In other words there are no definite solvent shifts, but the spectrum does broaden in polar solvents compared to non polar. This broadening is evident in figure 2.10 which shows the NOSI3 spectrum measured in acetonitrile compared to that in cyclohexane.

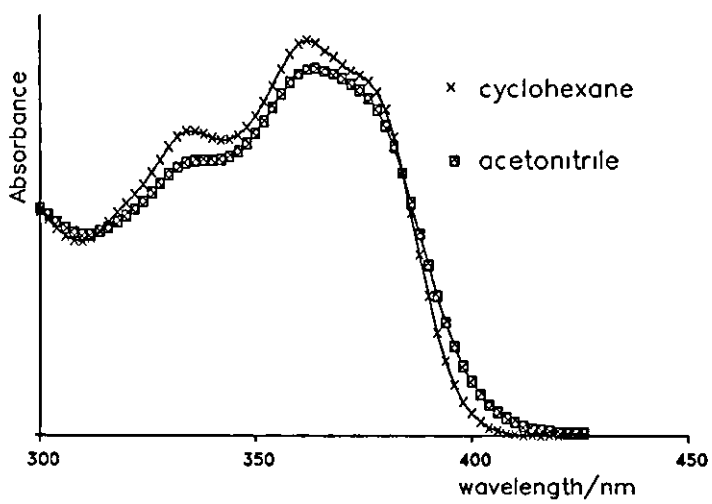

Figure 2.10. The NOSI3 A-form spectra in acetonitrile and cyclohexane.

2.3.2 The B-form absorption spectrum.

The present work demonstrates that the appearance of the B-form spectra is a broad band in non-polar solvents such as cyclohexane, but as the solvent polarity is increased the spectra become red shifted and the resolution in the spectral structure increases. For the compound NOSI1 changing the solvent from toluene to ethanol results in a shift in the position of the B-form peak maximum from 592nm to 612nm, this spectral shift is accompanied by an increase in the size of ϵ_B from 31000 $dm^3.mol^{-1}cm^{-1}$ to 51000 $dm^3.mol^{-1}cm^{-1}$. There is also an enhancement in the spectral resolution with the development of a shoulder on the higher energy absorption edge of the main absorption peak in the ethanol solution. This type of increase in spectral resolution, the corresponding increase in ϵ_B and the large solvent shifts are common phenomenon which occur for many

of the NOSI B-forms presently being investigated. These effects are clearly seen for the n-iso-butyl NOSI2 spectra determined in a variety of different solvents shown in figure 2.11. The solvent parameters for the different solvents used are given below in table 2.3. The positions of the B-form peak maxima and the corresponding values of ϵ_B obtained in the different solvents are given in tables 2.4.-2.6. In general the positions of the peak maximum absorbances for NOSI2 and n-iso-butyl NOSI2 shift towards longer wavelengths as the solvent polarity is increased. This is, however only a general trend. The position of the peak maxima determined for the NOSI2 and the n-iso-butyl NOSI2 B-forms in acetonitrile were 592nm and 595nm respectively.

Table 2.3. Solvent dielectric constants [13].

Solvent	Dielectric constant
cyclohexane	2.0
benzene	2.3
toluene	2.4
acetonitrile	35.9
1-propanol	20.5
methanol	32.7

Table 2.4. Peak maxima and ϵ_B values for NOSI2 determined using the anti-correlation method.

Solvent	Peak maximum/nm	ϵ_B at peak maximum./ 1000 $dm^3.mol^{-1}cm^{-1}$
cyclohexane	562	40
toluene	583	48
benzene	586	49
acetonitrile	592	51
polyurethane	600	54
1-propanol	606	56
methanol	611	58

Table 2.5. Peak maxima and ϵ_B values for n-iso-butyl NOSI2 determined using the anti-correlation method.

Solvent	Peak maximum/nm	ϵ_B at peak maximum./ 1000 $dm^3.mol^{-1}cm^{-1}$
cyclohexane	576	42
toluene	587	47
benzene	593	50
acetonitrile	595	51
polyurethane	605	56
1-propanol	611	59
methanol	615	61

Table 2.6. Values of Φ_B/Φ_A and ϵ_B determined using a krypton ion CW laser.

Compound	Solvent	Φ_B/Φ_A	ϵ_B at peak maximum./1000 $dm^3.mol^{-1}cm^{-1}$
n-iso-butyl NOSI2	toluene	<0.04	47
n-iso-butyl NOSI2	benzene	<0.02	49
n-iso-butyl NOSI2	polyurethane	<0.06	61
n-iso-butyl NOSI2	propanol	0.08±0.06	61
NOSI2	polyurethane	<0.04	55
NOSI3	toluene	<0.04	32
NOSI3	polyurethane	<0.03	57
NOSI4	toluene	<0.06	43
NOSI1	ethanol	-	51*
NOSI1	toluene	-	31*
NOSI1	cyclohexane	-	24*

* Determined assuming that $\Phi_B \ll \Phi_A$. All other values determined using the Fischer method [12].

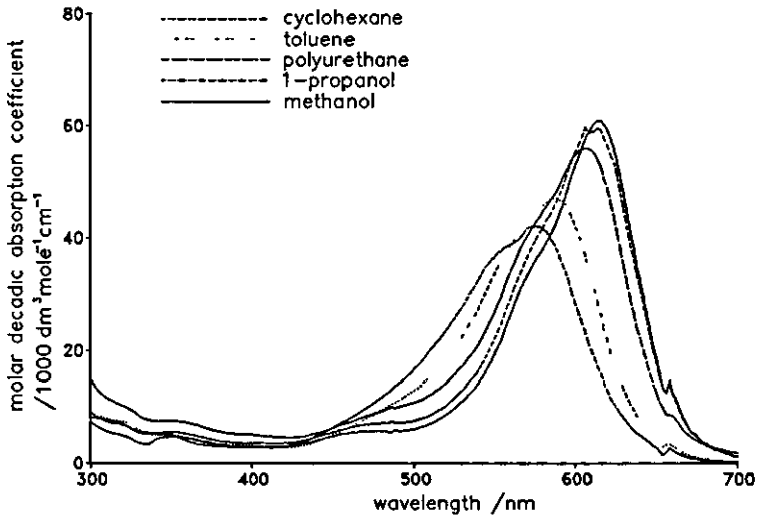

Figure 2.11. The B-form spectra determined using the anti-correlation method for n-iso-butyl NOSI2 in various solvents.

If solvent polarity were the only factor determining the positions of the B-form peaks, then it would be expected that the peak maximum determined for a given NOSI compound in methanol should be very close to the value determined in acetonitrile, since these two solvents have very similar dielectric constants. This is not found in practice and the actual measured positions of the peak maxima of NOSI2 and n-iso-butyl NOSI2 in methanol are 611nm and 615nm respectively compared with the values of 592nm and 595nm determined in acetonitrile. Hence for these two compounds there is a spectral shift of 19-20nm upon changing the solvent from acetonitrile to methanol. In actual fact the peak maximum for n-iso-butyl NOSI2 in acetonitrile is only red shifted by 2nm from its position determined in benzene despite the fact that benzene has a dielectric constant that is more than 10 times less than that of acetonitrile. A similar set of results is obtained for NOSI2 in these three solvents. The spectra of the NOSI2 B-form in these three solvents are shown below in figure 2.12. The fact that the observed spectral shifts do not correlate perfectly with the differences in solvent polarity is not altogether surprising in view of the other types of solvent interaction which can occur.

Methanol does posses the ability to form strong hydrogen bonds, this may be happening here resulting in an otherwise unstable B-form isomer being favoured in solution. Hydrogen bonding is not possible in the case of NOSI solutions in acetonitrile leading to the stabilisation of different isomers and different spectrum. Another factor which may influence the B-form spectral position is that the B-form can exist in different resonance forms. For the NOSI1 B-form there are two canonical forms which are possible, one being a zwitterionic species and the other a quinoidal species. The B-form exists as a hybrid made up

from the contribution from each of these. The relative contribution of each one of these to the hybridised B-form ground state will determine the overall charge separation of the ground state molecule.

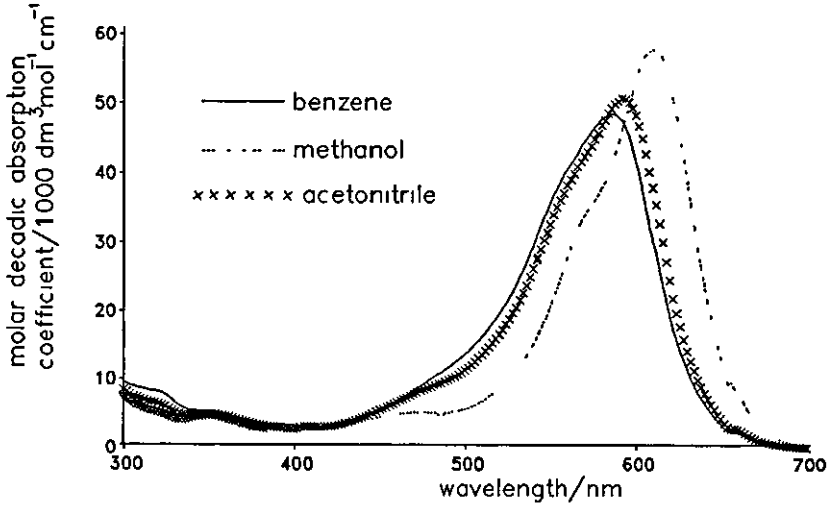

Figure 2.12. NOSI2 B-form spectra in benzene, acetonitrile, and methanol.

If the B-form ground state is predominantly the non charge separated quinoidal structure then the first excited singlet state of the molecule will mainly have resonance contributions from the more charge separated zwitterion when the hybrid forms. If this is the case then changing the solvent from a non-polar to a polar one will stabilise the S_1 state relative to the ground state and the S_1->S_0 energy gap will be reduced. The result of this would be a red shift in the B-form spectrum. The opposite effect has been observed for NPSI and BPSI [6], a result which has been explained in terms of the ground state of the B-form ground state being predominantly zwitterionic form which it is argued is then more charge separated than the first excited singlet state. Hence for BPSI's and NPSI's increasing the solvent polarity increases the S_1->S_0 energy gap by stabilising the S_0 level relative to the S_1 level. The solvent shifts observed for the BPSI's and NPSI's show the same trend with solvent polarity as is seen for the merocyanine dyes [14,15,16]. These dyes are highly charge separated in their ground state and in many cases show such pronounced solvent shifts that they have been proposed as solvent polarity indicators. The different canonical forms available to the unsubstituted and 6'-substituted NOSI compounds are shown in figures 2.13 and 2.14.

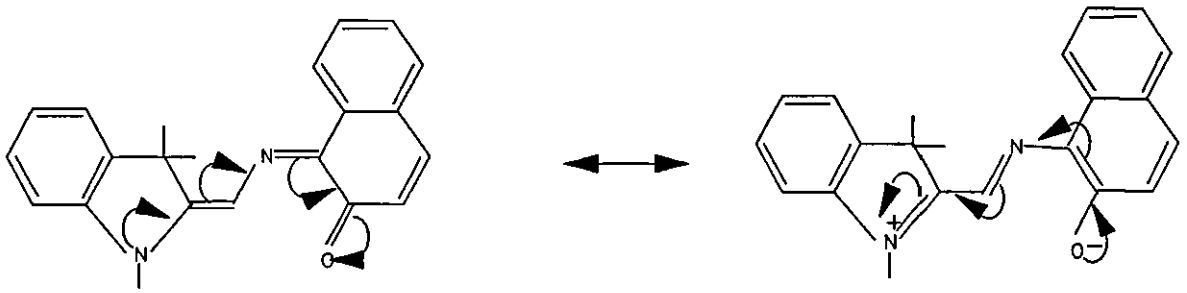

Figure 2.13. The Kekule forms available to the NOSI1 B-form resonance hybrid.

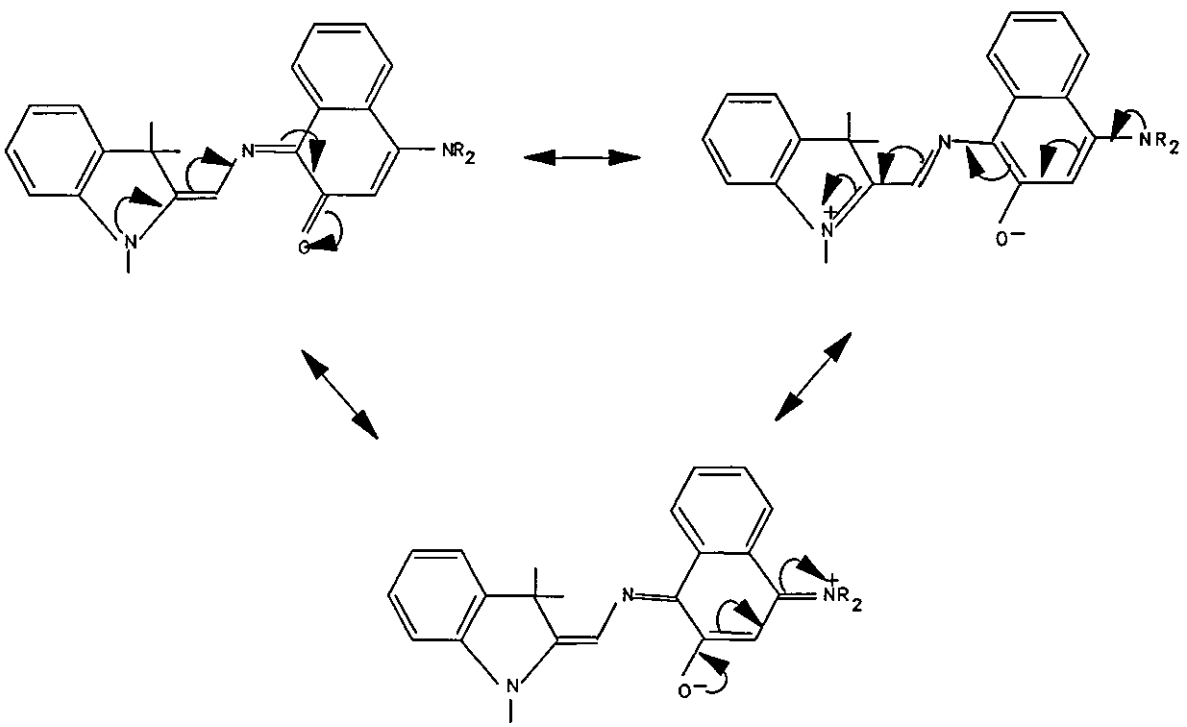

Figure 2.14. The Kekule structures available to the B-form resonance hybrids for NOSI compounds which have an electron donating 6'-substituent.

The dipole moments of the first excited singlet state and the ground state of NOSI1 have been calculated to be 5.4 and 3.8 Debyes respectively [17] this result is consistent with a predominantly quinoidal form for the ground state of the molecule and a zwitterionic form for the first excited singlet state. From the above discussions the spectral changes observed for the B-form upon changing the solvent polarity could be caused by changes in the distribution of B-form isomers in the different solvents or by the relative stabilisation of the zwitterionic excited singlet state compared to the quinoidal ground state. Equally both of these mechanisms may be contributing factors in determining the B-form spectra. The isomeric distribution theory is supported by the spectral positions determined for NOSI2

and n-iso-butyl NOSI2 in acetonitrile methanol and benzene. If the extent to which the B-form is zwitterionc was the sole cause of these solvent shifts then the solvent polarity of acetonitrile should influence the energy of the S_1->S_0 transition as much as and in the same direction as solvation in methanol does. This is not found to be the case and other factors such as changes in isomeric distribution must be influencing the resulting spectra. The presence of different B-form isomeric distributions in the different solvents has been proposed for NOSI compounds by Schneider *et al* [17] who measured CARS (coherent anti-Stokes Raman scattering) spectra for several NOSI compounds in several solvents. The results of their work suggested the presence of two or maybe even three isomers being present in solution with different relative concentrations depending upon the solvent type. Aramaki *et al* carried out time resolved resonance Raman (TR^3) spectroscopy on NOSI1 [18]. From their results it has been suggested that at least two B-form isomers are possible with their relative concentrations varying in each different solvent. These two transient studies will be discussed in more detail in chapter 5.

The presence of an electron donating group at the 6'-position on the oxazine has the effect of shifting the absorption maximum of the B-form to shorter wavelengths. Absorption maxima in toluene are summarised in table 2.7.

Table 2.7. ϵ_B and λ_{max} values for several NOSI compounds having different 6'-substituents.

Compound	ϵ_B/1000.dm^3.mol^{-1}cm^{-1}	λ_{max}/nm
NOSI1	31	592
NOSI2	48	583
NOSI3	32	560
NOSI4	43	588

The 6'-substituent electron donating power reduces in the order NOSI3>NOSI4>NOSI2>NOSI1, however the methyl group on the indoline substituent of NOSI4 probably has the effect of pushing this group out of the plane of the rest of the molecule thereby reducing the Π-cloud overlap lowering the effective electron donating power of the group. The effective electron donating power of the 6'-groups is therefore more likely to reduce in the order NOSI3>NOSI2>NOSI4>NOSI1. This order mirrors the ordering observed for the substituent shifts where λ_{max} reduces in the order NOSI1>NOSI4>NOSI2>NOSI3. It therefore appears to be the trend that the more electron donating the

6'-group the shorter the wavelength of λ_{max}. The observed trend may be due to electron donation stabilising a particular B-form isomer which may be less planar and therefore less conjugated than the other possible isomers.

Other workers have determined values of ϵ_B for NOSI1 which can be compared to the values obtained in the present work. Kholmanskii *et al* have determined the value of ϵ_B for NOSI1 in ethanol to be 52000 $dm^3.mol^{-1}cm^{-1}$ (20) whereas Chu determined the value in ethanol to be 71000 $dm^3.mol^{-1}cm^{-1}$ (7). Both authors used steady state irradiation at temperatures low enough to freeze out the thermal reaction resulting in the reformation of the A-form. Chu worked at a temperature of 198K wheres Kholmanskii worked at a temperature of 203-243K. Our value of 51000 $dm^3.mol^{-1}cm^{-1}$ measured at a temperature of 298K is in agreement with Kholmanskii's result at 203-243K. The present result for NOSI1 and the results of Kholmanskii *et al* and Chu for the same compound all assume that $\Phi_B \ll \Phi_A$ and are measured under conditions where $I\Phi_A\epsilon_A^* \gg k$.

Chapter 2 References

1. F. Wilkinson, J. Hobley, M. Naftaly, J. Chem. Soc. Farad. Trans. 1992, 88, 1511.
2. D.A. Reeves, F. Wilkinson, J. Chem. Soc. Farad. Trans, 2, 69, 1973, 1381.
3. R.S. Becker, N.W. Tyer, Jr. J. Am. Chem. Soc. 92, 1970, 1289.
4. H. Durr, H. Bouas-Laurent, Photochromism Molecules and Systems, Elsevier, ISBN 0-444-87432-1, 1990, 498.
5. S.A. Krysanov A. Alfimov, Chem. Phys. Lett. 1982,91, 77.
6. R. Heiligman-Rim, Y. Hirshberg, E. Fischer, J. Phys. Chem. 66, 1962, 2465.
7. N.Y.C. Chu, Can. J. Chem. 1983, 61, 300.
8. C. Bohnne, M.G. Fan, Z.J. Li, Y.C. Liang, J.C. Scaiano, J. Photchem. Photobiol. A, Chem. 66, 1992, 79.
9. A. Kellermann, F. Tfibel, R. Dubest, P. Levoir, J. Aubard, E. Pottier, R. Gugliemetti, J. Photochem. Photobiol. A, Chem. 49, 1983, 63.
10. S. Hadley, R.A. Keller, J. Phys. Chem. 73, 12, Dec. 1969, 4351.
11. H. Labhart, Helv. Chim. Acta, 47, 1964, 2279.
12. E. Fischer, J. Chem. Phys. 1967/71, 3704.
13. S.L. Murov, I. Carmichael, G.L. Hug, Handbook of Photochemistry, 2nd Ed. Marcel Dekker, ISBN 0-8247-7911-8, 1993, p284.
14. H. Takahashi, K. Yoda, H. Isaka, T. Ohzeki, Y. Sakaino. Chem. Phys. Lett. 18 Sept. 1987.
15. H. Takahashi, K. Yoda, H. Isaka, T. Ohzeki, Y. Sakaino. J. Photochem. Photobiol. A, Chemistry, 45, 1988, 233.
16. P. Sappan, J. Am. Chem. Soc. A, 1968, 3125.
17. C.B. McArdle, Applied Photochromic Polymer Systems, Blackie, ISBN 0-412-02971-5, 1991, 39.
18. S. Schneider, F. Bauman, U. Klutter, M. Melzig, Ber. Bunsenges, Phys. Chem. 1987, 91, 1225.
19. S. Aramaki, G.H. Atkinson, Chem. Phys. Lett. 170, 2,3, 1990, 181.
20. A.S. Kholmanskii, K.M. Dyumaev, Dokl. Akad. Nauk. SSSR. 1988, 303, 1189.

CHAPTER 3

THE NOSI GROUND STATE POTENTIAL ENERGY SURFACE.

Chapter 3 The NOSI ground state potential energy surface.

3.1. Introduction.

A typical NOSI compound is able to interchange between its A-form and its B-form in the absence of exciting photons [1]. This reaction proceeds along a ground state potential energy surface and not along an excited state surface as occurs following photo-excitation. The potential energy profile of the ground state surface can be investigated by establishing the changes that occur in the thermal equilibrium that exists between the A-form and the B-forms of the molecule as a function of temperature [1,2], as well as by measuring the rate constants for the thermal reformation of the A-form from the B-form at different temperatures [1,3,4]. The elucidation of the ground state surface and the effects of both solvent and substituent on this surface are described in this chapter. The study of these surfaces is important in order to predict the behaviour of photochromic systems whilst undergoing processes other than photochemical ones. Different NOSI compounds will have different ground state potential energy surfaces and will therefore tend to have different equilibrium constants for the equilibrium that exists between the A-form and the B-form as well as having different thermal fade reaction kinetics.

One type of situation for which the above factors are important considerations is when mixtures of photochromic compounds with different B-form absorption spectra are used in the manufacture of photochromic dispersions in polymer matrices to give neutral light transmitting characteristics [5]. Such dispersions are used in ophthalmic photochromic lenses. If the different compounds had very different thermal fade rates then this would show up to the wearer as changes in the matrix colour with time following the removal of the photo-excitation source, as the different components in the mixture faded with different rates. This effect is generally considered to be undesirable especially in photochromic lenses.

When the concentration of a NOSI compound in solution is high enough and the temperature of the solution is sufficient, enough B-form can be present in thermal equilibrium with the A-form for its colouration in the solution to be clearly visible to the human eye even without photoexcitation. This phenomenon is also considered to be a problem in applications such as ophthalmic photochromic lenses since the B-form colouration may become visible to the wearer at room temperatures even when no U.V. radiation is present to photochemically populate the B-form.

These effects are governed by the ground state potential energy surface of the NOSI molecule which is shown in figure 3.1.

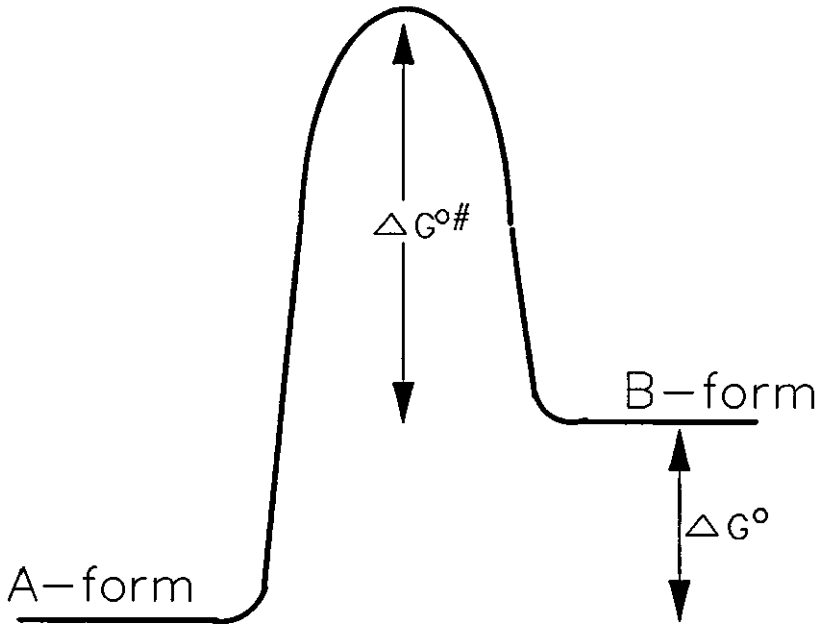

Figure 3.1. The ground state potential energy surface for a simple unimolecular reaction where $B \rightarrow A$.

Where $\Delta G^{\ddagger}$ is the Gibbs free energy for the activation of the reaction $B \rightarrow A$, and ΔG° is the free energy difference between the B-form and the A-form.

3.2. Experimental.

3.2.1. The determination of the activation barrier to the thermal fade reaction.

The thermal bleaching reaction of fresh solutions of various NOSI compounds have been reported to obey first order kinetics in polar solvents and bi-exponential kinetics in non-polar solvents [6,7]. In non-polar solvents the contribution from the faster component is reported to be very small and in general more than an order of magnitude faster than the slow component for all of the NOSI compounds studied. For this reason it would not be observed in the present study since it would be too fast for apparatus used here and only first order kinetics are measured. Even when the compounds being studied presently have been studied using nanosecond flash photolysis no faster components to the thermal decay were detected in toluene. The rate of the thermal isomerisation reaction from the B-form to the A-form is in part determined by the number of B-form molecules which possess sufficient energy to overcome the activation barrier for this process at any point in time. This in turn is determined by the thermal energy contained within the solution. Hence

there exists a relationship between the rate constant of the thermal fade reaction and the temperature of the solution. This relationship is given by an equation proposed by Arrhenius [3,4]:

$$k = Ae^{-\frac{E_a}{RT}} \qquad 3.1$$

Where;

k = the first order rate constant for the reaction,

A = the pre-exponential factor for the reaction,

E_a = the activation energy for the reaction,

R = the gas constant,

T = the reaction temperature.

If the first order rate constant for the thermal fade reaction, k, is determined at various thermostatically controlled temperatures and a graph of lnk against $1/T$ is plotted then $-E_a/R$ is slope of the resulting graph and A is the intercept.

If we assume that the B-form reforms the A-form via an activated species B$^{\#}$ and that the species B$^{\#}$ exists in steady state with the A-form and the B-form then the following argument can be applied:

$$\frac{da}{dt} = kb^{\#} \qquad 3.2$$

since a steady state exists between the B-form and B$^{\#}$ then,

$$K_e^{\#} = \frac{b^{\#}}{b} \qquad 3.3$$

the rate of formation of the A-form is proportional to the frequency of breakdown of the activated species B$^{\#}$, ν, i.e.

$$\frac{da}{dt} = \nu K_e^{\#} b \qquad 3.4$$

pseudo thermodynamic properties can be applied to the steady state species B$^{\#}$,

$$\ln K_e^{\#} = -\frac{\Delta G^{o\#}}{RT} \qquad 3.5$$

$$\Delta G^{o\#} = \Delta H^{o\#} - T\Delta S^{o\#} \qquad 3.6$$

Combining equations 3.5 and 3.6 gives;

$$K_e^{\#} = e^{\frac{\Delta S^{o\#}}{R}} . e^{-\frac{\Delta H^{o\#}}{RT}} \qquad 3.7$$

If $k = \nu K_e^{\#}$ then we can write;

$$k = \nu e^{\frac{\Delta S^{o\#}}{R}} . e^{-\frac{\Delta H^{o\#}}{RT}} \qquad 3.8$$

It is often assumed that $\nu = \frac{k_b T}{h}$ and therefore equation 3.8 can be re-written as;

$$\ln \frac{k}{T} = \ln \frac{k_b}{h} + \frac{\Delta S^{o\#}}{R} - \frac{\Delta H^{o\#}}{RT} \qquad 3.9$$

Where:

a = the concentration of the A-form,

b = the concentration of the B-form,

$b^{\#}$ = the concentration of $B^{\#}$

k = the first order rate constant for the reformation of the A-form,

$K_e^{\#}$ = the equilibrium constant for the equilibrium between the B-form and $B^{\#}$,

R = the gas constant,

T = the reaction temperature.

k_b = Boltzmans constant.

Plotting a graph of $\ln k/T$ against $1/T$ should give a straight line with a slope of $-\Delta H^{o\#}/R$, and an intercept from which the value of $\Delta S^{o\#}$ can be determined.

The first order rate constants for the thermal fade reaction were determined spectroscopically for several NOSI compounds in toluene in a 1 cm pathlength glass cell with optical quality windows. This cell was placed in a thermostated cell holder and was magnetically stirred throughout the experiment. Conversion to the B-form was brought about using a photographic flash gun placed above the cell. The B-form absorption was measured at various time delays after the solution was flashed using a Hewlett Packard HP8452A diode array spectrometer. From Beer's law the absorbance due to the B-form is directly proportional to the B-form concentration (see section 1.1.2). Hence by measuring the rate of change of B-form absorbance with time the rate of decay of the B-form can be established. The absorbance with time data was then analysed using a non-linear least squares fitting routine fitting the data to first order kinetics to obtain a value of the first order rate constant. First order rate constants were determined at various different temperatures and graphs of $\ln k$ against $1/T$ and $\ln k/T$ against $1/T$, respectively, were plotted for each of the compounds studied. These graphs are shown in figures 3.2 and 3.3. From the slopes of these E_a and $\Delta H^{o\#}$ can be found respectively.

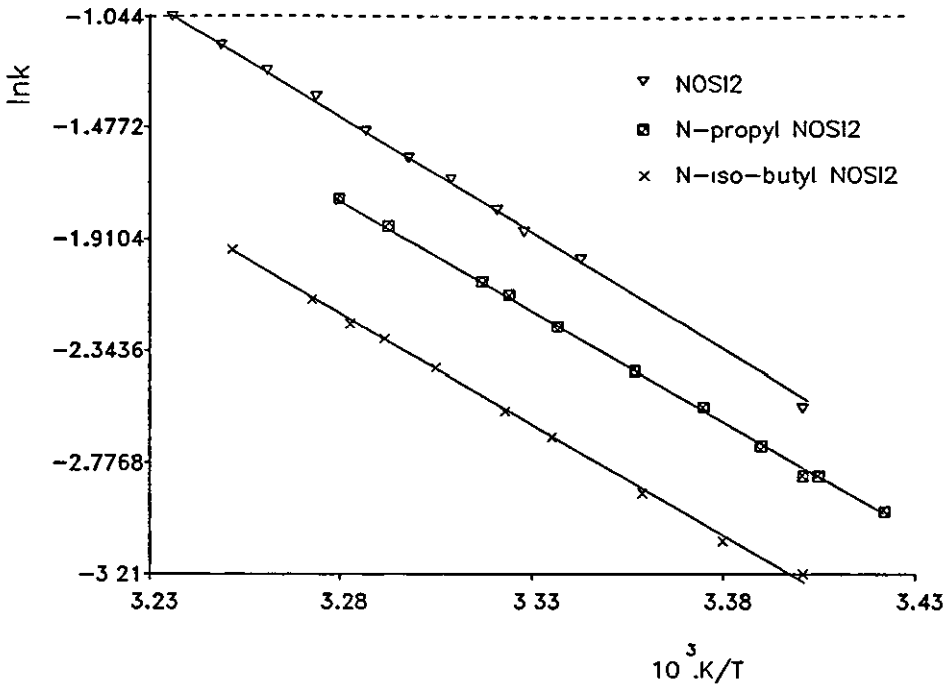

Figure 3.2. *lnk* plotted against $1/T$ for several n-alkyl NOSI2 compounds in toluene.

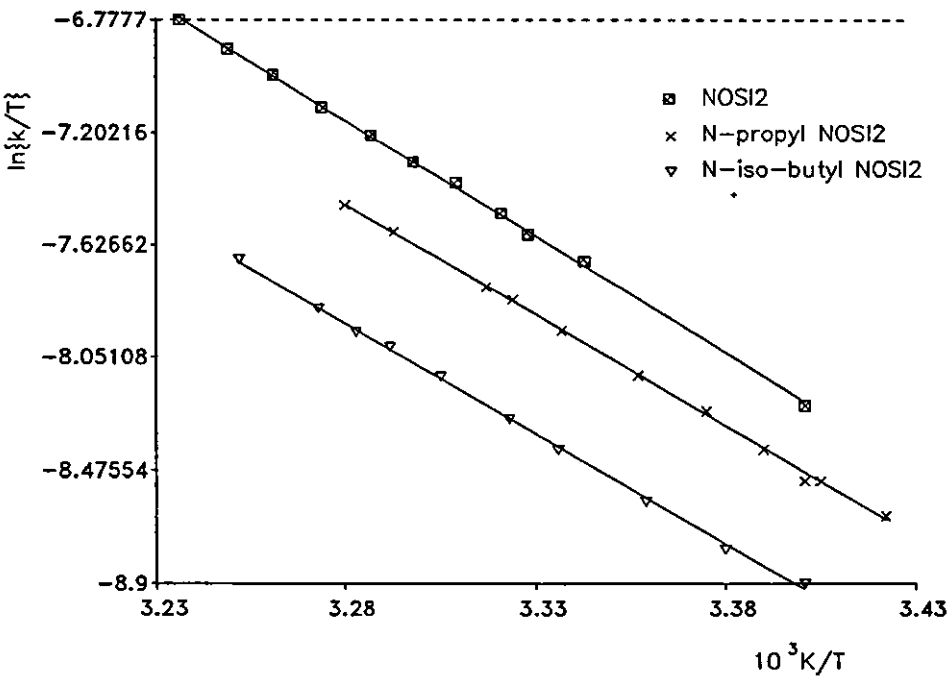

Figure 3.3. $\ln k/T$ against $1/T$ for several n-alkyl NOSI2 compounds in toluene.

In this piece of work the effect of the size of the substituent on the indoline nitrogen upon the values of $\Delta H^{\circ\ddagger}, \Delta S^{\circ\ddagger}$ and E_a were investigated, since increasing the size of this substituent has been reported to increase the lifetime of the B-form [8].
Values of $\Delta H^{\circ\ddagger}, \Delta S^{\circ\ddagger}$ and E_a were not determined for every NOSI system investigated in this piece of work, in many cases single values of first order rate constant were measured at 294K and these values were compared to each other. The effect of different substituents at the 6'-position was investigated in this way.

3.2.2. Thermochromism of NOSI compounds.

In solution the A-form and the B-forms of a NOSI compound can co-exist in thermal equilibrium with one another [1]. The free energy difference between the A-form and the B-form is such that it is often possible to detect measurable concentrations of the B-form of the molecule in thermal equilibrium with the A-form at room temperature.

As can be seen from figure 3.1 the B-form of a NOSI compound possesses more energy than the A-form does and as the temperature of a NOSI solution is increased the number of molecules possessing sufficient energy to adopt the B-form will increase. If the temperature is raised sufficiently then the concentration of B-form isomers becomes such that their spectrum and therefore their concentration becomes measurable.
When considering NOSI thermochromism the relevant energy gap on the above potential energy diagram is the energy difference between the A-form and the B-form. This energy gap is the thermodynamic property ΔG°. The size of ΔG° for a given NOSI compound will dictate the effect of temperature on the equilibrium concentration of the B-form. The relationship between temperature and the B-form concentration and absorption is derived below:

$$K = \frac{b}{a}$$

$$K = \frac{x}{a_0 - x} \qquad 3.10$$

If the conversion to the B-form is low enough that the condition, $x \ll a_0$ applies then equation 3.10 simplifies to equation 3.11

$$K = \frac{x}{a_0} \qquad 3.11$$

From Beers law $x = \frac{A_B}{\epsilon_B l}$ and equation 3.11 we obtain equation 3.12;

$$\epsilon_B l[a_o]K = A_B$$

$$\ln A_B = \ln \epsilon_B l + \ln[a_o] + \ln K \qquad 3.12$$

From basic thermodynamics we get the following equations;

$$-RT \ln K = \Delta G^\circ \qquad 3.13$$

$$\Delta G^\circ = \Delta H^\circ - T\Delta S^\circ \qquad 3.14$$

Which combined with equation 3.12 gives equation 3.15;

$$\ln A_B = -\frac{\Delta H^\circ}{RT} + \frac{\Delta S^\circ}{R} + \ln \epsilon_B l + \ln[a_o] \qquad 3.15$$

Where:

K = the equilibrium constant for the reaction $A \rightarrow B$.

a = the concentration of A-form.

b = the concentration of B-form.

x = the concentration of B-form.

a_o = the initial concentration of A-form.

A_B = the absorbance due to the B-form.

ϵ_B = the molar decadic absorption coefficient of the B-form.

l = the optical pathlength of the solution.

Plotting $\ln A_B$ against $1/T$ gives a straight line graph from which values of ΔH° can be derived from the slope.

The thermodynamic behaviour of various NOSI compounds in various solvents was examined in this study in order to establish both substituent and solvent effects upon the value of ΔH°. B-form absorbance values for the different solutions were measured in sealed 1 cm pathlength glass cells with optical quality faces using an HP8452A diode array spectrometer. The cell was sealed in order to prevent evaporation of the solvent and a corresponding increase in the NOSI concentration as the temperature of the solution was raised. The temperature of the various NOSI solutions could be varied since the glass cell was placed inside a thermostated cell holder. The temperature of the solution could easily be varied between ~290K and ~360K, this temperature being measured with a thermo-couple placed inside the cell. The B-form absorbance values were measured at wavelengths close to the peak maximum for each NOSI B-form studied. Solutions of the various NOSI compounds were made up to have a total NOSI concentration high enough to give a resulting equilibrated B-form concentration which gave easily measurable absorbances at the probe wavelength.

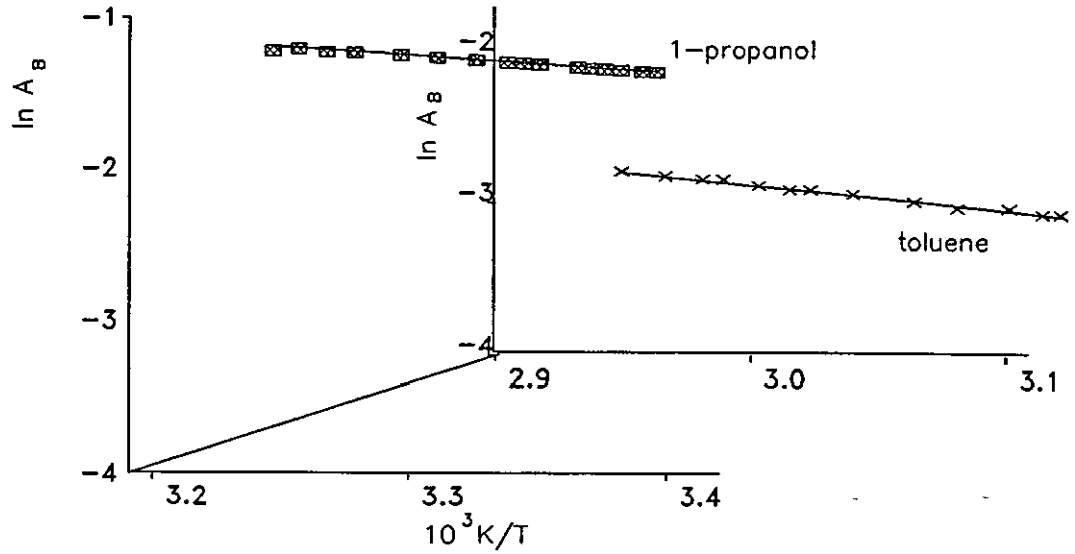

Figure 3.4. Vant Hoff isochores for n-propyl NOSI2 in 1-propanol and toluene.

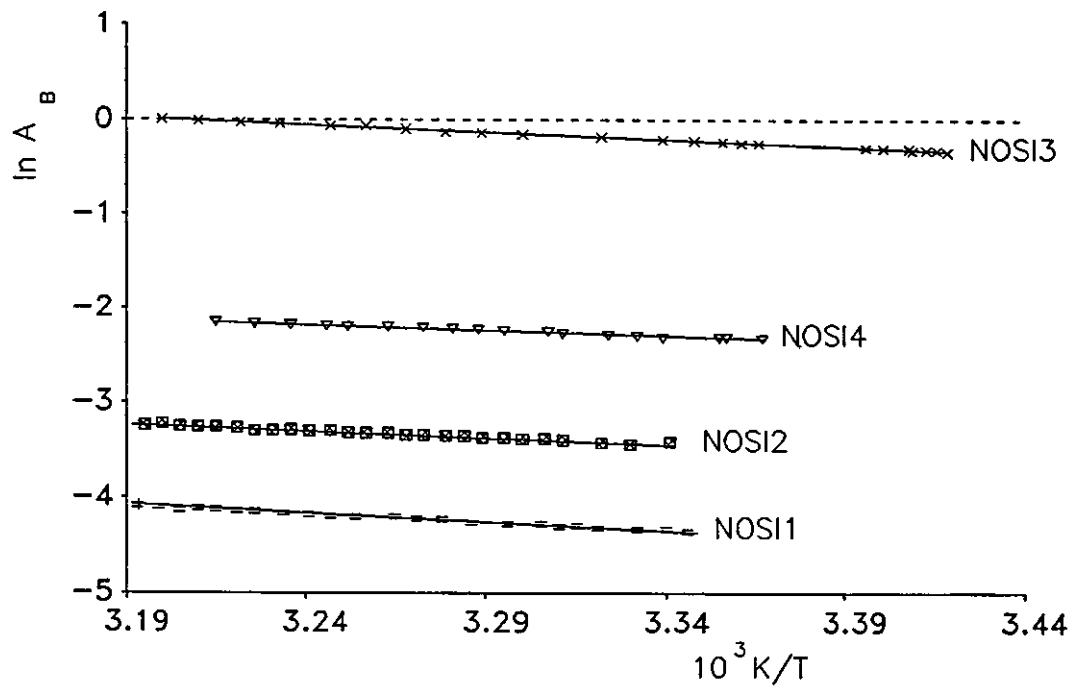

Figure 3.5. Vant Hoff isochores for NOSI1-4 in 1-propanol.

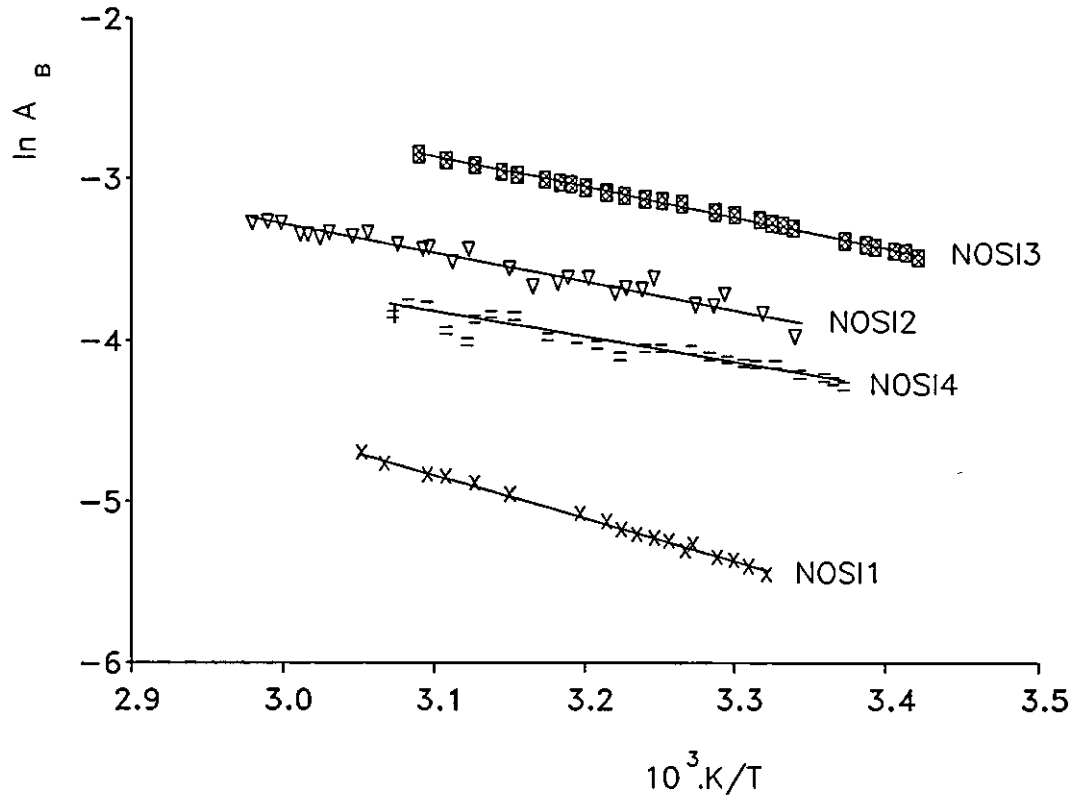

Figure 3.6. Vant Hoff isochores for NOSI1-4 in toluene.

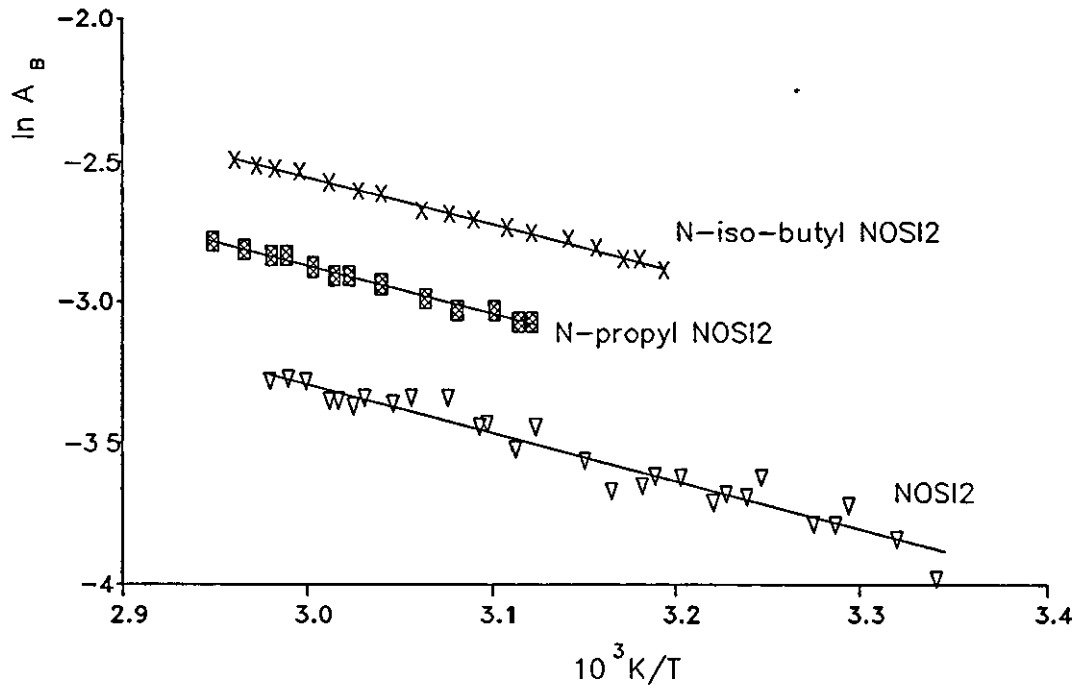

Figure 3.7. Vant Hoff isochores for the n-alkyl NOSI2 compounds in toluene.

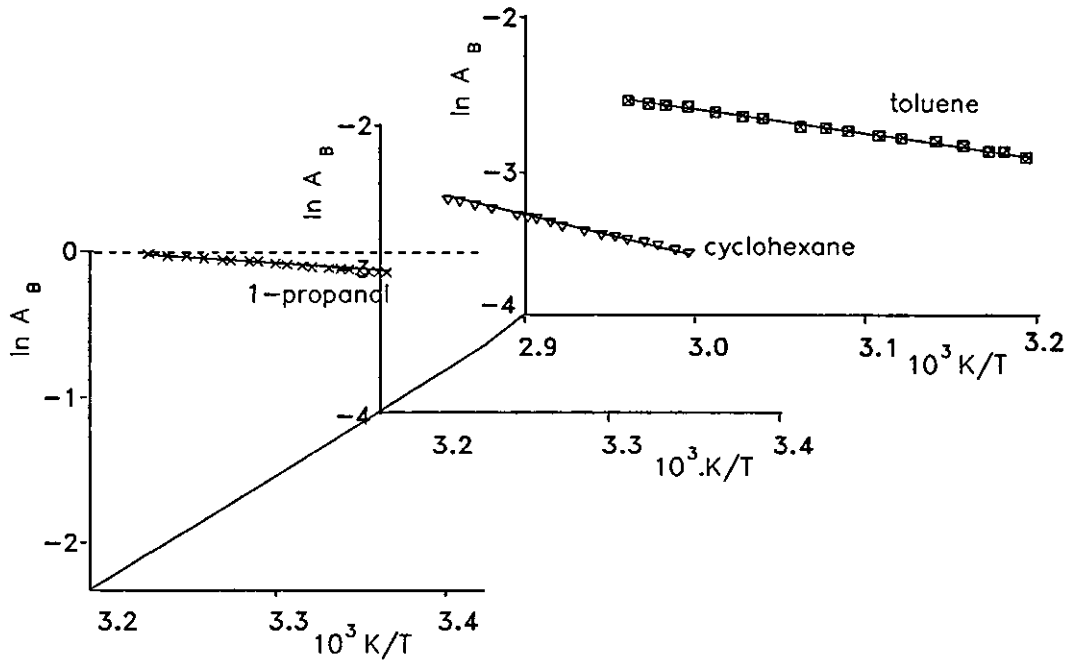

Figure 3.8. Vant Hoff isochores for n-iso-butyl NOSI2 in different solvents.

Absorption measurements at the probe wavelength were made over a range different temperatures and were recorded as the thermally equilibrated absorbance due to the B-form. From before a plot of $\ln A_B$ against $1/T$ should yield a straight line if the overall conversion to the B-form is small enough with respect to the A-form. If conversions are too high then curvature will occur in these plots. From the gradients of these graphs values of ΔH° for the equilibrium between the A-form and the B-form can be obtained. These graphs were plotted for all of the NOSI systems studied and are shown in figures 3.4-3.8.

3.3. Results and discussion.

3.3.1. The thermal fade reaction kinetics.

NOSI1-4, n-iso-butyl NOSI2 and n-propyl NOSI2, were investigated in this study.
The value of E_a, $\Delta H^{\circ\ddagger}$ and $\Delta S^{\circ\ddagger}$ for the thermal reverse reactions were determined for NOSI2, n-propyl NOSI2 and n-iso-butyl NOSI2 in toluene and the rate of the thermal reverse reaction was determined for all three of these compounds at 294K. In the case of all of the NOSI compounds for which the thermal fade kinetics have been measured only first order kinetics have been observed, these particular results are not necessarily in conflict with of the results of other authors [6,7], since using the method described above any faster component with a small contribution to the overall kinetics would not have been

observed. However, no faster component has been observed by us for these compounds even using the faster data collection available with flash photolysis. The results of these experiments are given in tables 3.1 and 3.2.

It has been observed that the rate of the thermal reverse reaction is slowed down by the addition of larger substituents on the indoline nitrogen [8]. It has been one of the aims of the present work to determine the reason for this effect. The present results confirm the finding that the addition of a larger alkyl chain at the indoline nitrogen does indeed slow down the thermal reformation of the B-form, this is clearly seen for NOSI2 and the n-propyl and n-iso-butyl substituted compounds from the results in table 3.1. The rate of the thermal reverse reaction is slowest for the n-iso-butyl derivative the next slowest is for the n-propyl derivative and the fastest is for the n-methyl compound NOSI2 itself. This effect could be due to the rotation of the molecule being hindered either by interaction of the longer side chain with the solvent or by steric hindrance to rotation caused by interaction with the other groups on the oxazine part of the NOSI molecule or by both of these effects. The stability of the transition state relative to the B-form stability will effect the energy barrier between the B-form and the A-form and this in turn will effect the rate of reformation of the A-form, however changes in the relative stabilities of these different transients in the NOSI thermal fade reaction upon changing either solvent or substituent are difficult to predict. If the observed trends in the rates of the reverse reaction for the n-alkyl NOSI2 compounds were caused only by solvent interactions with the side chain hindering the isomerisation process, then it would be expected that the values of $\Delta H^{o\#}$ would be larger for the compounds with the longer n-alkyl groups. However the values obtained for the n-alkyl NOSI2 compounds are given in table 3.2 and are very similar to one another. It is therefore unlikely that the interaction of the side chain with the solvent molecules is the main factor affecting the potential energy diagram and the rate of the thermal reverse reaction. It is however possible that the molecule has to adopt a certain orientation prior to the isomerisation for which the longer n-alkyl side chains are moved out of the way of the groups on the oxazine half of the molecule before the isomerisation proceeds. Such a specific orientation requirement may be the reason for the differences in the values of $\Delta S^{o\#}$ for the different molecules seen in table 3.2. These values of $\Delta S^{o\#}$ have been determined from the intercept of the graphs shown in figure 3.2 at 0K. Noticeable from this is the increasingly negative value of $\Delta S^{o\#}$ for NOSI2 series as the n-alkyl group increases in size. This is consistent with compounds with larger side chains having more stringent orientation requirements prior to isomerisation along the ground state potential energy surface with the n-alkyl group moved

Table 3.1. Thermal fade reaction first order rate constants for several NOSI compounds in toluene.

Compound	k/s^{-1} Measured at 294K
NOSI1	0.27±0.015
NOSI2	0.077±0.004
NOSI3	0.044±0.002
NOSI4	0.099±0.005
n-propyl NOSI2	0.059±0.030
n-iso-butyl NOSI2	0.040±0.002

Table 3.2. $\Delta H^{o\#}$, $\Delta S^{o\#}$ and ϵ_a values for various n-alkyl derivatives of NOSI2 in toluene.

Compound	$\Delta H^{o\#}$ /kJ.mol^{-1}.	$\Delta S^{o\#}$ /J.K^{-1}.mol^{-1}.	E_a /kJ.mol^{-1}.
NOSI2	70.6±4	-16.6±6	73.2±4
n-Propyl NOSI2	69.3±4	-32.8±5	71.8±4
n-iso-butyl NOSI2	69.0±4	-37.6±5	71.6±4

out of the path of the rotating oxazine part of the molecule before isomerisation can occur. This implies that the transition state is a species that has the n-alkyl group and the oxazine in close proximity to each other.

The presence of the electron donating groups at the 6'-position slows down the thermal reverse reaction as can be seen by comparing the rate constants for NOSI1 with NOSI2, NOSI3, and NOSI4. It may be that the differences in the rates obtained for the compounds NOSI1-4 could be due to differences in the relative stabilisation of an intermediate in the thermal reverse reaction caused by the different electron donating powers of the 6'-group. The B-form isomers are expected to be more planar than any intermediates in the thermal

reverse reaction. This means that electron donation will stabilise the B-form isomers by delocalising the positive charge of the zwitterionic form. This stabilisation would not be as efficient for a non-planar transient because the Π-electron overlap would not be as good. This means that 6'-electron donation will increase the activation barrier to the reaction by stabilising the B-form relative to the transition state.

3.3.2. NOSI thermochromism.

Values of ΔH° were obtained from slopes obtained from plots of $\ln A_B$ against $1/T$ these are given in table 3.3 These plots are shown in figures 3.4-3.8.

Table 3.3 can be summarised as follows:

ΔH° increases as the solvent polarity decreases for NOSI1-4.

ΔH° decreases as the alkyl side chain size on the indoline nitrogen increases in both 1-propanol and toluene.

ΔH° decreases in the order NOSI1>NOSI3>NOSI2>NOSI4 in both 1-propanol and toluene.

It is not a trivial matter to assign the trends observed here to specific characteristics of the particular NOSI-solvent systems under investigation. This is because the values of ΔH° for the reaction are dependant upon the relative stability of both the A-form and the B-form. The absolute stability of both forms may be altered by changing either the solvent or the substituents. The above results are pictorially represented in figure 3.9.

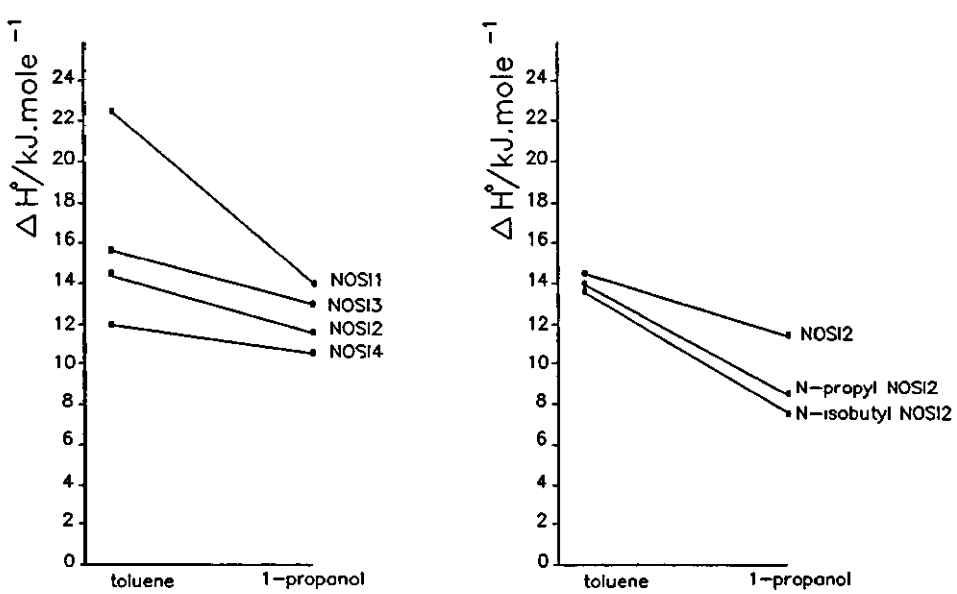

Figure 3.9. ΔH° values in different solvents for the different NOSI compounds studied.

Table 3.3. ΔH° values measured for several NOSI compounds in several solvents.

compound	Solvent	ΔH°/kJ.mol^{-1}.
NOSI1	Toluene	22.4±1
NOSI1	Propanol	14.0±2
NOSI2	Toluene	14.4±1
n-propyl NOSI2	Toluene	14.0±1
n-iso-butyl NOSI2	Toluene	13.6±1
n-iso-butyl NOSI2	Cyclohexane	21.4±2
n-iso-butyl NOSI2	Propanol	7.6±1
n-propyl NOSI2	Propanol	8.5±1
NOSI2	Propanol	11.6±1
NOSI4	Propanol	10.6±1
NOSI3	Propanol	12.9±1
NOSI4	Toluene	12.0±1
NOSI3	Toluene	15.5±1

The 6'-substituents increase in basicity with the following order; H < indoline < 2-methyl-indoline < piperidine.

i.e the 6'-group basicity varies for each compound in the order; NOSI1 < NOSI2 < NOSI4 < NOSI3.

The values of ΔH° are more spread out for the compounds NOSI1-4 in toluene than in

1-propanol as can clearly be seen from figure 3.9. In the case of NOSI1 upon changing the solvent from toluene to 1-propanol the value of ΔH° drops by 8.4 kJ.mol^{-1}. The values of ΔH° change by the following amounts for the other compounds upon changing the solvent from toluene to 1-propanol; NOSI2 (2.8 kJ.mol^{-1}), NOSI3 (2.6 kJ.mol^{-1}), NOSI4 (1.4 kJ.mol^{-1}). These latter compounds have electron donating 6'-substituents and can therefore delocalise any charge separation due to the zwitterionic form by allowing the presence of another, less charge separated zwitterionic form for which the positive charge is on the 6'-substituents' nitrogen, see figure 3.10 and 3.11. NOSI1 cannot delocalise the positive charge in the same way and will therefore be more charge separated. Hence although these NOSI molecules are presumed to be mainly quinoidal in nature the extra charge separation on NOSI1 will lead to a larger drop in the value of ΔH° upon changing solvent from toluene to 1-propanol than is seen for the other three compounds. The value of ΔH° is determined by the relative stabilities of the A-form and the B-form, the A-form does not have the B-forms ability to form a zwitterionic form, this means that the B-form will always tend to be more charge separated than the A-form and will in general be more stabilised in a more polar solvent.

The presence of an alkyl side chain on the indoline nitrogen relatively stabilises the B-form of the molecule. The stabilisation is more pronounced in 1-propanol than in toluene as can be seen from figure 3.9, however the reasons for this trend are not clear.

Only a few results have been obtained by other authors for the compound NOSI1 and these are given below in table 3.4:

Table 3.4. Results obtained by other authors for NOSI1.

Author	solvent	E_a/kJ.mol^{-1}.	ΔH°/kJ.mol^{-1}.
Kholmanskii[9]	ethanol	35	
Pottier [1,]	ethanol	69.3	
	toluene	56.7	
Chu [1,10]	ethanol	82.5	18
	ethanol	86.1	22.7

Although there are differences in the choice of solvent and compound for the values of E_a and $\Delta H°$ obtained by other authors and those values obtained in the present study, it can be commented upon that the present values are similar to values obtained by other authors for similar systems.

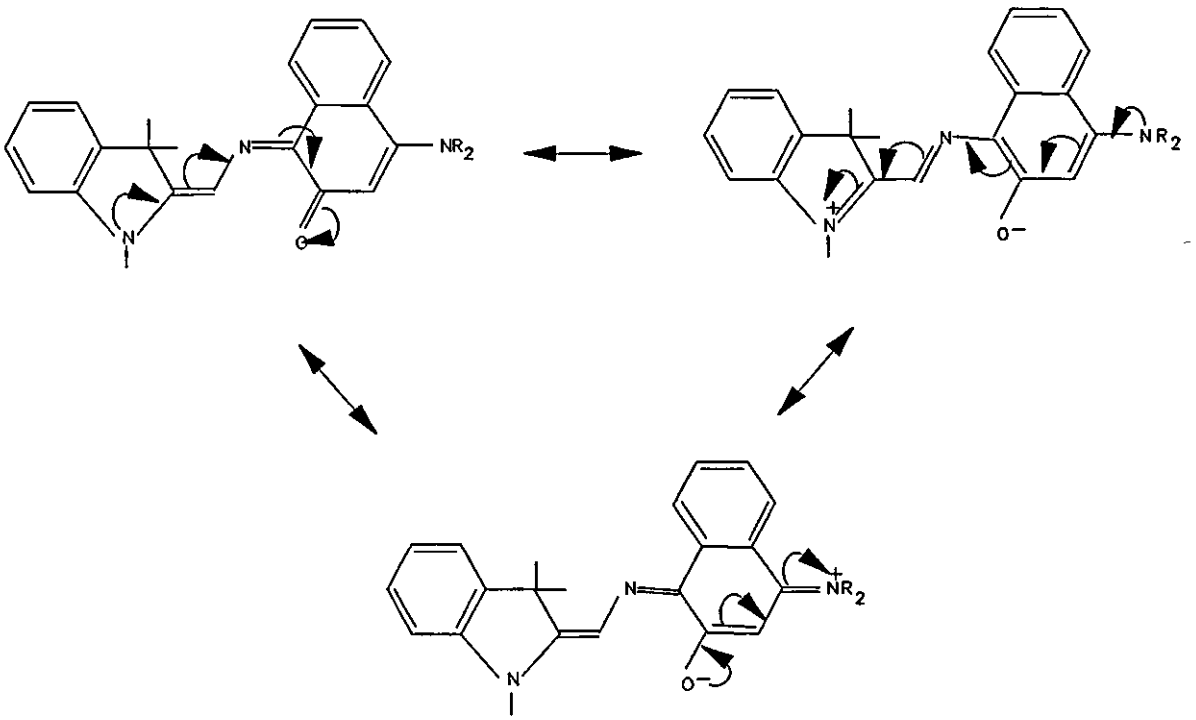

Figure 3.10. The resonance forms available to the NOSI2-4 B-forms.

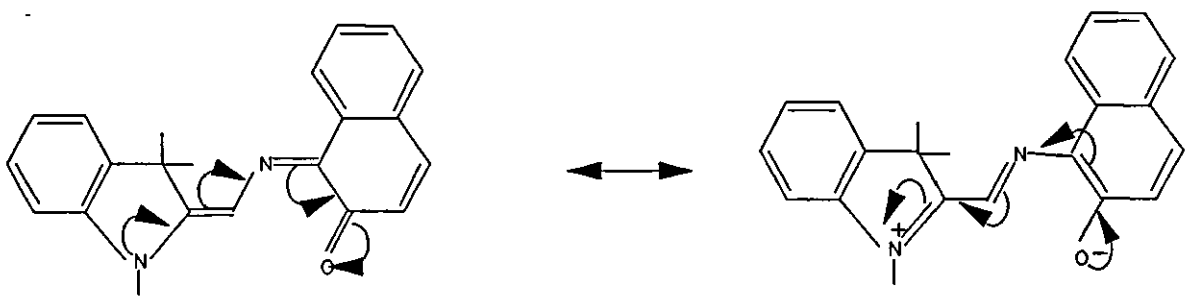

Figure 3.11. The resonance forms available to the NOSI1 B-form.

Chapter 3 References.

1. N.Y.C. Chu, Can. J. Chem. 61, 1983, 300.
2. P.W. Atkins, Pysical Chemistry, 3rd Ed. ISBN 0-19-855186-X, 1988, 221.
3. P.W. Atkins, Pysical Chemistry, 3rd Ed. ISBN 0-19-855186-X, 1988, 750.
4. F. Wilkinson, Chemical Kinetics and Reaction Mechanisms, Van Nostrand Reinhold, ISBN 0-442-30248-7, 1980, 95.
5. C.B. McArdle, Applied Photochromic Polymer Systems, Blackie, ISBN 0-412-02971-5, 1992, 76.
6. E. Pottier, R. Dubest, R. Guglielmetti, P. Tardieu, A. Kellmann, F. Tfibel, J. Aubard, Helv. Chim. Acta. 73, 1990, 303
7. A. Kellmann, F. Tfibel, R. Dubest, P. Levoir, J. Aubard, E. Pottier R. Guglielmetti, J. Photochem. Photobiol. A. Chem. 49, 1983, 63.
8. C.B. McArdle, Applied Photochromic Polymer Systems, Blackie, ISBN 0-412-02971-5, 1992, 52.
9. A. S. Kholmanskii, K.M. Dyumaev, Dokl. Akad, Nauk, SSSR, 303, 1988, 1189.
10. H. Durr, H. Bouas-Laurent, Elsevier, ISBN 0-444-87432-1, 1990, 504.

CHAPTER 4

DETERMINATION OF Φ_Δ FOLLOWING DIRECT EXCITATION AND FOLLOWING TRIPLET ENERGY DONATION.

Chapter 4. Determinations of Φ_A following direct excitation and after triplet energy donation, using nanosecond laser flash photolysis.

4.1. Introduction.

The photoisomerisation mechanisms of several NOSI compounds have been previously studied using both picosecond [1,2,3,4] and nanosecond [5,6] laser flash photolysis as well as using steady state irradiation [7,8]. The picosecond studies have led most authors to the conclusion that the photoisomerisation reaction occurs on the sub nanosecond timescale and therefore nanosecond laser flash photolysis cannot normally be used directly to probe transient states. However, the nanosecond pulsed laser studies on the compound NOSI1 by Kellmann *et al* [5] have suggested a microsecond rise time for the production of at least some of the B-form, this phenomenon has not been reported by any other authors. It has been suggested that the mechanism of B-form formation proceeds exclusively through an excited singlet state [1,2,9], this assumption was based on the absence of experimental data implicating any triplet state involvement in the overall reaction mechanism (i.e. no intermediate which can be assigned to a triplet-triplet absorption spectrum has been observed and the presence of oxygen has been reported to have no influence on the isomerisation process). In the case of the related nitro substituted BPSI's, the isomerisation reaction has been shown to occur at least in part via a triplet pathway [10], although no evidence for such a pathway has been found for BPSI and NPSI molecules without a nitro substituent, under conditions of direct excitation by sub-picosecond pulses at 308nm [11,12,13]. This has Lead the authors of these studies to propose a predominantly singlet route for the unsubstituted BPSI isomerisation reaction.

The aim of the work described here has been to determine the values of Φ_A for the compounds NOSI1-4 and n-iso-butyl NOSI2 following direct U.V. excitation in a variety of solvent media and solid polyurethane matrices. It was also aimed at establishing whether NOSI photo colouration can occur via an excited triplet pathway following triplet energy donation and if it can, with what yield.

The energy of the lowest energy NOSI triplet state has also been determined in this series of experiments by using triplet energy donation from a series of donor molecules of varying triplet energy.

4.2. Experimental.

4.2.1. Determination of Φ_A following direct excitation.

Values of Φ_A can easily be determined for most NOSI compounds simply by measuring the conversion to the B-form as a function of the exciting light intensity. A schematic diagram of the apparatus which was used here to determine these values of Φ_A is shown in figure 4.1. The exciting light source was a pulsed nanosecond Q-switched Nd/YAG laser operating in the third harmonic producing laser light at 354.7nm with a pulse duration of ~25ns.

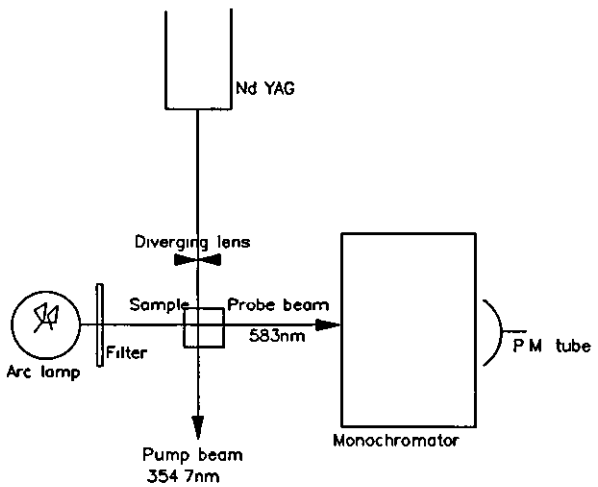

Figure 4.1. The apparatus used in these nanosecond flash photolysis studies.

The laser intensity incident upon the sample was varied by successively placing filters made from sodium nitrite solutions of different concentrations, between the laser and the sample. The percentage of light being transmitted by each of these filters at 354.7nm was measured using a PU8800 UV/VIS spectrophotometer operating in transmission mode. The conversion to the B-form was determined by measuring the absorbance change at the peak maximum wavelength for the NOSI B-form in that solvent. For example when studying NOSI2 in toluene the probe wavelength used was 583nm, and the molar decadic absorption coefficient used in the calculation of Φ_A was 48000 $dm^3.mol^{-1}.cm^{-1}$ (7). The probe beam was produced by an arc lamp source illuminating the sample at right angles to the laser excitation source. The U.V. and near visible light produced by the arc lamp was filtered out using a 480nm cut off filter. This prevented the absorption of any of the probe light by the A-forms of the photochromic compounds being studied avoiding any photoconversion to the B-form due to the probe beam. The A-forms of all of the photochromics being investigated stop absorbing light at wavelengths above 430nm.

The absolute laser intensity at the sample was determined for each of the sodium nitrite filters used in terms of the amount of benzophenone triplet that was initially produced following flash photolysis of a solution of benzophenone in benzene. This actinometer solution was irradiated using the same sample geometry as was used for NOSI sample. The benzophenone actinometer solution used in each case had an absorbance matched to that of the NOSI sample solution. The benzophenone triplet absorbance change at zero time were measured at 530nm, and the extent of conversion could then be calculated using a molar decadic absorption coefficient for this triplet state of 7225 $dm^3.mol^{-1}.cm^{-1}$ and a quantum efficiency of the triplet state formation of unity [14]. If the conversion to the triplet state is kept sufficiently low and the solution is thoroughly deoxygenated either by nitrogen purging or repeated freezing to 77K, followed by evacuation to $\sim 5x10^{-7}$ bar, then the benzophenone triplet state in benzene should decay with a first order lifetime of 6 microseconds [14]. The absorption at zero time can then be established from the amplitude of this decay determined from a first order fit to the absorption data with time using a least squares fitting routine.

Plotting the absorbance change due to the formation of the NOSI B-form against the absorbance due to the formation of benzophenone triplet state for each of the laser intensities used will then yield a straight line if the photochemical conversions involved are kept sufficiently low as shown in figure 4.2. If the photochemical conversion are too high then a significant proportion of the exciting photons will be absorbed by the photochemical products and curvature in the plot will result. It is a simple matter to ensure that the extent of photochemical conversion is low enough by plotting both the B-form absorption and benzophenone triplet state absorption against the percentage of laser light incident upon the sample. If both of these plots are linear then Φ_A can be determined from the slopes of these graphs or from the slope of a plot of the absorbance change due to the formation of the NOSI B-form against the absorbance due to the formation of benzophenone triplet state.

The value of Φ_A is evaluated for each particular photochromic system being investigated using equation 4.1.

$$slope = \frac{\epsilon_B \Phi_A}{\epsilon_{std} \Phi_{std}} \qquad 4.1$$

where;

ϵ_{std} is the benzophenone triplet extinction coefficient, and Φ_{std} is the quantum efficiency of benzophenone triplet formation, all other terms have previously been defined (see equations 2.4).

Once the value of Φ_A has been reliably determined for a particular NOSI system using benzophenone in benzene as an actinometer solution, it is then possible to use this NOSI system as an actinometer solution to evaluate Φ_A values for other similar systems. Using a NOSI system as an actinometer has the advantage that the absorption due to the formation of the NOSI B-form following nanosecond excitation rises to a plateau within the excitation pulse and remains constant for several seconds.

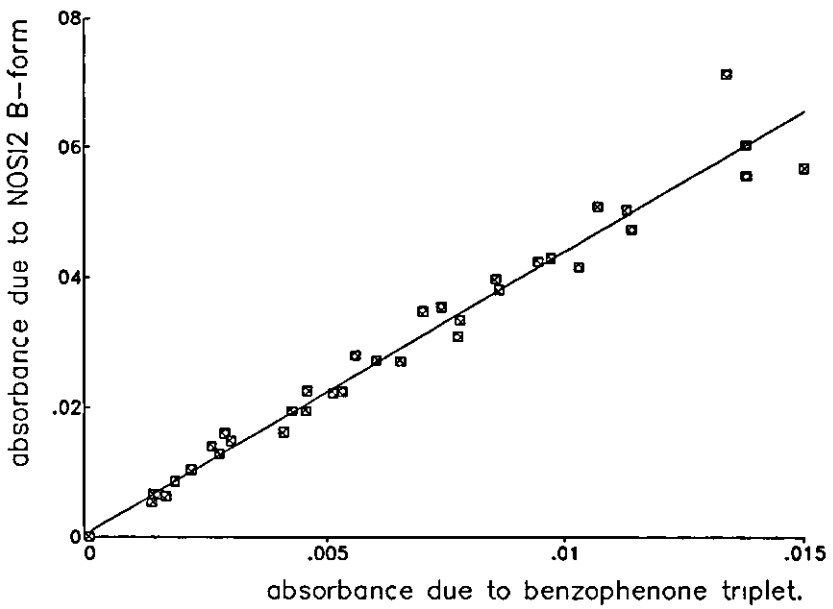

Figure 4.2. The absorbance change due to the formation of the NOSI2 B-form plotted against the absorbance due to the formation of benzophenone triplet.

The photochromic compounds NOSI1-4, n-iso-butyl NOSI2 and a flugide, Aberchrome 540(Tm), were dissolved in various organic solvents to give solutions having an absorbance of around 0.3 at 354.7nm in a 1cm pathlength cell. The benzophenone was dissolved in benzene to give a solution having the same absorbance at 354.7nm as the photochromic solutions. Aberchrome 540(Tm) is quoted, by the manufacturers, as having a quantum efficiency of colouration of 0.2 when excited at between 310-370nm in toluene [15], and was therefore used to check the accuracy of this method of Φ_A determination.
The photochemical yields of the NOSI2 and n-iso-butyl NOSI2 B-forms were also determined in several polyurethane matrices containing different proportions of cross

linking groups in the ploymer chains. The more cross linking groups in the polymer the "harder" the polyurethane. The property used to gauge the "hardness" of each polyurethane sample was its glass transition temperature. The higher this value the "harder" the polyurethane. These solid samples were comprised of a 1mm thick sample sandwiched between two optical quality quartz windows. In order for the laser induced B-form absorptions to be measured for the solid samples they had to be placed with an orientation of 45° to the incidence of each of the excitation and probe beams, with the probe passing through the laser excited area on the sample. The sample geometry used in these solid matrix studies had to be matched by that of the actinometer. The actinometer chosen was NOSI2 in toluene in a 1mm pathlength quartz cell. The solid samples and the actinometer solutions all had absorbances of 0.2.

For the compounds NOSI2-4, n-iso-butyl NOSI2 and Aberchrome 540(Tm), the efficiency of the photochemical closure reaction has been shown to be small compared with the value of Φ_Δ [7,15,16], and as such its contribution to the overall photocolouration process has been neglected here. In the case of NOSI1 the closure reaction efficiency has not been determined, however it has been assumed that its contribution in comparison with the forward isomerisation yield will negligible as was found to be the case with the other compounds being studied here. In any event the reverse photo-chemical reaction can be safely ignored if the degree of conversion to the coloured form is kept low, since under these conditions effectively none of the exciting light is absorbed by the B-form. This criterion is met when working under conditions of linearity between photochemical conversion and incident laser intensity. The use of nanosecond laser photolysis makes the contributions to B-form depletion from the thermal closure reaction negligible. This is because the thermal reverse reaction has a lifetime occurring on the order of seconds for most NOSI systems studied here [7] whereas the absorption data collection times used here was generally of the order of 20 microseconds.

4.2.2. Triplet sensitization studies.

4.2.2.1. The quenching rate constant k_q for triplet energy donors quenched by the NOSI A-form and the determination of the NOSI2 triplet energy.

Photochromic NOSI compounds can undergo photochemical conversions to the B-form via a sensitized triplet pathway (17). Experiments using triplet energy donation to the NOSI1 A-form by a series of triplet energy donors, with various triplet energies, have already established that the triplet energy of this compound is ~212 kJ mol^{-1} (17).
The aim of the present work is to establish the lowest triplet energy of the NOSI2 A-form in toluene.
In order to achieve this goal the following theory and method has been applied.

In the absence of a reaction which can repopulate the donor triplet state then the changes in the population of available donor triplet states which occur with time are either caused by interactions with quencher molecules or by the states natural decay with a rate constant k_d. The rate of these processes is given by equation 4.2.

$$-\frac{d[D_t]}{dt} = k_d[D_T] + k_q[D_T][Q]$$

$$-\frac{d[D_T]}{dt} = (k_d + k_q[Q])[D_T] = k_{obs}[D_T]$$

$$k_{obs} = k_d + k_q[Q] \qquad 4.2$$

If $[Q] >> [D_T]$ then k_{obs} will be a pseudo first order rate constant, where $[D_T]$= the concentration of triplets available to donate their energy to the quencher molecule and k_d = the natural lifetime of the donor triplet state.

The First stage in the process to determine the NOSI2 A-form triplet energy is the measurement of the observed first order quenching rate constant k_{obs} for each particular triplet energy donor over a range of NOSI2 concentrations. The method used to achieve this is described below:
Solutions containing mixtures of the NOSI2 A-form and the triplet energy donor were made up in toluene. The absorbance of the ground state of the triplet energy donors in these solutions was made to be ~1 at 354.7nm. This absorbance was kept constant in the determination of each value of k_{obs} for the particular donor/acceptor system being investigated. The absorbance due to the NOSI2 A-form was then varied between 0.1 and 1 at the same wavelength. These absorbance values correspond to a quencher concentration

range of $1.7x10^{-5}$ to $1.7x10^{-4}$ mol.dm^{-3}. These solutions were thoroughly deoxygenated by repeated freezing to 77K, followed by evacuation to ~$5x10^{-7}$ bar.

The apparatus used in this series of experiments was the same as shown in figure 4.1. These solutions were irradiated with the 354.7nm excitation pulse available from the Nd-YAG laser and the absorption changes were probed by light from an arc lamp which was again filtered out below 480nm. The laser intensity reaching the sample was reduced sufficiently to prevent second order effects occurring in the kinetics of the triplet donor-acceptor system being studied and ensuring that $[Q] >> [D_T]$. This was achieved as before by placing a sodium nitrite filter in the path of the excitation beam before the sample. The first order kinetics occurring for the natural decay of the donor triplet alone were measured in order to obtain the first order lifetime of the donor triplet state and from this a value of k_d. The solutions of NOSI2/donor mixtures were then irradiated and the kinetics of the sensitized B-form production were established for each NOSI2 concentration used. In each case the sensitized absorption rise due the B-form followed the kinetics of the donor triplet decay. The sensitized B-form absorption rise kinetics found in this way could then be used to determine values of k_{obs} by fitting the rise data to a first order model using a least squares fitting routine. A typical trace which shows the time dependence of the sensitized first order B-form absorption rise is shown in figure 4.3. For comparison a typical NOSI2 absorption rise following direct excitation is also shown. This clearly shows the absorption rise kinetics seen for the sensitized merocyanine formation and the lack of any absorption changes occurring after the prompt rise following direct excitation of a NOSI2 solution in the absence of triplet energy donation.

The values of k_{obs} so determined were then used to obtain the value of k_q for that particular donor acceptor mixture. This was done by plotting the measured value of k_{obs} against the corresponding NOSI2 quencher concentration. This should give a straight line from which the value of k_q can then be established from the slope. An example of this type of plot is shown in figure 4.4.

Values of k_q were determined in this way for a number of triplet energy donors, having a wide range of triplet energies which were again quenched by the NOSI2 A-form. This gave a series of k_q values corresponding to different triplet energies. A graph of k_q plotted against the triplet donor energy could then be plotted as shown in figure 4.5 the values of k_q determined for the different triplet energy donors are summarised in table 4.1.

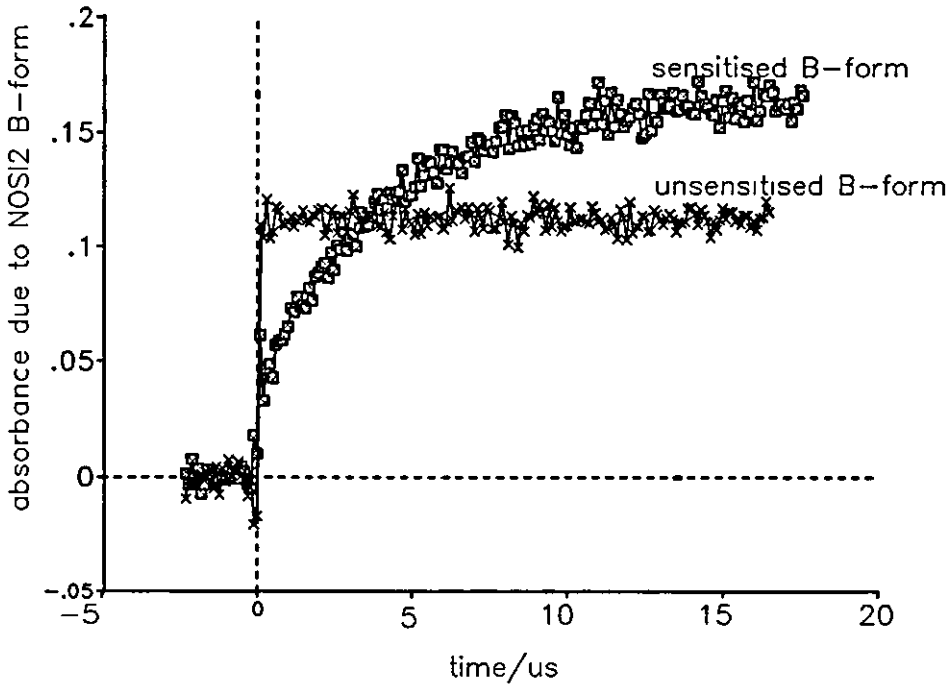

Figure 4.3. Absorption rises for two optically matched NOSI2 solutions, one directly excited and the other excited by triplet energy donation.

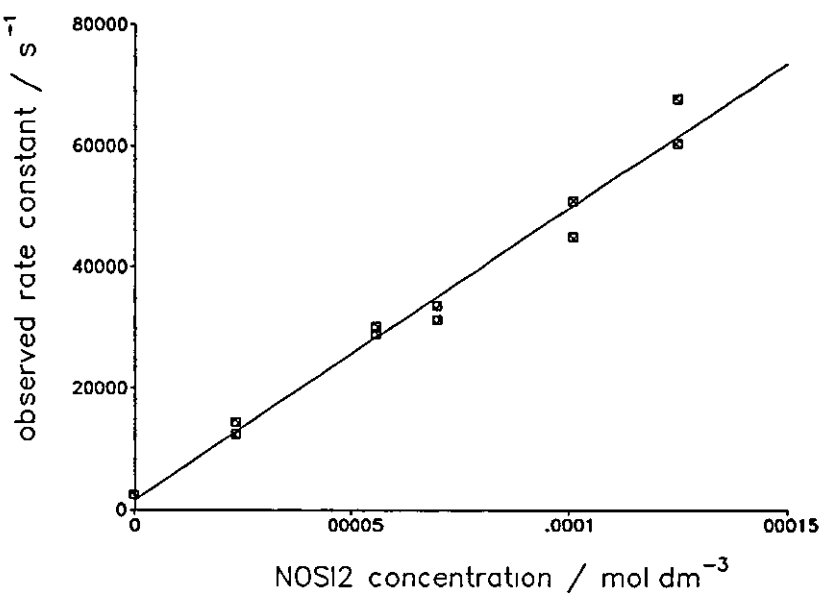

Figure 4.4. The observed quenching rate constant for the benzil triplet quenched by NOSI2 plotted against the NOSI2 concentration.

From this graph of k_q against donor triplet energy it was then possible to estimate the NOSI2 A-form triplet state energy. The theory behind this is given below.

These changes in the value of k_q measured as a function of the triplet donor energy can now be interpreted [18]. The values of k_q which are determined for NOSI2 quenching triplet energy donors with triplet energies much greater than the NOSI2 triplet energy should be close to diffusion controlled. This is because in these cases the energy gap between the donor triplet energy and the NOSI2 triplet energy is too large for donation to occur in the opposite sense from the NOSI2 triplet state to the donor ground state. As the donor triplet energy is reduced and approaches triplet energy of NOSI2 it becomes possible for donation to occur from the NOSI2 triplet state to the ground state of triplet energy donor. Generally for this reverse donation to happen at room temperatures, the donor triplet energy cannot generally be more than 12 kJ.mol^{-1} in excess of the NOSI2 triplet energy. When the donor and acceptor triplet energies are within 12 kJ.mol^{-1} of each other this activation energy barrier can be overcome by the thermal energy contained within the system. The k_q values determined for donors having triplet energies sufficiently low for this back donation to occur, will be less than diffusion controlled because the reverse quenching processes become of significance and equation 4.2 now becomes:

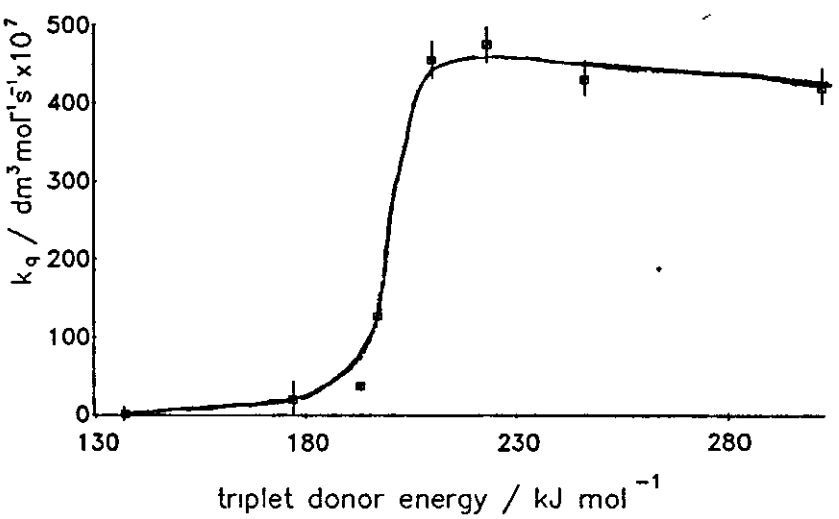

Figure 4.5. k_q values determined for NOSI2 plotted against the corresponding triplet donor energy.

$$-\frac{d[D_t]}{dt} = k_d[D_T] + k_q[D_T][Q] - k_q^R[D][Q_T] \qquad 4.3$$

Where k_q^R is the quenching constant of the reverse donation.

The measured value of k_q will therefore continue to fall as lower and lower donor triplet energies are employed and as the reverse donation process becomes more and more significant. The drop in the measured value of k_q will continue until the NOSI2 A-form

triplet state is no longer produced resulting in the effective cessation of sensitized B-form production. The donor triplet energies being employed at this point will probably be more than 12 kJ.mol^{-1} below the NOSI2 A-form triplet energy. The NOSI2 triplet state energy will be the energy that corresponds to the point halfway down the steeply sloping region of the graph in figure 4.5.

4.2.2.2. Determination of the yield of the NOSI B-form following triplet energy donation.

The efficiency of the B-form production occurring via the NOSI1-3 triplet states produced following triplet energy donation from the 2'-acetonaphthone triplet were determined by comparing the amount of NOSI1, NOSI2 and NOSI3 B-form produced by direct excitation with the conversions achieved following sensitization. In most instances the sensitized efficiencies were also determined by comparing the sensitized B-form conversion with the conversions to the benzophenone triplet state as described in section 4.2.1. The B-form yield of NOSI2 via the triplet state was also determined using para methoxy-acetophenone as the triplet energy donor.

For each NOSI system studied the absorbance change which follows photolysis that is caused solely by the sensitized B-form production, was plotted against the corresponding absorbance due to benzophenone triplet formation, or the absorbance due to the B-form produced following direct excitation, for a range of laser energies as described before in section 4.2.1. An example of such a plot is shown in figure 4.6.

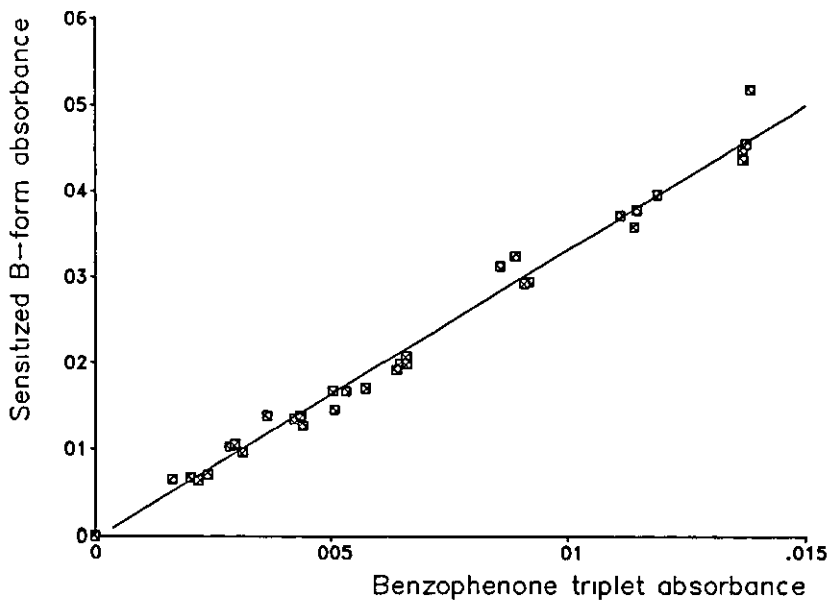

Figure 4.6. The sensitized NOSI2 B-form absorbance plotted against the benzophenone triplet state absorbance for a range of laser intensities.

The equation used to calculate the sensitized yields is given below. This equation will work for NOSI/donor solutions and standard solutions that have optically matched absorptions.

$$\Phi_A^S = \frac{A_B^S \Phi_{std} \epsilon_{std} I_{std}}{A_{std} \Phi_T f_i \epsilon_B I_S} \qquad 4.4$$

$\frac{A_B^S}{A_{std}}$ is the absorbance due to sensitized B-form formation divided by the actinometer absorbance and can be simply be obtained from the slope of a graph such as the one shown in figure 3.6 as long as the graph is behaving linearly.

Φ_T is the triplet yield of the triplet energy donor,

Φ_A^S is the B-form yield from the A-form triplet state,

f_i is the fraction of triplets intercepted,

$$f_i = \frac{k_q[Q]}{k_d + k_q[Q]} \qquad 4.5$$

I_s is the proportion of exciting light absorbed by the sensitizer alone in the solution.

I_{std} is the proportion of exciting light absorbed by the actinometer solution.

The other terms have previously been defined.

These calculations of sensitized B-form formation efficiency used a value for the quantum efficiency for the para methoxy-acetophenone triplet formation of unity [19] and a value for 2'-acetonaphthone triplet formation of 0.84 [14].

4.3. Results and discussion.

4.3.1. k_q values and the triplet energy of NOSI2.

Table 4.1 gives the values of k_q obtained for the different triplet energy donors used in this series of experiments quenched by different NOSI compounds. The work described here demonstrates that sensitization of a triplet state can indeed be brought about for several NOSI A-form compounds and further that its formation can result in the production of the B-form. It was established that in the case of the sensitization studies using 2'-acetonaphthone, the rate of decay of the 2'-acetonaphthone triplet was the same as the rate of production of the NOSI2 B-form. This suggests that the rate of formation of the NOSI2 coloured form resulting from diffusion of triplet energy donors and acceptors in solution is much slower than the rate of NOSI2 triplet decay.

Table 4.1. Values of k_q obtained for several NOSI compounds quenching various triplet states in toluene.

Triplet energy donor	Triplet donor energy \kJ.mol^{-1}	Quenching constant (k_q)\dm^3.mol^{-1}.s^{-1}	Photochromic
2'-acetonaphthone	246	5.03±0.25 x10^9	NOSI1
p-methoxy-acetophenone	301	4.22±0.21 x10^9	NOSI2
2'-acetonaphthone	246	4.29±0.2 x10^9	NOSI2
Benzil	223	4.75±0.2 x10^9	NOSI2
9-fluorenone	210	4.55±0.2 x10^9	NOSI2
1,2 benzanthracene	197	1.26±0.06 x10^9	NOSI2
Benz[ghi]perylene	193	0.36±0.02 x10^9	NOSI2
Anthracene	177	0.2±2 x10^9	NOSI2
Zinc Tetraphenyl -porphine	137	3±3 x10^5	NOSI2
2'-acetonaphthone	246	5.47±0.27 x10^9	NOSI3

The lowest triplet energy of the NOSI2 A-form was found to be less than 210 kJ mol^{-1} but greater than 193 kJ mol^{-1}. Other workers have determined the triplet energy of NOSI1 in toluene to be 212 kJ mol^{-1} [17]. This energy is probably most influenced by the naphthoxazine part of the molecule, since the two parts of the molecule are largely isolated by the spiro linkage. The triplet energy of the indoline part of the molecule would be expected be more in line with those of aniline or indole derivatives which have triplet energies in the region of 300 kJ mol^{-1} [14].

The largest values of k_q determined here for the compounds NOSI1, NOSI2 and NOSI3 in toluene were those values lying on the plateau region of the graph of k_q plotted against the donor triplet state energy. These values were between $4.2x10^9$-$5.5x10^9$ $dm^3.mol^{-1}.s^{-1}$. The diffusion controlled rate constant in toluene is quoted as $1.1x10^{10}$ $dm^3.mol^{-1}.s^{-1}$ as calculated from the Smoluchowski-Stokes-Einstein equations [19]. The fact that the k_q values obtained here are around half the diffusion controlled value merely suggests that not every collision that occurs is effective at transferring the triplet energy.

4.3.2. Determination of Φ_A following direct excitation and following triplet energy donation.

The values of Φ_A obtained in this study are summarised below in tables 4.2-4.4. It is interesting to note the differences between the present values of Φ_A measured in toluene using 354.7nm excitation and those measured previously in toluene with 352nm line from a krypton ion CW laser [7]. The yields for NOSI1 and NOSI4 are the same within the error of the two experiments, however the yields for NOSI2 and NOSI3 are very different. The two excitation wavelengths employed in the two studies were different to one another by less than three nanometers and it is therefore unlikely that this factor is the cause of the large discrepancies between the measured values of Φ_A. It must be noted that more individual parameter measurements are required with the CW laser method, these parameters being the B-form thermal fade rate, the incident laser energy, and the A-form and B-form absorption values. Of these parameters the most uncertain is the rate constant of the thermal fade reaction. Several factors may influence the rate of fade of the B-form one of these was found to be the presence of impurities in the solution being investigated due to photodecomposition products of the NOSI compound itself. The fade rate of a solution of NOSI2 B-form in toluene nearly doubled upon the addition of 1-2% by volume of an equimolar solution of NOSI2 photodegraded by extended exposure to U.V. light. In this way the presence of a small amount of photo-decomposition products could effectively halve the measured value of Φ_A. The extent to which this will effect the results obtained

by steady state irradiation is to some extent an unknown, because it is dependant upon several factors all which will be different for each particular NOSI system being studied. If the compound under investigation is resilient to prolonged U.V. irradiation then fewer decomposition products will form during the course of data acquisition and the fade rate will be only slightly altered. Also if the compound has a large rate constant for the fade reaction then the time required to achieve the photostationary state for each laser intensity used is reduced and the total U.V. dose received by the sample is therefore less. Again this will result in fewer decomposition products forming. As previously stated the worst agreement between the two data sets occurs for NOSI2 and NOSI3, of the four compounds studied these two have the smallest B-form fade reaction rate constants. The fact that the colouration efficiency of Aberchrome 540(Tm) measured in the present study is the same as that quoted by the manufacturers gives more confidence in these newer results than those obtained by steady state irradiation. It has been reported by Boule et al (16) that the reaction scheme of Aberchrome 540(Tm) is more complicated than the manufacturers initially claimed, since after prolonged irradiation the measured efficiency of the ring closure reaction decreases. Boule did find that initially the conversion to the coloured form with photon flux is linear up to 10% conversion and that the light intensities so derived are consistent with those obtained with other chemical actinometers. Hence if the Aberchrome solutions are used for a single Φ_A determination and the extent of conversion to the ring closed form is less than 10%, then there is no reason to believe that the quantum efficiencies measured for Aberchrome(Tm) are unreliable. In the present study the maximum conversion to the ring closed form was always less than 10% and fresh solutions were employed for each determination. Hence the value of Φ_A measured should be the same as the value quoted by the manufacturers (15).

It must be noted that the only doubt in the steady-state studies (7) lies with values of Φ_A measured using steady state irradiation and not with the extinction coefficients and efficiency ratios obtained using the Fischer method and used in the present study in order to calculate values of Φ_A. These values did not require the measurement of the thermal fade reaction rate constant and are therefore not subject to the same type of errors, also the total UV dose received by the sample is much less, since the extent of conversion to the B-form was measured for a single photostationary state rather than for several photostationary states as was the case with the determination of Φ_A values. Therefore the effect of the photo-decomposition products is not expected to have had a significant effect on the measured values of ϵ_B.

Table 4.2. Φ_A values obtained for several NOSI systems following direct excitation and following triplet energy donation.

Photochromic	Solvent	Φ_A	$\epsilon_B x10^{-3}$/ $dm^3.mol^{-1}.cm^{-1}$	Previously reported Φ_A values.
NOSI1	cyclohexane (degassed)	0.41±0.06	24@	-
NOSI1	cyclohexane	0.43±0.06	24@	-
NOSI1	ethanol	0.24±0.04	51@(7)	0.26#,0.44(8)
NOSI1	toluene	0.33±0.05	31@(7)	0.23±0.1(7), 0.43*
NOSI3	toluene	0.74±0.11	32@(7)	0.42±0.2(7)
NOSI2	toluene	0.64±0.1	48@(7)	0.2±0.1(7)
NOSI2	toluene (degassed)	0.60±0.09	48@(7)	
NOSI4	toluene	0.58±0.11	43@(7)	0.85±0.2(7)
NOSI2	cyclohexane	0.72±0.11	40@	-
Aberchrome 540(Tm)	toluene	0.20±0.04	8.2(15)	0.2(15)
2'-acetonaphthone / NOSI1	toluene	1.07±0.18	31@(7)	-
2'-acetonaphthone / NOSI3	toluene	0.98±0.15	32@(7)	-
2'-acetonaphthone / NOSI2	toluene	0.98±0.15	48@(7)	-
P-methoxy- aceto-phenone/ NOSI2	toluene	0.97±0.15	48@(7)	-

* Recalculated from the Φ_A value given by Kellmann et al (5) using the same values of ϵ_B for NOSI1 given in this table.

Recalculated using the Φ_A value given by Kellmann et al [5] for NOSI1 in methanol using the value of ϵ_B given in this table for ethanol solutions.
@ These values are given in chapter 2, tables 2.4-2.6.

Table 4.3. Φ_A Values for n-iso-butyl NOSI2 in various solvents.

Solvent	dielectric constant ϵ^e	Φ_A	$\epsilon_B x10^{-3}$ /$dm^3.mol^{-1}.cm^{-1}$
cyclohexane	2.0	0.70±0.10	42
toluene	2.4	0.67±0.10	47
benzene	2.3	0.62±0.09	50
acetonitrile	35.9	0.29±0.04	51
1-propanol	20.5	0.22±0.03	59
methanol	32.7	0.06±0.01	61

The values of ϵ_B used here are given in chapter 2, tables 2.4-2.6.

Table 4.4. The values of Φ_A determined for NOSI2 and n-iso-butyl NOSI2 in polyurethane matrices having varying "hardness."

Compound	Glass transition temperature of the polyurethane matrix/°C	Φ_A
NOSI2	45	0.11
n-iso-butyl NOSI2	33	0.17
n-iso-butyl NOSI2	45	0.11
n-iso-butyl NOSI2	>45	0.09

The values of ϵ_B used for the polyurethanes were 54000 $dm^{-3}.mol.cm^{-1}$ for NOSI2 measured at 606nm and 56000 $dm^{-3}.mol.cm^{-1}$ for n-iso-butyl NOSI2 measured at 605nm. These values are given in tables 2.4-2.6.

Evident from the present results is the much higher value of Φ_A, determined following direct excitation, for the compounds substituted with an electron donating substituent on the 6'-position of the oxazine ring, the highest of these being for NOSI3 which has a piperidine substituent at the 6'-position, see table 4.2. The measured quantum efficiencies decrease as the basicity of the 6'-substituents decrease, i.e. the efficiencies decrease in the order NOSI3 > NOSI2 > NOSI4 > NOSI1. Note that the methyl group on the 6'-indoline of NOSI4 most probably has the effect of forcing the 6'-substituent out of the plane of the oxazine ring thereby reducing its electron donating power compared with the unsubstituted 6'-indoline. This increase in Φ_A could be due to either of two reasons. The first of these is that the 6'-position on the oxazine ring is resonantly coupled to the C-O in the spiro linkage therefore electron donation here would result in an overall reduction in the C-O bond order thereby weakening the bond. If this is so then the step in the photoisomerisation where the C-O bond breaks would be more efficient. The other possible reason for the increase in Φ_A is that there is a transient structure in the isomerisation mechanism that is in some way affected by 6'-electron donation. Both of these possibilities can be investigated by fast spectroscopic methods such as the picosecond transient absorption spectroscopy (PTA) described in chapter 5. It is interesting to note that the above ordering in the values of the quantum efficiencies for the different NOSI molecules mirrors the ordering in the values of the B-form thermal fade rate constants at 294K, these values decrease in the order NOSI1 > NOSI4 > NOSI2 > NOSI3 [7]. Again in the thermal fade reaction this could be due to the 6'-electron donation hindering the step involving the C-O bond reformation or some relative stabilisation or destabilisation of another transient species.

In summary, electron donation at the 6' position of the oxazine ring assists photochemical ring opening and reduces the rate of thermal ring closure reaction occurring at room temperature. These two factors lead to higher photostationary B-form concentrations during U.V. exposure and therefore these compounds will give more colouration during steady state irradiation.

Changing the solvent from toluene to cyclohexane slightly increases Φ_A for NOSI2 B-form formation from 0.64 to 0.72. Changing the solvent from cyclohexane to toluene to ethanol reduces Φ_A of NOSI1 photo-colouration from 0.43 to 0.33 to 0.24 respectively, see table 4.2.

Solvent effects have been most extensively studied for n-iso-butyl NOSI2, see table 4.3. These results have shown that there is a general trend towards a lower value of Φ_A as the solvent polarity increases. This trend is only general since n-iso-butyl NOSI2 should give a similar yield in acetonitrile to that measured in methanol if solvent polarity is the

only consideration, however the value obtained in acetonitrile is in fact much higher than in methanol. The general increase in the Φ_A values determined for NOSI1, NOSI2 and n-iso-butyl NOSI2 in the different solvents tends to support the hypothesis that there is an intermediate state in the photoisomerisation reaction which is in some way sensitive to solvent polarity.

Another result from this work is that in the polyurethane matrices the value of Φ_A is lower in the "harder" plastics where the hardness is gauged by the glass transition temperatures, see table 4.4. The "hardness" of each plastic is increased by increasing the number of cross linking groups in the polymer which may be increasing the viscosity of the sites containing the NOSI molecule.

The values of Φ_A measured for NOSI2 and n-iso-butyl NOSI2 were the same in toluene. This result implies that the n-iso-butyl group does not hinder the photochemical isomerisation either by viscosity effects or by steric effects. The values of Φ_A for these two compounds were also found to be the same when irradiated in polyurethanes matrices having the same "hardness". The fact that no effect is seen upon increasing the size of the n-alkyl may suggest that this group does not increase the viscous drag experienced by the NOSI molecule during the photochemical isomerisation and further that it does not cause any steric effects in the photochemical isomerisation process whereas the ground state fade reaction described in chapter 3 is affected by the presence of bulky n-alkyl substituents.

The present values of NOSI1 colouration efficiency in toluene of 0.33, using a molar decadic absorption coefficient of 31000 $dm^3.mol^{-1}.cm^{-1}$, and 0.24, using a molar decadic absorption coefficient of 51000 $dm^3.mol^{-1}.cm^{-1}$ in ethanol, can be directly compared to those obtained by Kellmann et al [5] of 0.22 using a molar decadic absorption coefficient of 60000 $dm^3.mol^{-1}.cm^{-1}$ in toluene and 0.19 using a molar decadic absorption coefficient of 70000 $dm^3.mol^{-1}.cm^{-1}$ in methanol. When Kellmanns values are adjusted for the differences in the values of extinction coefficient used in the Φ_A calculation they are in agreement, within error, with the present values given in table 4.2. The present value of 0.24 for the efficiency of B-form formation in ethanol is different to Kholmanskii's value of 0.44 in the same solvent using a similar molar decadic absorption coefficient of 52000 $dm^3.mol^{-1}.cm^{-1}$ [8]. Two differences exist between the methods used to determine these two Φ_A values. Kholmanskii's value was obtained using 366nm steady state excitation and at a temperature of 243K as opposed to the 354.7nm pulsed irradiation at 294K used in the present study. Either or both of these factors could account for the differences between the values obtained. Light at both 366nm and 354.7nm is absorbed by the oxazine half of the molecule

and would therefore be expected to bring about the photochromic reaction with a similar efficiency. Lowering the temperature may be expected to cause a lowering of the measured isomerisation efficiency due to increases in the solvent viscosity at 243K.

The measured yields of B-form formation for NOSI3, NOSI2 and NOSI1 in toluene via the triplet pathway are close to unity, however the yields following direct excitation at 354.7nm are 0.74, 0.64 and 0.33 respectively. These results are shown in table 4.2. If the yields obtained via the triplet state had been less than those measured after direct excitation, the implication would be that at least some degree of direct singlet involvement in the photocolouration process is present, however this cannot be said. This enhanced colouration efficiency is clearly shown in figure 4.3, which shows the rise kinetics, following excitation by the ~25 nanoscond 354.7nm pulse from a NdYAG laser, for two optically matched solutions one containing 2'-acetonaphthone plus NOSI2 and one containing NOSI2 alone. Even though both solutions absorb the same number of exciting photons the solution containing the 2'-acetonaphthone gives a greater yield of the B-form.

This absorption trace following direct excitation is interesting in that no rise or decay kinetics are seen which was the finding throughout this work. The microsecond absorbance rise time for the formation of some of the B-form product under conditions of direct excitation reported by Kellmann et al [5] was not observed in the present nanosecond study, in fact all of the absorption rises resulting from direct excitation occurred within the 25ns pulse from the laser.

References.

1. S. Schneider, A. Mindl and G. Elfinger, Ber. Bunsenges. Phys. Chem. 91, 1987, 1222.
2. S. Aramaki and G. Atkinson, Chem Phys. Lett. 170, 181, 1990, 1189.
3. H. Masuhara, N. Tamai, Chem. Phys. Lett., 191, 12, 27 1992, 189.
4. F. Wilkinson, D. J. McGarvey, J. Hobley, D. R. Worrall, A. Langley, W. Shaikh, and W. Noad, Central Laser Facility Annual Report 1993, 156.
5. A. Kellmann, F. Tifbel and R. Guglielmetti, P. Levoir, J. Aubard, E. Pottier, J. Photochem. Potobiol, A, Chem. 1988, 61, 300.
6. C Bohne, M.G. Fan, Z.J. Li, Y.C. Liang, J.C. scaiano, J. Photochem, Photobiol, A, Chem. 66, 1992, 79.
7. F. Wilkinson, J. Hobley and M. Naftaly, J. Chem. Soc. Farad. Trans. 1992,88(11), 1511.
8. A.S. Kholmanskii and K.M. Dyumaev, Dokl. Akad. Nauk. SSSR, 1988, 303.
9. N. Y. C. Chu, Can. J. Chem., 61, 1983, 300.
10. C. Lenoble and R. Becker, J. Phys. Chem. 90, 1, 1986, 62.
11. N. P. Ernsting and Arthen-Engeland, J. Phys. Chem. 1991, 95, 5502.
12. N.P. Ernsting, Chem. Phys. Lett. 159, (5,6), 1989, 526.
13. N.P.Ernsting, Arthen-Engeland, Pure and App. Chem. 62, 8, 1990, 1483.
14. J. C. Scaiano, Handbook of Photochemistry, C.R.C. Press, Cleveland, 1989.
15 H. Heller. Technical Report provided with Aberchrome 540.
16. P. Boule and J. F. Pilichowski, J. Photochem. and Photobiol., A: Chem., 1993, 51-53.
17. D. Eloy, P. Escaffre, R. Gautron, P. Jardon, J. Chim. Phys, 1992, 89, 897.
18. H.L.J. Backstrom, K. Sandros, Acta Chem, Scand, 14, 1960, 48.
19. S.L. Murov, I. Carmichael, G.L. Hug, Handbook Of Photochemistry, 2nd Ed. Marcel Dekker, ISBN 0-8247-7911-8, 1993, 4.

CHAPTER 5

PICOSECOND TRANSIENT ABSORPTION SPECTROSCOPY (PTA) AND PICOSECOND TIME RESOLVED RESONANCE RAMAN SPECTROSCOPY (PTR^3) OF NOSI COMPOUNDS.

5. Picosecond transient absorption spectroscopy (PTA) and picosecond time resolved resonance Raman spectroscopy (PTR^3) of NOSI compounds.

5.1. Introduction.

The photoisomerisation reactions of NOSI, NPSI and BPSI compounds have been studied by several authors using both picosecond transient absorption (PTA) [1,2] methods and nanosecond laser flash photolysis [3,4,5,6,7], as well as using picosecond and nanosecond time resolved resonance Raman spectroscopy (PTR^3) [8,9,10]. Of all NOSI compounds presently being investigated in this thesis it is NOSI1 which has been the most extensively studied by other authors. Where the time resolution of the apparatus has permitted, it has been shown that the initial step in the NOSI1 isomerisation process occurs within the first few picoseconds following the absorption of a photon by the A-form [1,2], but some authors have also observed the presence of at least one other component in the isomerisation reaction having a lifetime of some tens of picoseconds [1,2]. PTR^3 studies on NOSI1 in methanol have shown an initial build up in the intensity of the bands in the resonance Raman spectrum which occurs within the 50 picosecond time resolution available to them but observed no change in the relative band intensities or position occurring after 50 picoseconds [10]. Bohne *et al* [6] have investigated NOSI1 and 2'-methyl NOSI1 using nanosecond laser flash photolysis, they found that whereas photolysis of NOSI1 leads to the spectrum expected from the B-form, photolysis of 2'-methyl NOSI1 gave an intermediate with a lifetime in the order of microseconds decaying to the initial A-form. This transient, was suggested to be a non planar species, cis about the central C-N bond, which due to the presence of the 2'-substituent cannot form the final trans isomers which give the characteristic B-form spectrum. This transient state could be a common intermediate involved in the isomerisation mechanism for a number of NOSI compounds. From the work described above it is apparent that several transient states have been identified in several NOSI reactions, however the assignation of these states to particular conformations of the NOSI1 molecule has not always been possible. The present work aims to expand on the previous studies carried out on NOSI1 as well as investigating the photochemical isomerisations of the compounds NOSI2-4 and n-iso-butyl NOSI2 in a range of solvents. Masuhara *et al* [1] investigated the reaction of NOSI1 in 1-butanol using PTA. The transient spectra they obtained were consistent with the formation of a merocyanine isomer after a few picoseconds that is trans about the central C-N bond but which then has to undergo

some conformational changes before the distribution of merocyanine isomers that is stable in a hydrogen bonding polar solvent is formed with a 40-50 picosecond lifetime. The spectrum initially formed was similar to a NOSI1 B-form spectrum in a non polar solvent.

5.2 Experimental.

5.2.1. PTA studies on the compounds NOSI1-4 and the n-alkyl NOSI2 series.

The photochemical reaction kinetics of several NOSI compounds were investigated in solution during the first few picoseconds of the photoisomerisation reaction and up to 4 nanoseconds after the arrival of the excitation pulse at the sample. This was achieved with the PTA method mentioned before using an excitation beam which was essentially a train of U.V. laser light pulses having sub picosecond temporal widths. As well as generating a sub picosecond excitation source the PTA method also requires the generation of a train of sub picosecond probe pulses from the same initial source in order to achieve picosecond timescale temporal resolution for the transient absorption measurements. The apparatus that was used to obtain these transient absorption measurements is shown below in figure 5.1.

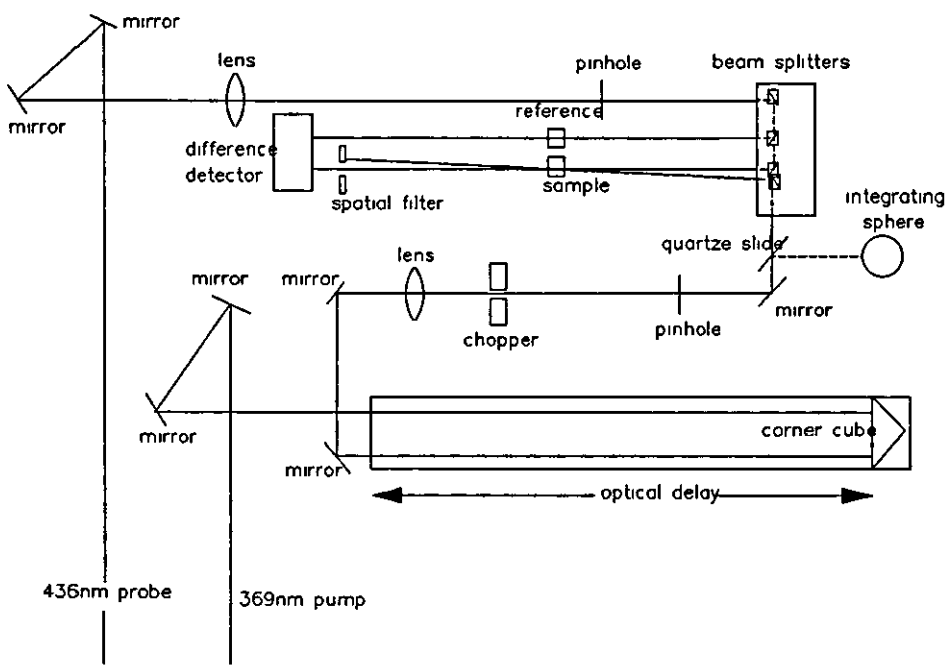

Figure 5.1. The optical layout used for the measurement of picosecond transient absorption changes.

The initial source of sub picosecond pulses was a Spectra Physics 171 argon ion laser pumping a Spectra Physics Tsunami femtosecond titanium sapphire oscillator. The Tsunami produced an 82 MHz train of pulses having a wavelength of ~736nm with each pulse having a ~150 femtosecond duration. The resulting train of pulses was then amplified using a Spectra Physics PDA1 three stage dye amplifier being pumped by a Q-switched Nd-YAG laser operating at 532nm. The pulses, once amplified, were then frequency doubled using a BBO crystal to give a final pump beam with a wavelength of 368nm and an energy of 1uJ per pulse. The probe beam was generated by mixing the 736nm light pulses from the Tsunami oscillator with the 1064nm light pulses from the Nd-YAG laser in a KDP crystal which gave a final probe wavelength of 435nm.
At this point in their journey to the sample the pump and the probe beams were each comprised of 10 Hz trains of subpicosecond pulses.

The pump and probe beams were then collimated and directed around an optical bench to the sample using the optical set up shown in figure 5.1. At the sample the two beams spatially overlapped with one another at some point within the sample cuvette. The optical layout of this bench was such that the pump and probe beams both travelled over a similar optical pathlength from the PDA1 dye amplifier to the sample, the only difference in their pathlengths being that the pump beam was directed into a laterally translatable corner cube which facilitated the production of an optical delay between the two beams. This made it possible to delay the time of arrival of the probe pulses at the point of overlap inside the sample with respect to the time of arrival of the pump pulses. The distance over which the corner cube could be physically moved was 610mm which allowed a maximum time delay of 4 nanoseconds to be set up between the pump and probe pulses.
The probe beam was split before reaching the sample with one portion passing through the sample cell along with the pump beam and the other passing through a reference cell containing an identical solution without the pump beam. These two beams were then sent to a difference detector capable of monitoring very slight differences between the probe absorbances that resulted in each of these cells, in other words the absorbance could be measured for the sample with the pump and for the reference without the pump.
Prior to its arrival at the sample the pump beam was chopped to 5 Hz but the probe beam still arrived at the detectors at 10Hz. This enabled the differences between the probe absorption by the sample and that of the reference cell to be alternately measured with and without the pump pulse. In order to achieve good statistics for the data collected it was generally necessary for 200 probe shots to be taken at each optical delay used. These 200 shots were made up of 100 absorption measurements with the pump on alternating

with 100 made with the pump off. This interweaving of probe pulses arriving at the sample with the pump on and those arriving with the pump off made it possible to correct for any non pump induced changes in the measured absorption which occurred over the extended timescale of the experiment. These non pump induced differences were caused by changes in the relative amounts of probe light reaching the difference detectors with time due to slight optical dealignments. Shot to shot variations and long term drift in the pump energy arriving at the sample during the data collection process will affect the magnitude of the transient absorption signal being monitored. These changes can easily be taken into account by splitting off a small portion of the pump beam before its arrival at the sample and then directing it into an integrating sphere containing a photodiode which registered a voltage that was proportional to the amount of pump beam entering the sphere. This data was then be used to normalise the pump induced transient absorption changes to the average pump energy.

In this way absorption data could be collected at several different optical delays and the transient induced changes in the probe absorption that occur with time could be measured less than 1 picosecond after the initial U.V. photon absorption by the NOSI molecule being investigated and up to 4 nanoseconds thereafter.

The photoisomerisation reactions of NOSI1, NOSI2-4 and n-iso-butyl NOSI2 in 1-propanol, 1-butanol, 1-decanol, acetonitrile and cyclohexane were investigated using the apparatus and methods described. These solvents were chosen in order to examine the effect of changes in the solvent polarity, viscosities and hydrogen bonding ability upon the photoisomerisation reaction. The properties of all of the solvents used in this study are given in table 5.1. The NOSI compounds studied here were chosen in order to determine what effects the basicity of the 6'-substituent or the size of the n-alkyl substituent had upon the photoisomerisation kinetics.

Table 5.1. The properties of the solvents used in the PTA experiments at 298K [11].

Solvent	Viscosity/cp	Dielectric constant ϵ^e
1-propanol	1.9	20.5
1-butanol	2.5	17.5
1-decanol	10.9	8.1
acetonitrile	0.4	36.0
cyclohexane	0.9	2.0

The alcohols and the acetonitrile used here were Aldrich chemicals 99+% pure spectrophotometric grade reagents which had been dried prior to use by distillation over calcium carbide under dry nitrogen, these were then stored in sealed glass containers until used. The cyclohexane was used as supplied by Aldrich chemicals.

Several compounds with well characterised photochemical reactions were used as standard compounds to ensure that all results obtained here were in fact due to real photochemical effects and not due to instrumentation errors or optically induced artefacts. The model systems that were chosen gave a rapid absorption change following photoexcitation reaching a plateau value that was constant for the time delays being used. If after photoexcitation the absorption value of the model systems did not plateau as expected then it was likely that either the spatial overlap of the pump and probe was drifting or that the pump energy distribution was not remaining constant as the corner cube moved from one end of its slide to the other. The two model systems which were used to ensure that the pump and probe overlap and the pump energy distributions remained constant throughout the experiment were the 2'acetonaphthone triplet state in benzene and the haematoporphine singlet state in ethanol. These two excited states are rapidly formed and do not significantly decay over the available 4 nanosecond time delay.

Standard compounds were also used to locate the position of the corner cube on its translation slide for which the pump and probe arrived simultaneously within the sample cuvette, this position on the slide is often referred to as t_0. The compounds used to locate t_0 will ideally give a transient absorption change following photoexcitation which occurs on a much shorter timescale than the temporal resolution limit set by the pump and probe pulse duration. If the model system has an initial absorption rise or decay which lasts for less time than the pump and probe pulse duration then it can also be used to estimate the temporal resolution available with the optical system that is being used. This is because the initial reaction kinetics of the model system, although resulting in the measured absorption changes, will not contribute to the profile of the absorption rise. The rise will then be able to closely follow the temporal intensity profile of the convoluted pulses which itself determines the time resolution of the optical system described here. The pulse component to the absorption rise was determined using the Zinc tetraphenylporphine singlet state formation reaction in acetonitrile as a model system. The resulting absorption rise had an ~800 femtosecond mean lifetime. Pulse components of <200 femtoseconds have been measured previously using this particular model system [1] which means that the value of ~800 femtosecond for the pulse component lifetime determined here should be a good estimate of the time resolution of the system described above. The standard compounds were used as supplied by Aldrich chemicals and were 99+% pure

spectrophotometric grade reagents.

The NOSI and the standard solutions which were used here were made up to give absorbances of ~0.6 at the excitation wavelength. The sample cuvette was a flow cell which was mechanically pumped to give a flow rate that was fast enough to remove any photochemical products from the area being probed before the arrival of the next probe pulse. This was done to ensure that the NOSI solution was fresh upon the arrival of the individual probe pulses at the sample avoiding the build up of photochemical products in the path of the probe beam.

The transient absorption changes that were measured over the first 10-20 picoseconds of the photoisomerisation reaction were analysed using a least squares fit to a biexponential function. The faster of these two components was used as an estimate of the temporal profile of the convoluted pump and probe pulses and the slower component gave the lifetime of the absorption changes arising as a result of the NOSI transformations that occur during this time. Even though the pulse component of the absorption rise will not necessarily follow an exponential function a biexponential model was still used here. This model was decided upon because the actual temporal profile of the convoluted pump and probe pulses are not easily determined for pulses this short, and for this reason any other models which could have been developed would also require assumed pulse profiles and would not necessarily give a better estimate of the pulse component to the rise. In any case the same model was applied throughout to fit absorption rises measured during the first 10-20 picoseconds which meant that direct comparisons could still be made between the fits obtained for each different system. The longer timescale reaction kinetics did not require a knowledge of the convoluted pulse profile because its contribution to the kinetics of these slower absorption changes is insignificant. This data could be fitted using the same least squares fitting routine to either first order or bi-exponential kinetics.

5.2.2. PTR^3 used to probe the photochemical isomerisation of NOSI3.

The picosecond time resolved resonance Raman (PTR^3) experiments described here are complimentary to the PTA studies described in the previous section. In many instances PTR^3 can be used to give both structural and kinetic information about short lived intermediates. In PTR^3 the resonance Raman effect is used to probe the behaviour of transient states which have an electronic transition giving an absorption at the probe wavelength. This method will not give direct spectroscopic information about transient states that don't absorb the probe beam. Preliminary studies had shown that out of the NOSI systems which were studied using PTA, NOSI3 in cyclohexane and NOSI3 in 1-butanol were the most suited to further investigation using the PTR^3 apparatus available.

Unfortunately the other NOSI systems that gave interesting PTA results and were considered for further investigation using PTR^3, gave too much fluorescence for this method to be of much use.

In these experiments the probe beam was generated using a Spectra Physics 3500 dye laser that was pumped by frequency doubled mode locked Nd-YAG laser with an 82 MHz repetition rate which gave a train of 6 picosecond pulses which had an energy of ~7 nJ per pulse. This beam was injected into a six stage dye amplifier which was synchronously pumped by the 511nm and 578nm laser lines produced by an Oxford laser Cu40 copper vapour laser operating at 4.46 kHz and at a power of 30W. The dye amplifier gave a tuneable wavelength range of between 550-655nm peaking in pulse energy at 610nm. For these experiments the probe wavelength chosen was 580nm because the B-form of NOSI3 absorbs strongly here in both cyclohexane and 1-butanol. The energy of the probe at this wavelength was 0.5uJ per pulse. The pump beam was generated by frequency doubling the probe in a BBO crystal which gave a train of 290nm pulses with an energy of 0.2uJ per pulse. Once generated the pump and the probe were sent around an optical bench which was set up essentially the same as the one shown in figure 5.1. Once again the pump and probe pulses arrived at the sample optically delayed with respect to each other. This delay was facilitated using a laterally translatable corner cube in just the same way as the delay generated for PTA experiments. The convolution of the pump and probe beams gave a temporal intensity profile of 6 picoseconds FWHM. The sample solutions were flowed through a 0.5 mm jet which gave a steady stream of the sample solution onto which the pump and probe beams were focussed together at the same point to a diameter of 40μm. The resonance Raman scattering from the sample was then collected at right angles to the incoming pump and probe beams and then analysed using a CCD detector. It was found that it was necessary to cool the NOSI3 solution in 1-butanol to 273-268K in order to reduce the concentration of the B-form that existed in solution due to thermal equilibrium with the A-form. This was not found to be necessary with NOSI3 in cyclohexane which, in any case, would freeze at the lower temperatures which were necessary for the NOSI3 solutions in 1-butanol.

TR^3 spectra were collected at a number of time delays ranging from t_0 up to a positive time delay of 1.5 nanoseconds. A further spectrum was measured for the B-form isomers which exist in solution due to their thermal equilibrium with the A-form at room temperature to use a spectrum which was effectively taken at an "infinite" time delay that could

be compared to the transient spectra. The spectral range covered in this work was 1100-1630 cm^{-1}, with a spectral resolution of 12 cm^{-1}, these wavelengths were calibrated using cyclohexane Raman bands.

The background signal was collected for an optical delay of -100 picoseconds the minus implying a time delay that is before t_0. This background signal was comprised of the solvent Raman bands and the thermally generated B-form resonance Raman spectrum, but also included any fluorescence. This background was then subtracted from each of the spectra that were measured at positive time delays. The fluorescence which occurred at positive time delays was actually different to the fluorescence at negative delays in that at the positive time delays as well as signal from the fluorescence from the A-form there were also contributions probably resulting from B-form fluorescence. Since this pump/probe induced fluorescence could not be obtained in the absence of a transient signal it had to be subtracted from the spectra collected at positive time delays as a 2^{nd} order polynomial with variables chosen which gave a flat background. In this way the resonance Raman spectra were obtained for the transient species that form during the photochemical reaction.

5.3. Results and discussion.

5.3.1. PTA results obtained for NOSI compounds.

Absorption changes with time due to several different transient species were identified in this series of experiments. The lifetimes and occurrence of these species for the different NOSI compounds studied in various solvents are given below in table 5.2.

5.3.1.1a. Absorption changes occurring within the convoluted pump and probe pulses.

The lifetimes τ_1 which are given in table 5.2 were obtained from biexponential fits to the initial absorption rise data due to the absorption of the 435nm probe beam with time. The temporal width of the convoluted pump and probe pulses determines the limit of the time resolution of the apparatus. This was estimated to be ~800 femtoseconds from the initial absorption rise time measured for the formation of the zinc tetraphenylporphine singlet state. The convoluted intensity profile of these pulses with time will give a contribution to the subsequent absorption values that were determined at the different time delays. This pulse contribution will only be significant when measuring absorption rises and decays that occur over say the first 20 picoseconds. After ~20 picoseconds the pulse width is <4% of the total timebase.

Table 5.2. Lifetimes of transient species observed for several NOSI compounds in several solvents being pumped at 368nm and probed at 435nm.

Compound	Solvent	τ_1/ps	τ_2/ps	τ_3/ps
NOSI1	1-butanol	2±0.3 D	-	-
NOSI2	1-butanol	7±0.7 R	790±40 D	-
n-iso-butyl NOSI2	1-propanol	7±0.7 R	560±30 D	-
n-iso-butyl NOSI2	1-butanol	7±0.7 R	790±40 D	-
n-iso-butyl NOSI2	1-decanol	7±0.7 R	1100±55 D	-
n-iso-butyl NOSI2	acetonitrile	80±8 D	1600±80 D	-
n-iso-butyl NOSI2	cyclohexane	5±0.5 R	-	-
NOSI3	1-butanol	5±0.5 D	30±3 D	1400±70 D
NOSI3	cyclohexane	9±0.9 D	70±7 D	-
NOSI4	1-butanol	not measured	1000±50 D	-

In this table an R after a lifetime value indicates that it was determined for a transient absorption rise and D implies that the value is associated with a transient absorption decay.

As mentioned, the pulse duration is significant to the shorter timescale absorption changes and its contribution to the absorption rise kinetics will be measurable. This is so even in instances when no transient states are formed within the pulse which absorb at the probe wavelength, because the temporal intensity profile of the pulses will contribute to the profile of the absorption rise. The pulse contribution to the initial absorption rise data was estimated for each NOSI system by fitting it to one of the exponentials of a bi-exponential function. In every case this contribution was found to fit to a lifetime of 800±200 femtoseconds. Out of all of the NOSI systems which were studied only the photoisomerisations of NOSI1 in 1-butanol, n-iso-butyl NOSI2 in acetonitrile, NOSI3 in 1-butanol and NOSI3 in cyclohexane, gave obvious absorption rises occurring with lifetimes that were of the same order as the 800 femtosecond lifetime determined for the pulse component using model systems. With these four systems the absorption rises within the pulse and then decays with a lifetime that is longer than the pulse duration. Such rise traces are shown in figures 5.2 and 5.3. These traces show absorption changes with time that can best be explained by the formation of a transient within the pulse which absorbs the 435nm probe more than the species which forms thereafter with a lifetime longer than the pulse component. These traces demonstrate that for some if not all NOSI systems there are rapid transformations resulting from photoexcitation which occur with lifetimes much less than

the 800 femtosecond pulse component lifetime. The initial rises of the NOSI3 systems shown in figure 5.3 at first appear to be slower than that of n-iso-butyl NOSI2 in acetonitrile which is shown in figure 5.2, however these initial rises all fit to similar lifetimes and this apparent difference only occurs because the NOSI3 systems have subsequent absorption decays which are much faster than the subsequent decay that occurs for n-iso-butyl NOSI2 in acetonitrile. The absorption rise measured for n-iso-butyl NOSI2 in cyclohexane is also shown in figure 5.2.

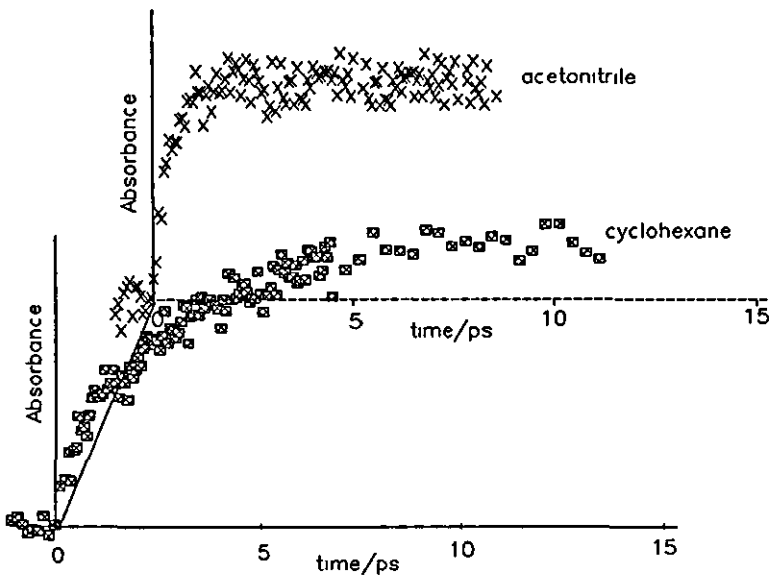

Figure 5.2. The initial absorption rise kinetics of n-iso-butyl NOSI2 in acetonitrile and in cyclohexane solutions.

This latter trace appears at first glance to follow still different rise kinetics, but once again despite the apparent differences between this absorption rise and the other three rise/decay traces shown in figure 5.2-5.3, it also gives a similar value for the lifetime of the initial pulse component. The major differences between these absorption rise profiles are probably caused by the species forming within the pulse component of the n-iso-butyl NOSI2 rise in cyclohexane absorbing less strongly at 435nm than similar species forming for the other systems. In fact all of the NOSI systems which were investigated here gave lifetimes for the initial component to the absorption rise of 800±200 femtoseconds which is consistent the pulse component lifetime determined from model systems. From these results it can be stated that the first transient species that forms during the NOSI3 photoisomerisation in 1-butanol and cyclohexane and for n-iso-butyl NOSI2 in acetonitrile probably does so with a lifetime that is similar to or shorter than the ~800 femtosecond lifetime of the pulse component. Although no definite absorption rises within the pump

and probe pulses were observed for the other NOSI systems that were studied, this does not necessarily mean that the same transients do not form in these cases, it may just mean that the spectrum of this species is shifted such that it gives a much lower absorption or even no absorption at all at the 435nm probe wavelength.

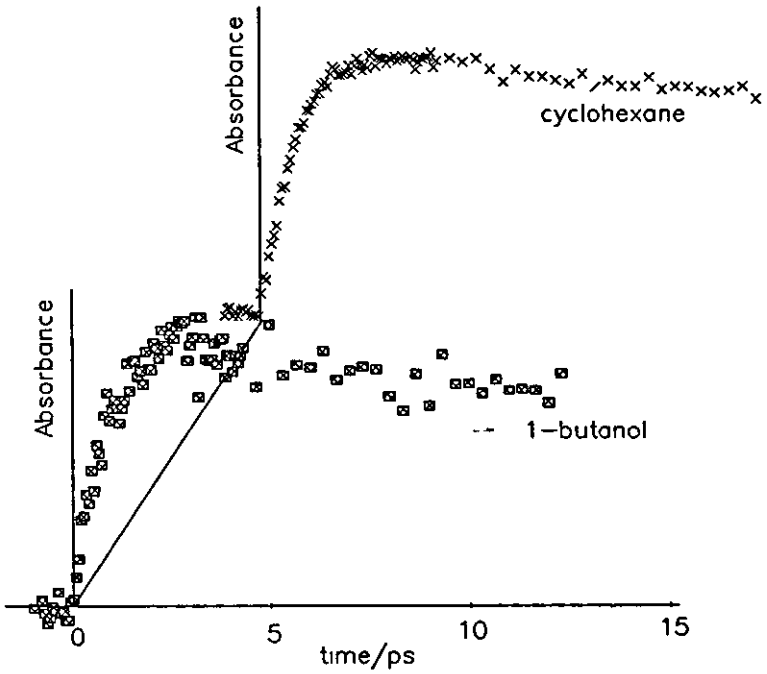

Figure 5.3. The initial absorption rise kinetics of NOSI3 in 1-butanol and cyclohexane solutions.

The types of transformation which could account for the initial absorption rise within the pulse are the formation of A^* [12] and the breaking of a bond [12], possibly the spiro C-O bond. It is likely that when the spiro C-O breaks it does so heterolytically [2,7] rapidly forming a species which still retains a negative charge on the oxygen but with the positive charge from the carbon atom delocalised onto the nitrogen. This species would still have the orthogonal A-form geometry and has previously been proposed as an intermediate in BPSI, NPSI and NOSI photochemical isomerisations to the B-form [2,7] being referred to as X. The structure of X is given below in figure 5.4 along with the structures of the other possible transient states which could be formed directly from X and the possible B-form isomers that form thereafter. The absorption changes that occur within the convoluted pulses are probably due to the formation of X and although similar rapid absorption rises are not seen for every NOSI system, it is argued here as above that this isn't because X does not form within the pulse in these cases, but that with these systems X does not absorb at 435nm due to spectral shifts caused by

changes in the solvent and the substituents.

The transient species X and A^* are both assigned as transients species that are formed within the pump and probe pulse convolution for all of the NOSI systems being presently studied.

5.3.1.1b. A description of the structures which may be involved in the photochemical formation of the B-form.

Apart from X the other eight structures shown in figure 5.4, are the possible merocyanine structures which could be formed as a result of isomerisations or conformational changes arising from X. The merocyanine isomers that are shown here are named according to whether they are cis or trans about each of the three central bonds that bridge the two halves of the molecule. The same nomenclature has been used by several authors to describe the similar unsubstituted BPSI and NPSI merocyanine forms [7,9].

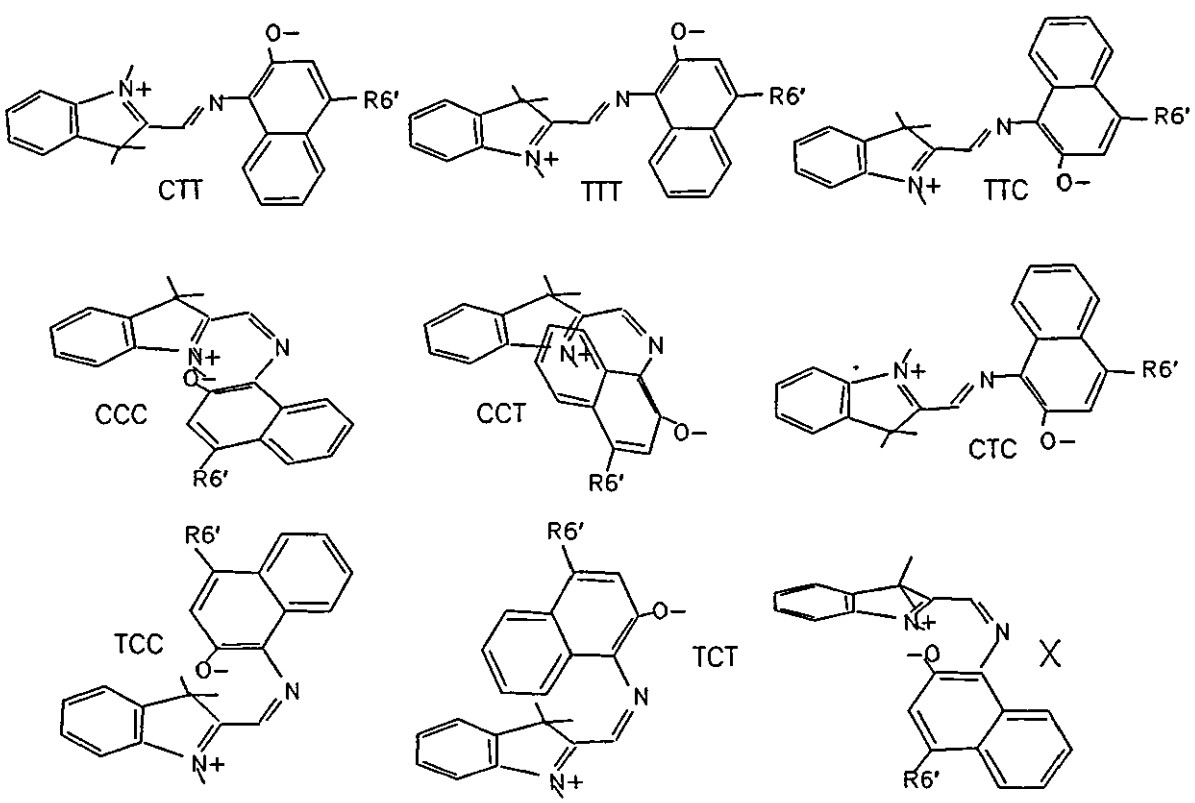

Figure 5.4. The structures that could result from the photolysis of the NOSI A-form and which are possible transients in the photoisomerisation reaction.

In the same articles that use this naming system the stabilities of some of these different isomeric forms in different solvents have either been calculated or inferred from their structures. For the BPSI isomers which are trans about the central C-C bridging bond, it

is TTC that is suggested to be the most stable in non polar solvents [7,9]. This is because it has the shortest distance between the partial negative charge on the oxygen and the partial positive charge on the nitrogen this reduces the overall charge separation of this isomer. In the same works TTT is suggested to be the least stable form in non polar solvents since it has the greatest charge separation, however the TTT isomer is suggested as the most stable of the isomers in hydrogen bonding solvents. The CTC and CTT are said to be the stable forms in polar solvents [7,9]. For NOSI1 it is suggested that TTC is the stable merocyanine isomer in non polar solutions [2] with TTT again only being stabilised by hydrogen bonding solvents. Of the BPSI isomers which are cis about the central bridging bond some dispute exists as to the most stable form, with either CCT [7] or TCC [9] given as the most stable form.

5.3.1.1. The photoisomerisation kinetics of NOSI2, n-iso-butyl NOSI2 and NOSI4 in alcohol solutions.

As can be clearly seen from figures 5.5 and 5.6 NOSI2 solutions and n-iso-butyl NOSI2 in the alcohols gave very similar absorption rises which corresponded in each case to a 7 picosecond lifetime for τ_1, these results are given in table 2. Neither increasing the size of the n-alkyl group from a methyl to an iso-butyl group nor increasing the length of the alkyl chain on the alcohol from a propyl to a decyl group had any effect upon the value of τ_1.

The transient that formed here in the alcohol solutions with τ_1 of 7 picoseconds gave a subsequent absorption decay that went to an end of trace absorption value that was broadly consistent with the absorption that would be expected from the equilibrated B-form in the alcohols. The absorption decays measured for n-iso-butyl NOSI2 in the alcohols occurred with a lifetime τ_2 of 560 picoseconds in 1-propanol, 790 picoseconds in 1-butanol and 1.1 nanoseconds in 1-decanol, these decay traces are shown in figure 5.7. As is apparent here τ_2 was found to be sensitive to variations in the size of the alkyl chain length on the alcohol its value doubling from 560 picoseconds to 1100 picoseconds upon changing from 1-propanol to 1-decanol. However this same transformation was totally unaffected by substituting the n-methyl group on NOSI2 with an n-iso-butyl group and both of these compounds had τ_2 values of 790 picoseconds measured in 1-butanol. However the addition of the 2-methyl group on the 6'-indoline on the compound NOSI4 increased the value of τ_2 to 1 nanosecond, measured in 1-butanol, from the value of 790 picoseconds obtained for NOSI2 in the same solvent.

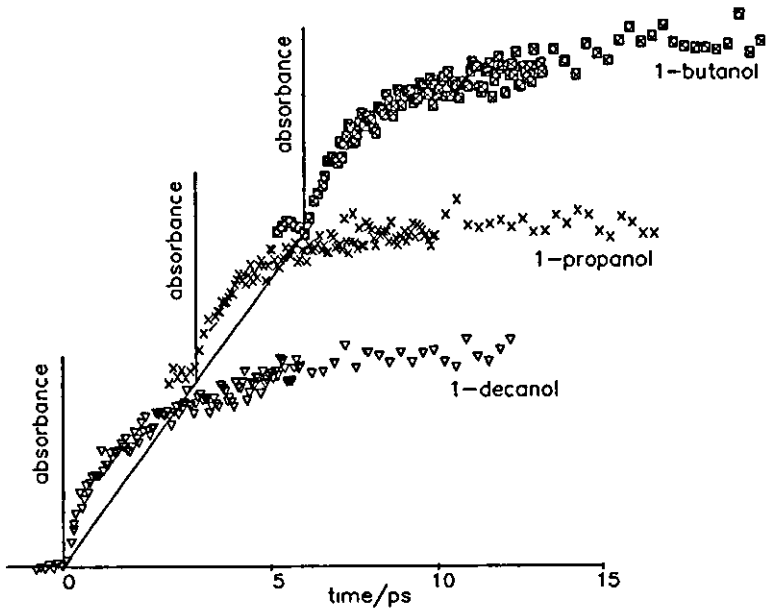

Figure 5.5. The initial absorption rises measured for n-iso-butyl NOSI2 in different alcohols with different alkyl chain lengths.

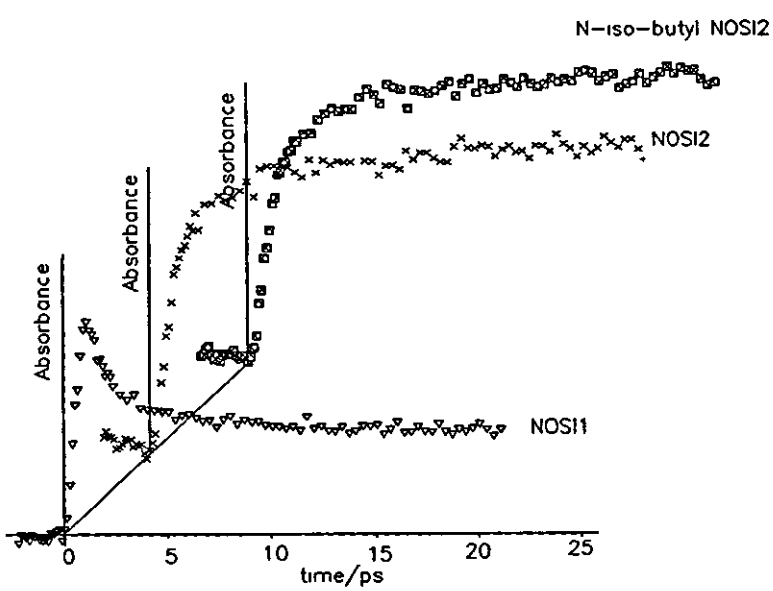

Figure 5.6. The initial absorption rise kinetics of NOSI1, NOSI2 and n-iso-butyl NOSI2 in 1-butanol.

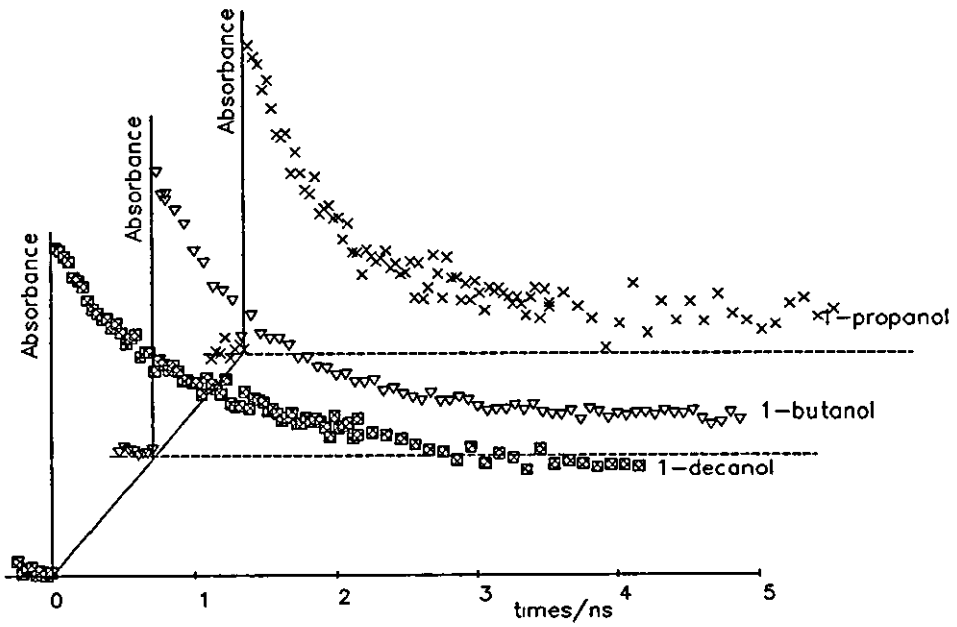

Figure 5.7. The absorption decay giving τ_2 measured for n-iso-butyl NOSI2 in different alcohols with different alkyl chain lengths.

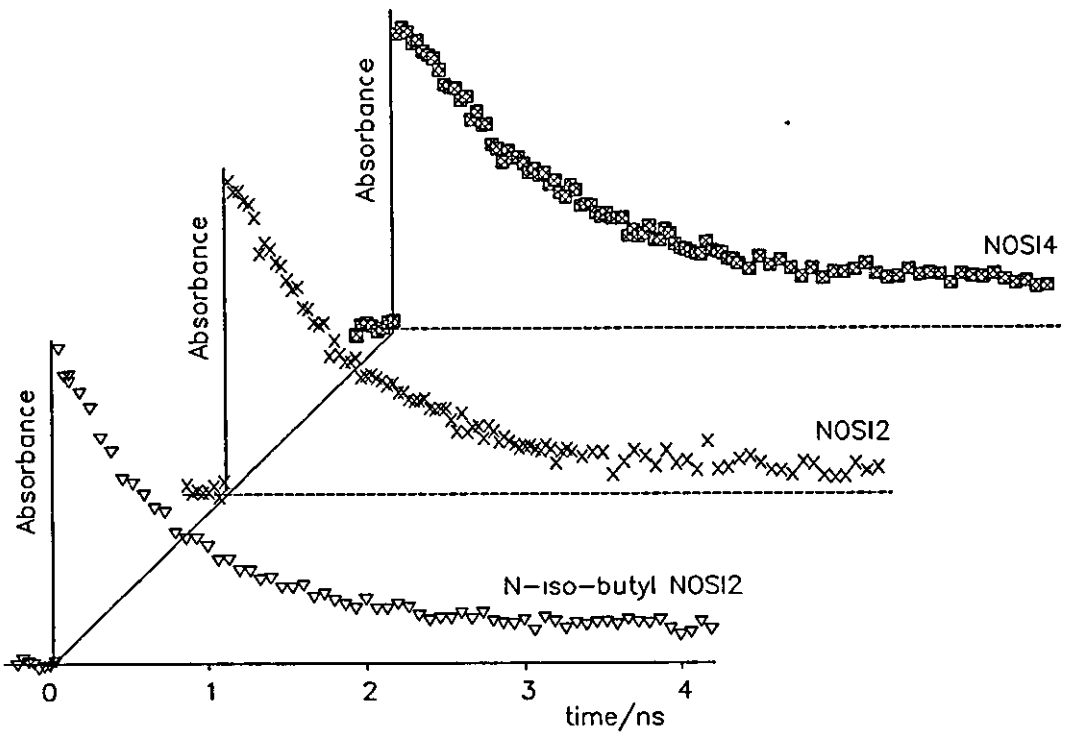

Figure 5.8. The absorption decay giving τ_2 measured for NOSI2, n-iso-butyl NOSI2 and NOSI4 in 1-butanol.

The solvent and substituent effects upon the absorption traces from which the values of τ_2 were obtained are shown in figures 5.7 and 5.8 and the corresponding values for τ_2 are given in table 5.2.

The increase in the value of τ_2 as longer alkyl chain alcohols were used is most probably the result of a solvent viscosity effect rather than an effect due to solvent polarity, since in the case of n-iso-butyl NOSI2 τ_2 has its largest value in 1-decanol. Out of the alcohols that were used here 1-decanol has got the lowest dielectric constant as shown in table 5.1 and in view of the fact that the τ_2 absorption decays were not observed at all for n-iso-butyl NOSI2 in cyclohexane (see later) it is suggested that polar solvents stabilise the species which decays with the lifetime τ_2.

The results obtained here for n-iso-butyl NOSI2 in alcohol solutions tell us that the τ_2 decays result from a transformation that is hindered in viscous solvents and further it is a transformation from a species which is stabilised in polar solvents. These results lead to the assignment of the τ_2 decays to an isomerisation which occurs from a species which is charge separated. The value of τ_2 is unaffected by the size of the n-alkyl group which suggests that this isomerisation is one from a species on which the n-alkyl group and the oxazine ring are placed apart from each other. This can be said because it is known, from the results presented in Chapter 3 of this thesis, that the ground state thermal fade isomerisation is slowed down by bulkier n-alkyl groups. This further suggests that the τ_2 isomerisation is not one occurring along the ground state potential energy surface. The fact that replacement of the NOSI n-methyl group with an iso-butyl group does not increase the transient lifetime implies that the size of these n-alkyl groups is small compared to the free volume of the solvent and that even the n-iso-butyl group does not significantly increase the viscous drag as the molecule isomerises.

One set of isomers which can interchange between each other with minimum steric hinderance from the n-alkyl group are those which are trans about the bridging C-N bond. These are the TTC, TTT, CTT and CTC isomers which equilibrate to make up the B-form. If an isomer which is trans about the C-N bond forms as a common intermediate in the photochemical isomerisation then it may be that this species would then undergo further conformational changes to form the equilibrated distribution of B-form isomers in the particular solvent being used. It could be argued that such isomeric equilibration may be the cause of the absorption decay resulting in τ_2. However, such an isomeric redistribution of NOSI2 B-form isomers cannot be the only transformation responsible for the large drop in absorption that occurs during the τ_2 decays. This statement can be

made here in view of the B-form spectra obtained in chapter 2, for which the extinction coefficients of the NOSI2 B-form and n-iso-butyl NOSI2 B-form at 435nm in polar solvents were found to be very similar to those measured in non polar solvents and as such a redistribution of B-form isomers to equilibrate in 1-butanol would not result in the large decreases in absorbance that are apparent in figures 5.7 and 5.8. The absorption changes with time that are observed for NOSI2 and n-iso-butyl NOSI2 at 435nm must therefore be due to some other transformation. A redistribution of B-form isomers may also be required before the equilibrated B-form is produced but this would not result in a large absorption change at 435nm and may not be show up in these experiments.

One possible transformation that could account for the τ_2 decay is an isomerisation step from a species such as the TCT isomer or the TCC structure both of which are given in figure 5.4. The oxazine ring on either TCT or TCC can rotate to form the final B-form distribution of merocyanine isomers following a single rotation about the bridging C-N bond without any intramolecular interactions occurring between the oxazine ring and the n-alkyl group. If either CCC or CCT were the conformations adopted prior to an isomerisation step then we would undoubtedly see an effect on the transients lifetime upon changing the size of the n-alkyl chain. The involvement of TCT as an intermediate in the isomerisation can be rejected, since it is more sterically crowded than TCC. The TCC isomer is therefore the most likely assignment as the transient giving the τ_2 absorption decay. TCC would not be as planar as the B-form isomers due to steric considerations therefore the subsequent conversion to final B-form isomers would almost certainly lead to an increase in the molecules Π-electron overlap which would result in a red shift in the measured absorption spectrum. This red shift could then be responsible for the large absorption decays measured at 435nm. The lack of planarity of TCC would also mean that delocalisation of the charges on the oxygen and nitrogen would not be efficient and the resulting structure would probably be partially charge separated.

Another result which implies that the isomerisation does not proceed along the ground state surface is that the absorption decay measured with a lifetime τ_2 for NOSI4 in 1-butanol is in fact slower than the τ_2 decay measured for NOSI2 in 1-butanol, this trend in the isomerisation rates is reversed for the thermal fade reaction and the isomerisations are therefore suggested to proceed along different pathways.

In summary the results obtained for NOSI2 and n-iso-butyl NOSI2 in the alcohols are consistent with the formation of A^*/X within the convoluted pulses, these then form the TCC isomer with a 7 picosecond lifetime, TCC then isomerises to form the final B-form distribution of merocyanines probably via the TTC structure which can form most easily from TCC following a single rotation about the C-N bond in the bridged region. TTC is

suggested to be the most stable isomer in non-polar solvents [2,7,9] and may therefore be required to undergo further structural changes in order to equilibrate itself in the alcohols however, due to similarities in their B-form absorptions at 435nm these changes would not necessarily be detected.

5.3.1.2. The kinetics of the NOSI1 photoisomerisation reaction in 1-butanol.

For NOSI1 in 1-butanol an initial fast absorption rise was measured within the pulse. This rise was followed by an absorption decay with a lifetime τ_1 of ~2 picoseconds. The absorption rise data for NOSI1 in 1-butanol is shown above in figure 5.6. No further absorption changes occurred after the first 10 picoseconds of the reaction as can be seen in figure 5.9.

The fact that no absorption changes occurred with time after 6 picoseconds in the present work, carried out on NOSI1 in 1-butanol, appears to be in contrast with the results obtained by Masuhara *et al* [1]. These authors measured a transient absorption change occurring with a lifetime of 40-50 picoseconds for the same compound in the same solvent.

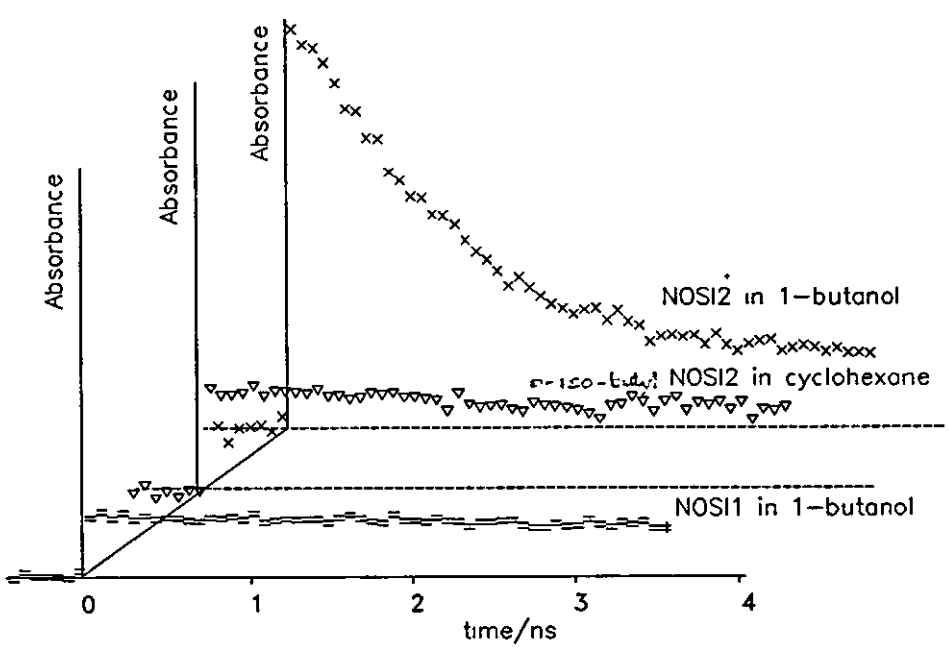

Figure 5.9. Absorption with time data for NOSI1 in 1-butanol and n-iso-butyl NOSI2 in cyclohexane showing no longer timescale absorption changes, the decay of NOSI2 in 1-butanol is shown here for comparison.

However upon closer inspection, Masuhara's time resolved spectra show little to no absorption changes at 435nm after the first few picoseconds. The spectral changes occurring with time measured by Masuhara *et al* [1] were assigned to an equilibration of the isomers

which are trans about the C-N bond to form an isomeric distribution that is stable in 1-butanol. This explanation was based upon the fact that the spectrum which evolved after a few picoseconds was very similar to NOSI1 spectra obtained in non polar solvents such as cyclohexane. This initial non polar B-form spectrum then evolved into the spectrum that is usually measured for the NOSI1 B-form at equilibrium in 1-butanol. As mentioned above these spectral changes do not show up at 435nm, and such an isomeric equilibration would not show up at this probe wavelength. The present data is consistent with the results of Masuhara *et al* (1) in as far as our absorption changes occur. Masuhara's transient spectra evolved within the 200 femtosecond pulse convolution to give a maximum absorption value at ~490nm. This then rapidly evolved into a species which had an absorption maximum at 680nm and another band with a maximum absorbance at ~460nm. This spectrum has similarities to the transient spectrum measured by Bohne *et al* (6) for 2'-methyl NOSI1 which was assigned as a charge separated intermediate cis about the bridging C-N bond and which had an absorption peak maxima at 470nm and one at 680nm both in acetonitrile. As mentioned previously, Masuhara's spectrum then formed the B-form type spectrum that would be expected in a solvent such as cyclohexane, this development occurred after a further 2-6 picoseconds. This spectrum could be largely due to the TTC isomer since it is similar to the B-form spectra normally measured in non polar solvents. TTC would be the most stable B-form in such solvents and may also be the predominant species in the 2 picosecond spectrum obtained by Masuhara (1). This non polar B-form spectrum then evolved into the B-form spectrum that would be expected in 1-butanol with a 40-50 picosecond lifetime for these spectral changes. With our time resolution the first two transients observed in Masuharas time resolved study would form within the convoluted pulse duration. The decay then seen with a 2 picosecond lifetime τ_1 would therefore be due to the formation of the typical non polar B-form spectrum which is probably due mainly to the TTC B-form isomer. This would imply that A^* and X and TCC are all formed within the pulse duration for NOSI1 in 1-butanol and TTC then forms with a 2 picosecond lifetime. The fact that no further absorption changes are seen for NOSI1 after 6 picoseconds, in the present work, supports the rejection of a B-form isomeric equilibration as a possible cause of the observed transient decays measured for n-iso-butyl NOSI2 NOSI2 and NOSI4 in the alcohols, because just as predicted no absorption changes do occur with time after 6 picoseconds in our or Masuhara's PTA study on NOSI1, whereas Masuhara did observe a typical non polar B-form spectrum evolving into a typical polar solvent NOSI1 B-form spectrum with a 40-50 picosecond lifetime. This process may be occurring for most of the NOSI compounds presently being studied but would not necessarily be seen at 435nm.

5.3.1.3. The photoisomerisation reaction kinetics of n-iso-butyl NOSI2 in acetonitrile.

The initial absorption rise of n-iso-butyl NOSI2 in acetonitrile is described above and is consistent with the formation of A^*/X within the convoluted pulses. This prompt rise is then followed by an absorption decay which has a lifetime τ_1 of ~80 picoseconds. The lifetime of this transient, proposed here as X, is longer than the lifetimes of the transients assigned as X in the alcohols. This increased lifetime could be caused by stabilisation of the transient due to the increased polarity of acetonitrile. Such an increase in τ_1 with solvent polarity is consistent with its assignment to a charge separated species such as X. The kinetic traces obtained for n-iso-butyl NOSI2 in some of the other solvent systems and measured over the first one hundred picoseconds of the reaction are shown below in figure 5.10. These show that there was no evidence to imply the existence of any transient decays having similar lifetimes occurring for these systems.

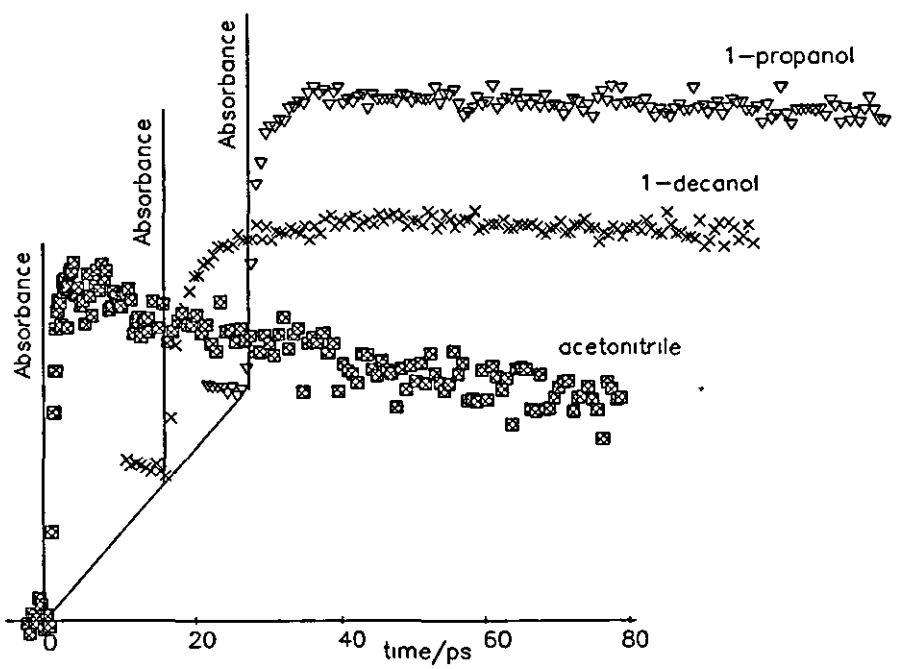

Figure 5.10. The absorption changes that occur over first 80 picoseconds of the n-iso-butyl NOSI2 reaction measured in 1-propanol, 1-decanol and acetonitrile.

The 80 picosecond τ_1 decay follows the formation of another species, probably the partially charge separated TCC isomer, which itself decays with a lifetime, τ_2, of 1.6 nanoseconds as shown in figure 5.11. The magnitude of the absorption decrease measured during the 1.6 nanosecond decay was again too great to be assignable solely to a B-form isomeric equilibration, as was the case with the same compound in the alcohols. Therefore the τ_2 decay measured here could be explained by a TCC->TTC

isomerisation in a similar manner to the τ_2 decays measured in the alcohols, but with the lifetime of TCC measured here increased by the greater polarity of acetonitrile.

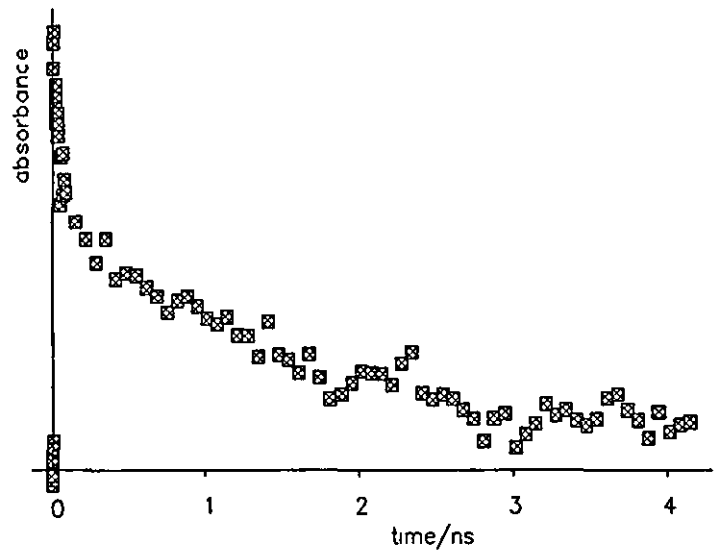

Figure 5.11. The absorption decay measured for n-iso-butyl NOSI2 in acetonitrile.

In summary n-iso-butyl NOSI2 in acetonitrile probably forms X rapidly within the excitation pulse. Its absorption spectrum is shifted sufficiently for it to be measurable at 435nm. X is stabilised in this system and has an extended lifetime of 80 picoseconds after which time it forms the TCC structure. TCC then isomerises to the B-form isomers with a lifetime of 1.6 nanoseconds. The TCC isomerisation lifetime is increased compared to its lifetime in the alcohols this again could be because of the higher polarity of acetonitrile. Further isomeric equilibration may also be occurring but may not result in an absorption change at 435nm.

5.3.1.4. The photoisomerisation reaction kinetics of n-iso-butyl NOSI2 in cyclohexane.

The initial absorption rise observed after the pulse component which was measured for n-iso-butyl NOSI2 in cyclohexane was slightly faster than the rise determined for the same compound in 1-butanol which is described above. No further absorption changes were seen for n-iso-butyl NOSI2 in cyclohexane after this initial fast step as shown in figure 5.9. The absorption rise data is shown in figure 5.3. The fact that in cyclohexane the n-iso-butyl NOSI2 photochromic reaction is over within the first 10-20 picoseconds after the excitation pulse adds weight to the argument that the transients observed in the polar solvents are in fact charge separated intermediates stabilised only in a polar media.

In summary the n-iso-butyl NOSI2 B-form is probably produced directly from a species that is formed within the pulse, in this case the species A^*, X and TCC probably all form

within the pulse however TCC is is probably the species which then isomerises with a lifetime τ_1 of 5 picoseconds to give the final B-form. No isomeric redistribution is expected or seen in this case as TTC should be formed directly from TCC and is not expected to undergo any further transformations since it is proposed to be the most stable isomer in cyclohexane [2].

5.3.1.5. The photoisomerisation reaction kinetics for NOSI3 in 1-butanol.

The initial absorption rise that was determined for NOSI3 in 1-butanol has similarities to those obtained for NOSI3 in cyclohexane and which are described below. The initial rise is consistent with a sub-picosecond component due to the convoluted pump and probe pulses. Any absorption rise happening within the pulse can again be assigned to A^*/X which then forms another species probably TCC with a corresponding τ_1 absorption decay lifetime of 5 picoseconds. The initial absorption rise traces are shown in figure 5.3. The absorption decay resulting from the formation of TCC is then followed by a further absorption decay with a lifetime, τ_2, of 30 picoseconds. This latest species itself gives a further absorption decay τ_3 which occurs with a 1.4 nanosecond lifetime. The absorption drop that occurs during this long decay is not large enough for a B-form isomeric redistribution to be ruled out as a possible cause of these longer absorption changes. The absorption with time traces for these last two transients are shown in figures 5.12, 5.13, and 5.14.

These observations can be explained as an A^*/X species forming inside the pulse which subsequently forms TCC with a 5 picosecond lifetime τ_1. The TCC absorption then further decays with 30 picosecond lifetime, τ_2, possibly to form the TTC B-form isomer. TTC then has to equilibrate with the other B-form isomers in order to establish a more stable B-form isomeric distribution for solvation in 1-butanol and this occurs with a lifetime τ_3 of 1.4 nanoseconds.

5.3.1.6. The photoisomerisation reaction kinetics of NOSI3 in cyclohexane.

In cyclohexane NOSI3 has an initial absorption rise which is again consistent with a sub-picosecond pulse contribution and a second component which decays but this time with a lifetime, τ_1, of around 9 picoseconds. The initial rise and the 9 picosecond decay is shown in figure 5.3. The most likely assignment of the states formed within the pump and probe pulses are the A^*/X states. The species formed from A^*/X then gave an absorption decay, shown in figure 5.14 occurring with a 70 picosecond lifetime, τ_2, to form a species which gave no further absorption changes during the next 4 nanoseconds.

The 70 picosecond lifetime intermediate could be similar in its origins to those previously assigned as the charge separated TCC state isomerising to form TTC, an event which has until now only been proposed to occur in polar solvents.

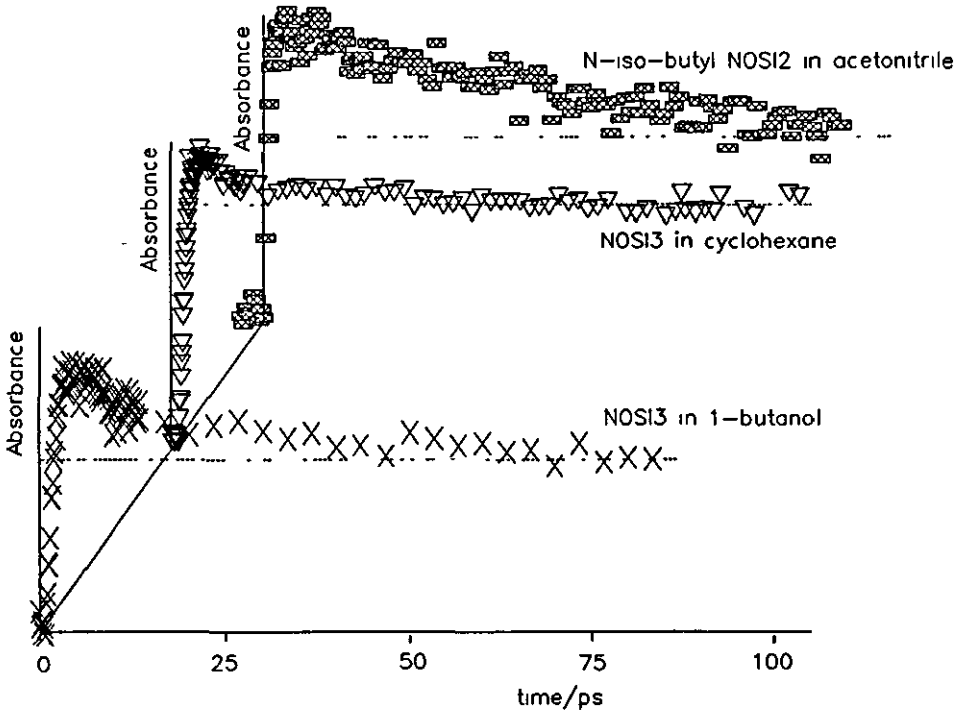

Figure 5.12. The absorption changes with time measured for NOSI3 in 1-butanol and cyclohexane and for n-iso-butyl NOSI2 in acetonitrile over 100 picoseconds.

It is possible that TCC is stabilised here by strong electron donation from the 6'-piperidine group allowing the delocalisation of some of the positive charge on the NOSI indoline nitrogen thereby reducing the overall charge separation of this state. Such delocalisation would not be expected to be a very efficient process for the non planar TCC isomer but some resonance may still be possible. The final absorption value that results after 4 nanoseconds was consistent with that expected if it were due to the final B-form in cyclohexane. The main criticism of this scheme is that the proposed TCC transient in cyclohexane has a longer lifetime than in 1-butanol, however it is argued below that electron donation to TCC will lessen the charge separation on this species. The transient lifetimes measured and assigned to the TCC state in 1-butanol decrease as the electron donating power of the 6'-group is increased. This increase occurs with the following order; NOSI3 < NOSI2 = n-iso-butyl NOSI2 < NOSI4. The reason for this may be that an increased electron donating power from the oxazine 6'-group can delocalise the positive charge residing on the NOSI indoline nitrogen more effectively. This would result in a less charge

separated transient which will be less stable in polar solvents. This explanation could account for the fact that the transient assigned as TCC for the NOSI3 systems lives for longer in cyclohexane than it does in 1-butanol.

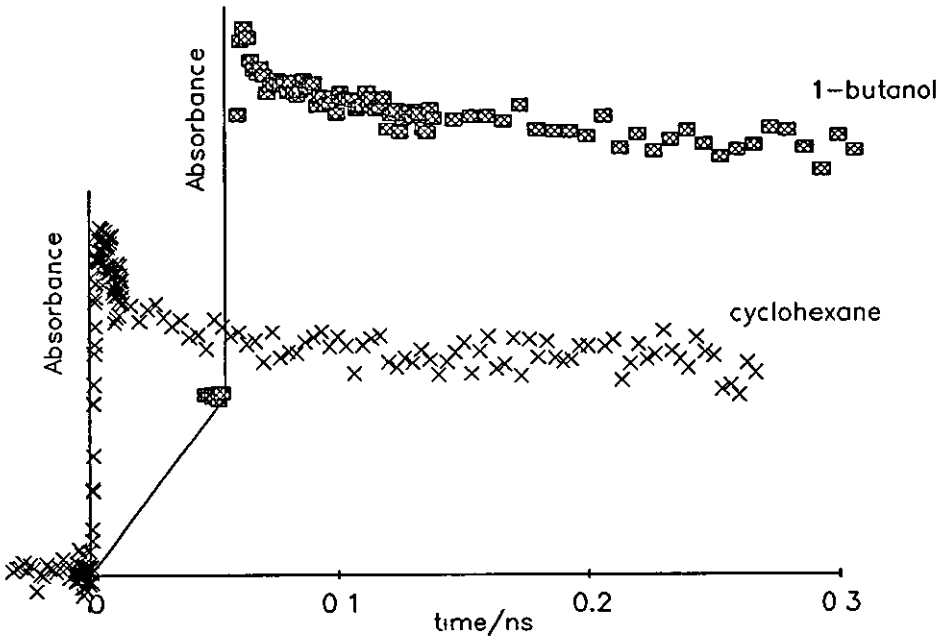

Figure 5.13. The absorption changes measured with time for NOSI3 in 1-butanol and in cyclohexane during the first 300 picoseconds.

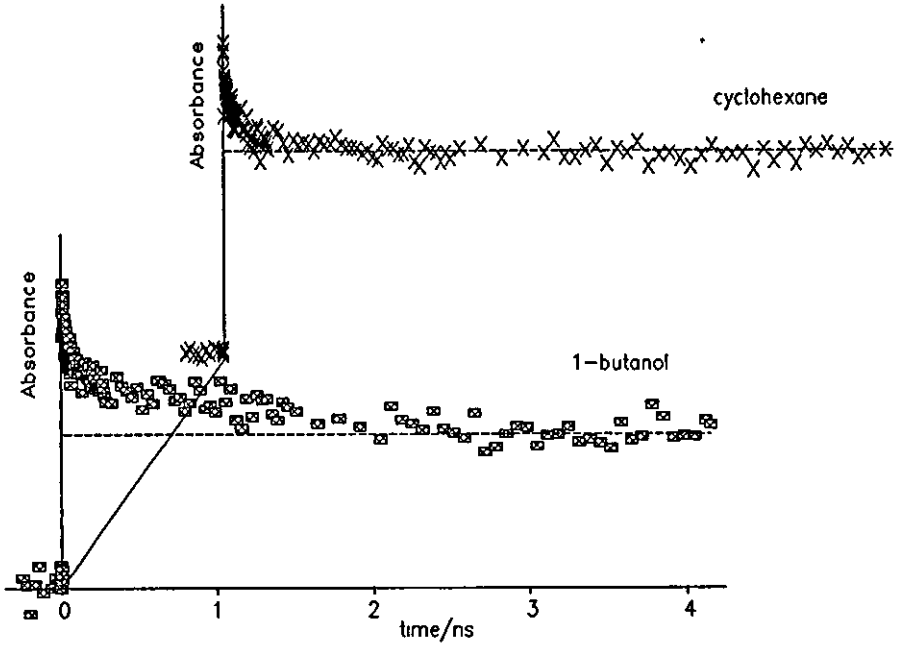

Figure 5.14. The absorption changes with time determined for NOSI3 in 1-butanol and in cyclohexane over 4 nanoseconds.

5.3.2. PTR^3 studies on NOSI3.

5.3.2.1. PTR^3 studies on NOSI3 in 1-butanol.

The NOSI3 solutions in 1-butanol gave rise to resonance Raman spectra which developed with time both in terms of their overall spectral shape and in their relative band intensities these spectra are given in figure 5.15. It was apparent from the results obtained here for NOSI3 in 1-butanol that the observed spectral evolution with time could only be explained by the presence of at least two, but maybe even three transient species. Each of these species is associated with groups of related peaks situated within the overall spectral envelope which grow in with different time constants. The time evolution of the relative contributions from these peaks to the overall spectrum was different for each of the groups identified. For simplicity it will be attempted to assign the observed bands to a model based on the presence of just two states since the presence of a third set of transient resonance Raman bands contributing to the measured spectra, although not ruled out, has not been established. The two species which are invoked in this description of the data will be referred to as the α and the β states. The resonance Raman peaks which are associated with the α component are centred at 1284 cm^{-1} and 1425 cm^{-1}. The β peaks are generally located on either side of the two α bands. The α bands seen in the transient spectra measured for NOSI3 in 1-butanol appear to grow in faster than the β peaks. The α peaks are essentially fully developed after 100 picoseconds but then appear to decay very slightly with a much longer time constant. The 100 picoseconds taken for the full development of these α components allows us to associate them with the transformation assigned to the isomerisation from TCC to TTC which in the PTA experiments on NOSI3 in 1-butanol gave an absorption decay with a mean lifetime τ_2 of 30 picoseconds. A mean lifetime of 30 picoseconds would give a decay that is essentially complete after three lifetimes therefore the grow in time of the α peaks matches the lifetime of the proposed TCC isomerisation to TTC. The TTC B-form isomer will be unstable in 1-butanol and would need to isomerise to form more stable B-form isomers. This process may result in the slower grow in of the β peaks occurs. The growth of these is essentially over after ~200 picoseconds but the bands do appear to continue to rise slightly over the remainder of the 1.5 nanosecond time delay which was available. It could well be that the longer grow in time of the β peaks results from an equilibration with the α components, this would also explain the longer decay of the α peaks. These longer components in the PTR^3 spectral evolution may then be linked to the longer 1.4 nanosecond lifetime transient decay that was also observed in the PTA work for NOSI3 in 1-butanol.

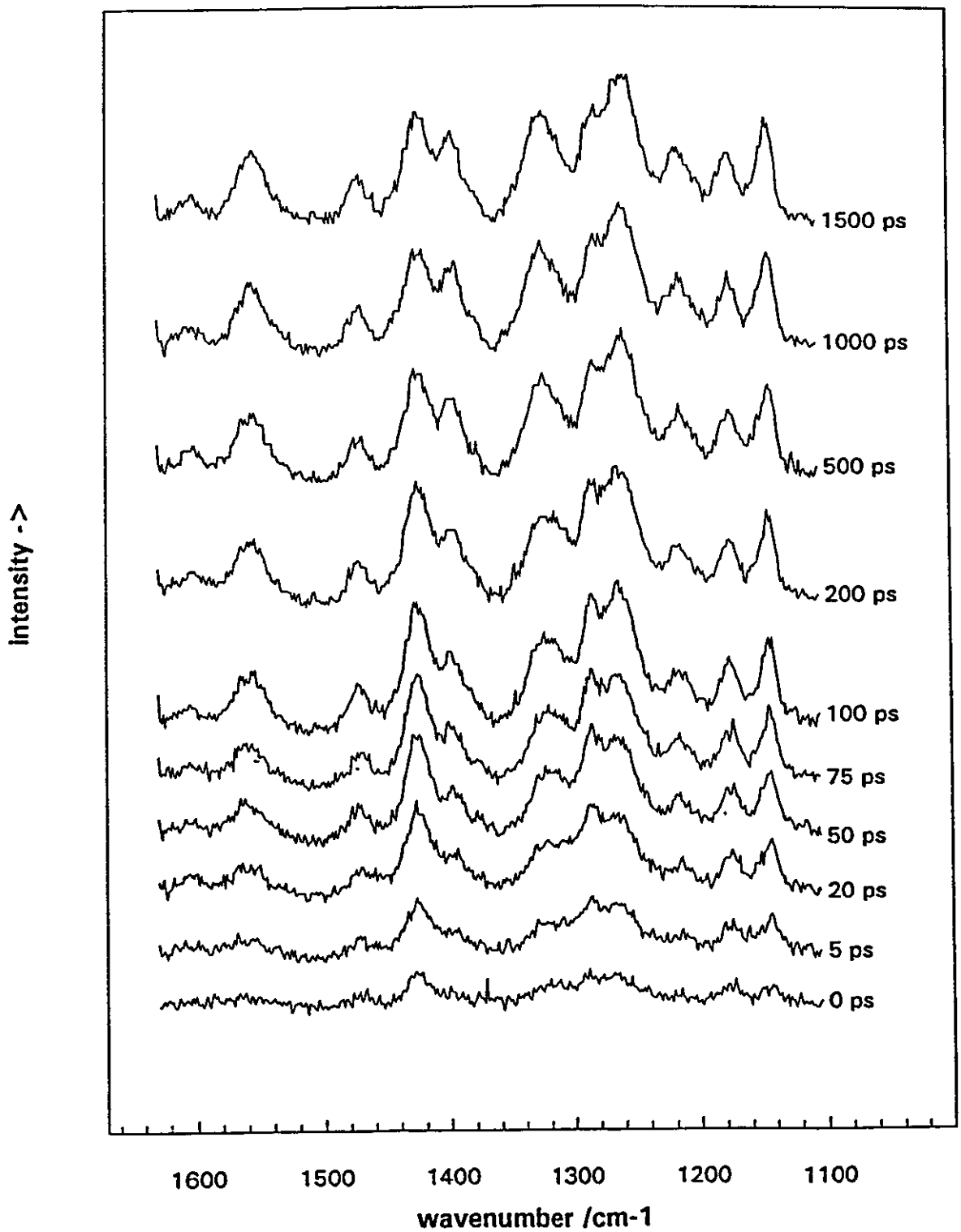

Figure 5.15. Picosecond TR^3 spectra of NOSI3 in 1-butanol.

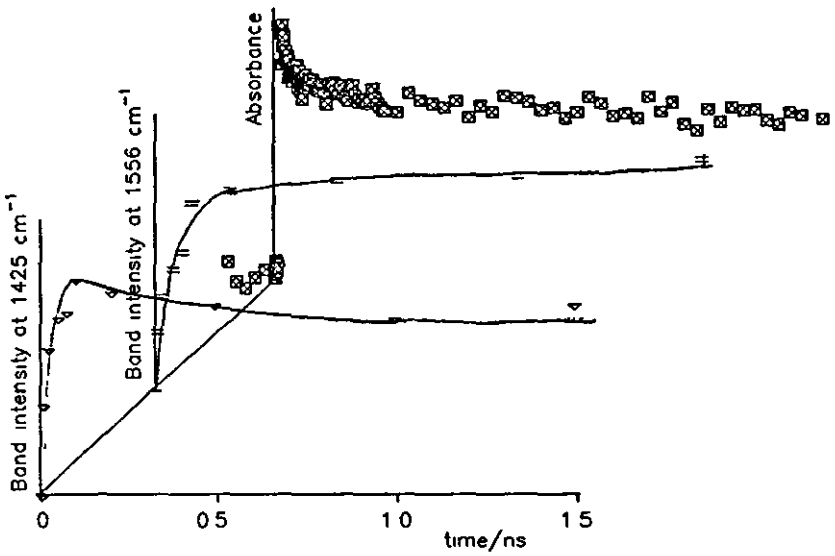

Figure 5.16. The growth of the PTR^3 spectral components with time compared to the PTA data collected over the same timescale for NOSI3 in 1-butanol.

The associations between the PTA and the PTR^3 transients are as yet only tentative and more experiments are required in order to measure kinetics for the Raman band evolution of sufficient quality for these bands to be unambiguously assigned to the PTA transients or to other species. Interpretation of the present data does suggest that the observed PTR^3 spectral changes follow the formation of the final B-form isomeric distribution, since both the α and β bands are present in the infinite time spectra and the transient spectra evolve with time to become more and more like the infinite time spectrum. This evolution in band intensity with time that was seen for NOSI3 in 1-butanol is shown in 5.15 and 5.16. Also shown on the latter plot are the PTA absorption changes that were measured for NOSI3 in 1-butanol over the same timescale. The solid lines on these plots are there merely as a visual guide and do not represent a fit to the data. The positions and relative intensities of these spectral bands are given in table 5.3.

5.3.2.2. PTR^3 studies on NOSI3 in cyclohexane.

The NOSI3 solutions in cyclohexane showed no spectral changes after t_0. It is possibile that the t_0 spectrum is slightly different to those obtained at longer time delays, however the signal was very small compared with the solvent bands that had to be subtracted and this result needs confirmation. The positions and relative intensities of the spectral bands are given in table 5.4.

Although there is no evolution in spectral shape with time for NOSI3 in cyclohexane after t_0, there may be an increase in the band intensities with time. In other

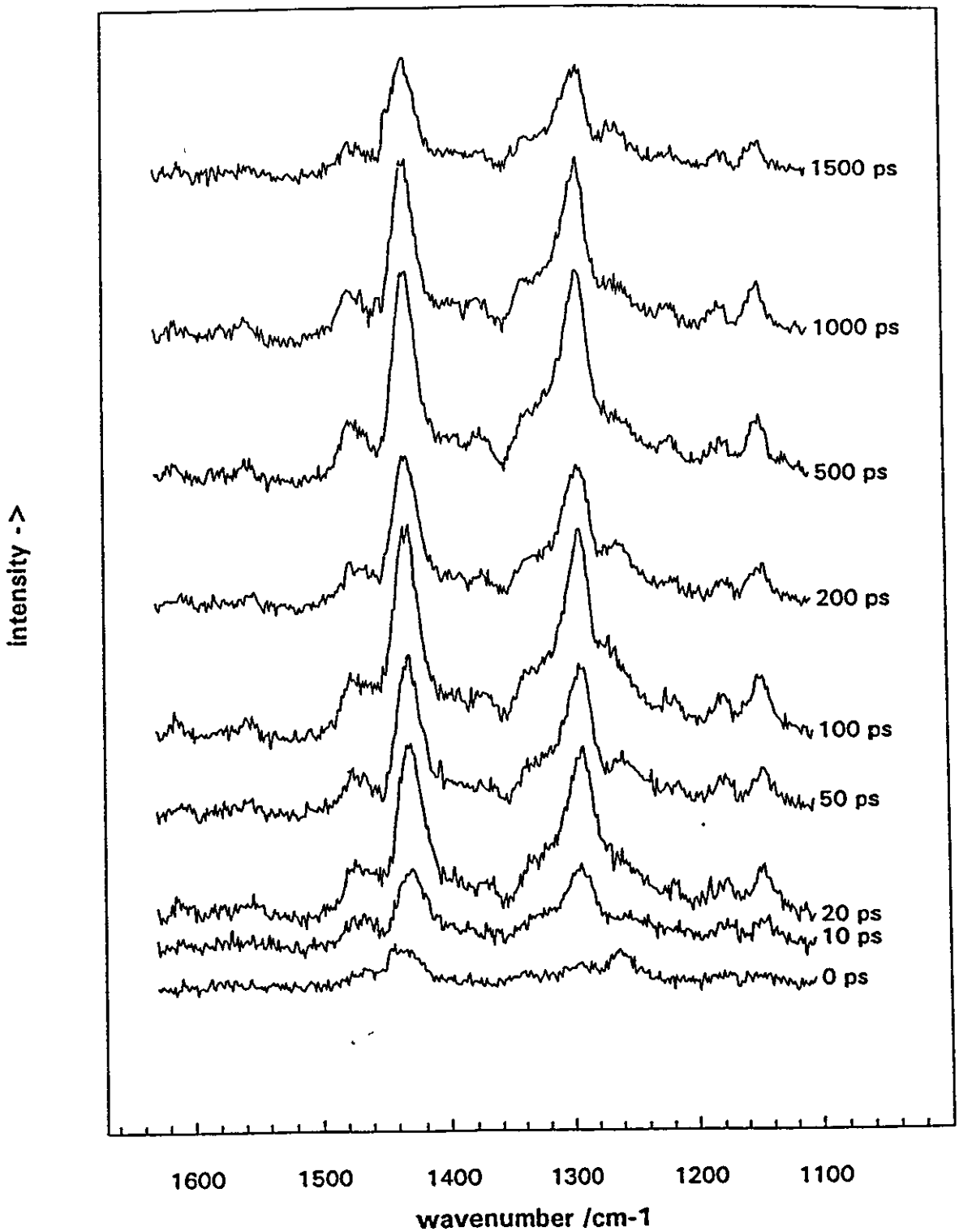

Figure 5.17. Picosecond TR[3] spectra of NOSI3 in cyclohexane.

words a single isomeric species or maybe a group of isomers may be forming with time. If there is more than one species present then they each form with the same lifetime. This increase in band intensity over the first 100-200 picoseconds is suggested from figure 5.17, however this phenomenon has yet to be confirmed. The possibility that there is a growth in the measured band intensities with time occurring over 100-200 picoseconds is consistent with the results of the PTA experiments which gave a 70 picosecond mean lifetime transient absorption decay value which was constant over the next 4 nanoseconds and which was consistent with the expected B-form absorption value. In other words the PTA work also suggests that the formation of the B-form distribution of merocyanine isomers is essentially complete after 200 picoseconds. The transient spectra obtained for NOSI3 in cyclohexane were the same shape as the infinite time spectrum throughout the full 1.5 nanosecond delay available.

Table 5.3. Band positions and intensities relative to the band centred at 1556 cm^{-1} obtained at 500 picoseconds time delay for NOSI3 in 1-butanol.

Wavenumber/cm^{-1}	FWHM/cm^{-1}	relative intensity	Assignment or Band origin.
1144	18	0.71	β
1175	19	0.47	β
1213	23	0.56	β
1259	29	1.75	β
1283	17	0.60	α*
1310	16	0.26	?
1323	18	0.51	?
1333	19	0.35	?
1396	22	0.66	β
1425	24	1.10	α*
1472	17	0.30	β
1556	33	1.00	β
1607	36	0.50	β

* These bands also correspond to the strongest bands observed in the spectrum of NOSI3 in cyclohexane and may be caused by the same species or one with a similar structure.

Table 5.4. Band positions and intensities relative to the band at 1293 cm^{-1} at 500 picoseconds time delay for NOSI3 in cyclohexane.

Wavenumber/cm^{-1}	FWHM/cm^{-1}	relative intensity	Assignment or band origin.
1146	22	0.26	β
1178	20	0.12	β
1218	22	0.13	β
1254	31	0.24	β
1293	25	1.00	α
1325	39	0.43	?
1373	12	0.07	?
1395	27	0.15	?
1428	18	0.56	α
1435	12	0.24	?
1473	19	0.22	β
1558	26	0.10	β
1614	26	0.10	?

This further implies that the only species being probed here are the final B-form merocyanine distribution of isomers. Both the α and the β forms are seen in the spectra obtained in cyclohexane however the β peaks seen here are very much smaller relative to those seen in 1-butanol. The PTR^3 spectra which were obtained for NOSI3 in cyclohexane are assigned to the TTC merocyanine isomer.

5.3.2.3. The assignment of the resonance Raman bands.

The photoisomerisation of NOSI1 in cyclohexane, benzene, acetonitrile and methanol has previously been investigated using PTR^3 by Aramaki *et al* [7]. These authors saw no spectral evolution occurring after the 50 picosecond convoluted pump and probe pulses in any of the solvents. This result is unusual in view of the work carried out by Masuhara *et al* [1] using PTA on NOSI1 in 1-butanol. These authors did detect spectral evolution occurring between the t_0 spectrum and the spectrum collected at a 400 picosecond delay. Their PTA spectral evolution was still occurring at time delays longer than the 50 picosecond resolution of the apparatus used by Aramaki *et al.* It may be that the increase in solvent viscosity upon changing solvent from methanol to 1-butanol increases the lifetimes of the transformations which occur after photoexcitation.

In the PTR^3 work of Aramaki *et al* (7) the spectra obtained for NOSI1 were different in the different solvents used, also the spectra obtained for a similar NOSI compound, with a nitrogen replacing the carbon at the 7'-position, were substantially different to the NOSI1 spectra. In view of this latter result they concluded that the observed bands were predominantly due to both the oxazine and bridged regions of the molecule. They further suggested that, since the B-form absorption in the visible region is due to Π-electron conjugation between the NOSI indoline nitrogen and the oxygen, the bands with the strongest intensities should also be associated with this part of the molecule. They found that these bands were not affected by structural changes that occurred elsewhere on the molecule. In this way the strongest bands were assignable to C=N, C-C, and C=C stretches. These bands were generally positioned at 1410-1420 cm^{-1}, 1290-1300 cm^{-1} and 1550-1560 cm^{-1}. Their apparatus produced a probe wavelength of 574nm whilst the present PTR^3 study uses a probe wavelength of 580nm, these two wavelengths will be probing the same events occurring at the same regions on the molecule.

In cyclohexane there were two main bands in Aramaki's spectrum which were located at 1293 cm^{-1} and 1419 cm^{-1} and a third smaller band at ~1560 cm^{-1}. In methanol similar bands were found at 1293 cm^{-1}, ~1424 cm^{-1} and 1551 cm^{-1}. The present study places these bands at 1293 cm^{-1}, 1428 cm^{-1} and 1558 cm^{-1} for NOSI3 in cyclohexane and at 1283 cm^{-1} 1425 cm^{-1} and 1556 cm^{-1} in 1-butanol.

It was notable from the spectra obtained for NOSI1 by Aramaki *et al* (7) that the sharpest bands occurred in cyclohexane solutions with other bands tending to form around these positions as the solvent was changed from non polar cyclohexane to more polar solvents, such as acetonitrile and hydrogen bonding solvents, such as methanol. This effect is also observed in the present work as the solvent is changed from cyclohexane to 1-butanol. This phenomena can be explained if a single isomeric species is predominant in cyclohexane, with other species becoming stabilised in 1-butanol and the other polar solvents. The bands forming around the bands seen in cyclohexane would then be due to the same C=N, C-C and C=C stretches but occurring on the other isomeric species, with the bands shifted slightly because of differences in the conformations of the different isomers. Further PTR^3 experiments are required on the NOSI3 systems in 1-butanol and cyclohexane in order to establish better kinetic data for the growth of the individual bands with time. Such work will enable us to determine whether the α peaks form initially and the β peaks form as these decay or if the two sets of peaks develop individually but with different rates. It could also be established if a third set of peaks is also developing on this timescale.

5.3.2.4. Summary of the PTA and PTR^3 results and conclusions.

The model used to explain the results of these picosecond studies is summarised in the scheme given below.

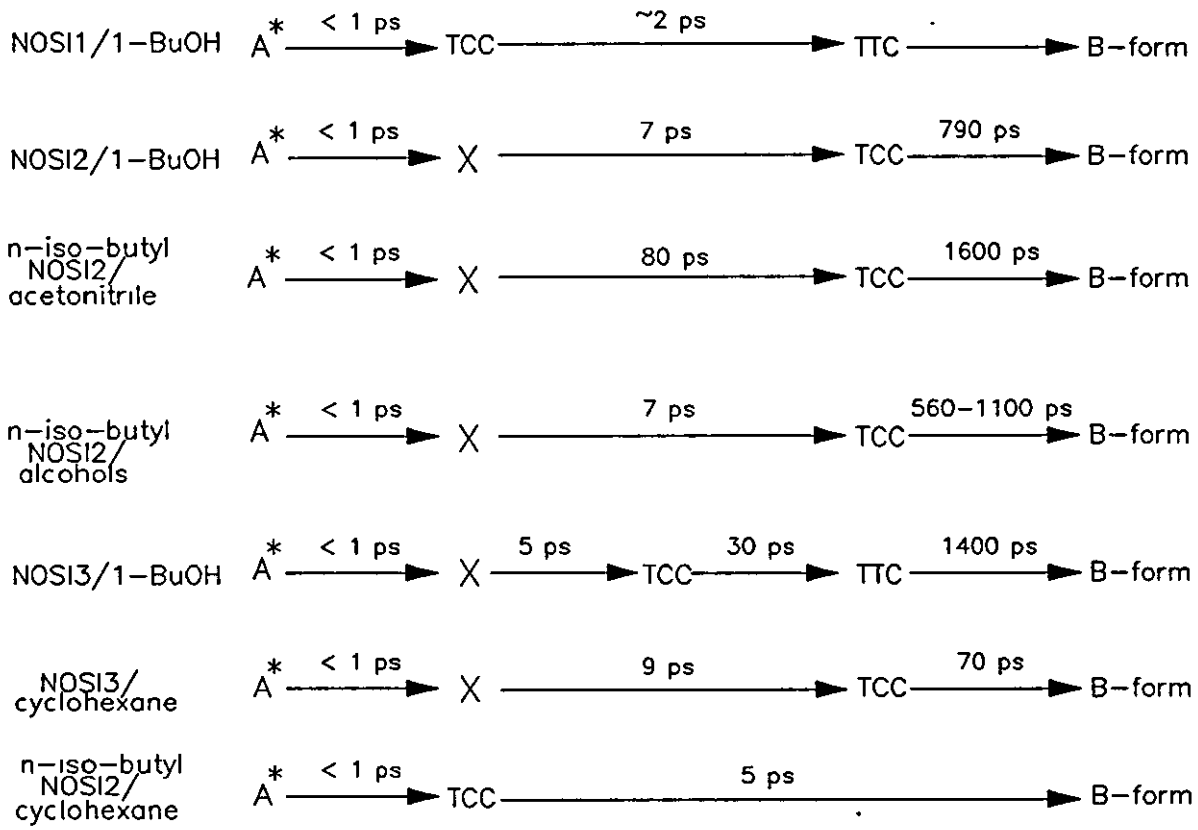

The initial rise kinetics are not obviously affected by the choice of solvent, with the initial step occurring within the convoluted pump and probe pulse overlap. The initial rise within these pulses is most probably due, in part, to the formation of the first excited singlet state A*. The spiro C-O bond of A* would then break forming X this would probably also occur within the pulse overlap. The transient states occurring after this primary step can be accounted for as follows:

For the alcoholic solutions of NOSI2 and n-iso-butyl NOSI2 the initial formation of A*/X within the pulse is followed the formation of TCC with lifetime of ~7 picoseconds. TCC then forms TTC with lifetimes varying from 560 picoseconds in 1-propanol to 1100 picoseconds in 1-decanol. These decays have end of trace values that are consistent with those expected from the equilibrated B-form absorption. The TTC isomer will probably be required to equilibrate in the alcohol to give the most favourable B-form isomeric distribution

For n-iso-butyl NOSI2 in cyclohexane the B-form forms directly from the transients which are formed within the pump and probe pulse convolution assigned here as $A^*/X/TCC$. The B-form is formed with a lifetime of ~5 picoseconds. No effects due to isomeric redistributions are observed since the TTC isomer formed initially, from TCC, will be most stable B-form in cyclohexane.

For n-iso-butyl NOSI2 in acetonitrile it is likely that A^*/X forms within the excitation pulse. X then isomerises to the TCC isomer with a lifetime of 80 picoseconds. The final B-form is then produced following an isomerisation from TCC to TTC with a 1600 picosecond lifetime. The TTC isomer may also undergo an isomeric redistribution to give the most stable B-form.

For NOSI3 in 1-butanol the initial absorption rise occurs within the excitation pulse and is probably due to the formation of A^*/X. X then directly forms TCC with a lifetime for this process of ~5 picoseconds. The TCC absorption then decays with a 30 picosecond lifetime forming the un-equilibrated TTC B-form isomer. The TTC state that originally forms should be the most stable in cyclohexane [2] but not in 1-butanol. It may therefore undergo an isomeric equilibration to give the most stable B-form distribution.

NOSI3 in cyclohexane forms A^*/X within the pulse convolution. X then forms the TCC isomer with a lifetime for this process of ~9 picoseconds. TCC can then directly form the TTC isomer a process which occurs with a 70 picosecond lifetime. There is one criticism of this scheme and that is that TCC is supposedly a charge separated state which should have a shorter lifetime in cyclohexane than in 1-butanol. This is not found in practice and the assignments of TCC to the 70 picosecond transient observed in cyclohexane and the 30 picosecond species seen in 1-butanol may not be correct in both cases.

The band evolution observed in the PTR^3 experiments has given some interesting conclutions. From this work it is suggested that at least two transient states, α and β, are involved in the formation the NOSI3 B-form. The α state is predominant in cyclohexane and both α and β species are seen evolving in 1-butanol. The changes seen in the PTR^3 spectra will probably be due to transformations to and between the possible B-form isomers and not to any other transient species. For NOSI3 in cyclohexane the α peaks predominate, a result which may imply that a single isomeric species is formed in this solvent which does not require further equilibration. This is in agreement with the PTA results. It is suggested that the single species which gives the α peaks is in fact the TTC isomer.

In 1-butanol solutions of NOSI3 the PTR[3] spectra show 2-3 components. The component formed with the fastest grow in time results in the development of the α peaks. These grow over ~100 picoseconds then start to decay slightly. The β peaks rise rapidly in intensity over ~200 picoseconds changing to a slower rate of increase similar to the rate of decay seen for the α peaks. The α peaks observed for NOSI3 in 1-butanol could correspond to the strongest absorption bands measured for the same compound in cyclohexane. The spectral changes that occur with time lead eventually to the thermally equilibrated infinite time B-form spectrum.

A reaction scheme is given below, based on the results presented here, showing some of the transformations which may be occurring during the photochemical formation of the B-form.

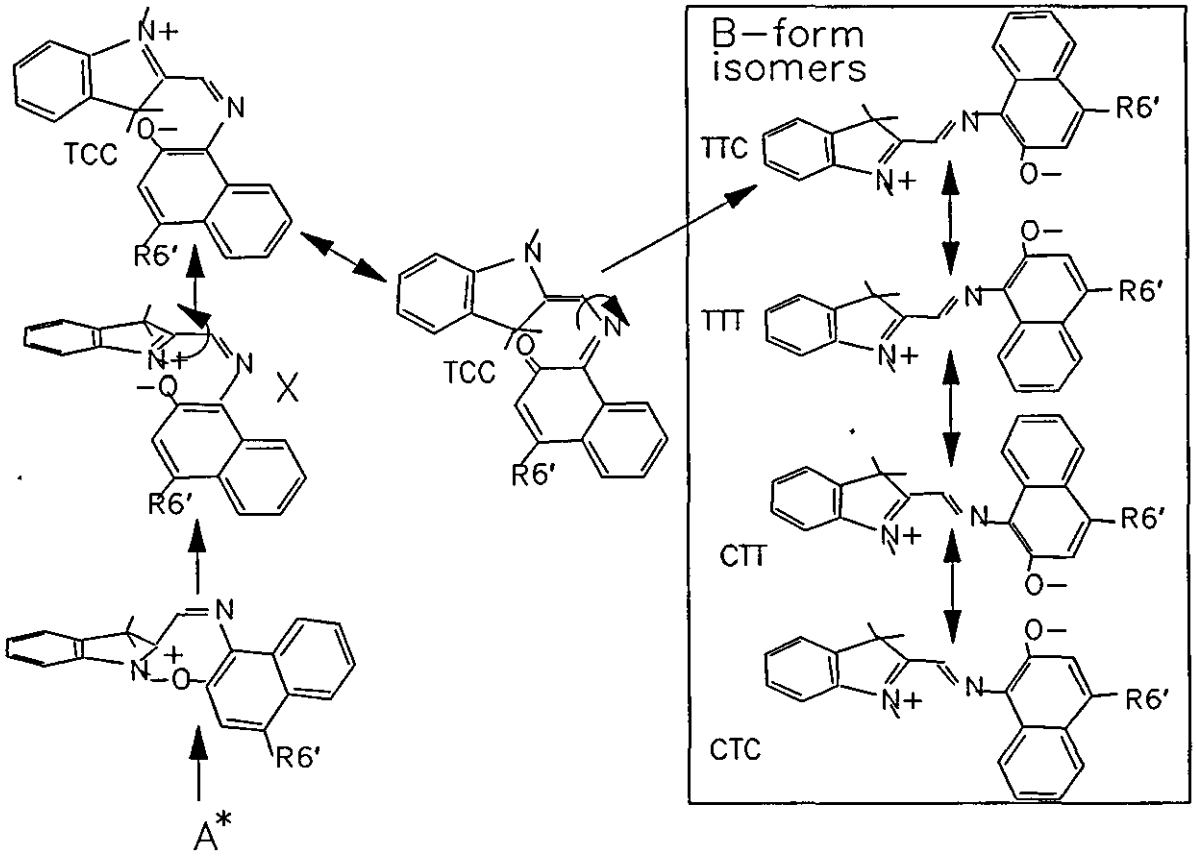

References.

1. H. Masuhara, N. Tamai, Chem. Phys. Lett., 191, (1,2), 1992, 189.

2. S. Schneider, A. Mindl and G. Elfinger, Ber. Bunsenges. Phys. Chem. 91, 1222-1224. 1987.

3. C. Bohne, M.G. Fan, Z.J. Li, Y.C. Liang, J.C. Scaiano, J.Chem. Soc. Chem. Comm. 1990, 571.

4. A. Kellmann, F. Tifbel, J. Photochem. Photobiol, A, Chem. 41, 1988, 299.

5. N. W. Tyer and R. S. Becker, J. Am. Chem. Soc., 92(5), 1970, 1289.

6. C. Bohne, M.G. Fan, Z.J. Li, Y.C. Liang, J. Lusztyk, J.C. Scaiano, J. Photochem. Photobiol. ,A, Chem. 66, 1992, 79.

7. N.P. Ernsting, Arthen Engeland, J. Phys. Chem. 95, 1991, 5502.

8. S. Aramaki, G. Atkinson,

9. N. Takahahshi, K. Yoda, H. Isaka, T. Ohzeki, Y. Sakaino, Chem. Phys. Lett., 140, 1987, 90.

10. S. Aramaki and G. Atkinson, Chem Phys. Lett. 1990, 170, 181.

11. S.L Murov, I. Carmichael, G.L. Hug, Handbook of Photochemistry, 2nd Ed. Marcel Dekker, ISBN 0-8247-7911-8, 1993, 284.

12. N.J. Turro, Modern Molecular Photochemistry, Benjamin Cummings Pub. Co. 1978 ISBN- 0-8053-9353-6, 7.

CHAPTER 6

CONCLUSIONS.

Chapter 6 Conclusions.

6.1. Introduction.

The aim of this thesis and the work described within it has been to obtain a concise picture of the behaviour of naphthoxazine spiro indoline or NOSI systems over a wide range of conditions in order to gain a fundamental understanding of the processes involved in their different photochemical and thermal reactions. The Basic photochemical and thermal isomerisation reactions are shown below in figure 6.1.

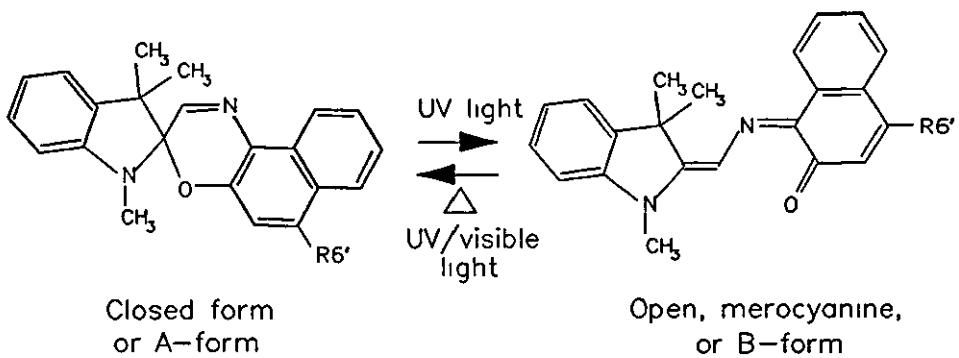

Figure 6.1. The basic NOSI reaction.

In particular the effects of different 6'-substituents and n-alkyl substituents upon these NOSI reactions have been investigated. The naming of these compounds is given below in table 6.1.

Table 6.1. The nomenclature used for the different NOSI compounds.

6'–substituent	Compound
H	NOSI1
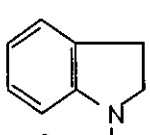	NOSI2
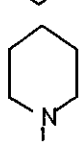	NOSI3
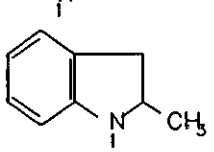	NOSI4

n-propyl NOSI2 and n-iso-butyl NOSI2 have also been investigated in this work.

Several aspects of NOSI chemistry have been studied using a wide range of experimental techniques some of which can be undertaken in most modern chemical laboratories and some, which use more advanced apparatus and methods, that are available only in highly specialised facilities. The photochemical methods used in this work range from simple U.V/visible spectroscopy using a photographic flash gun as the excitation source to create photochemical products, as described in chapter 2, to the picosecond pump probe experiments, described in chapter 5, which use state of the art modern laser systems which are capable of producing laser excitation pulses of less than 1 picosecond in duration. The NOSI systems investigated here were chosen in the hope that the different solvents and substituents would produce changes in the potential energy surfaces of both the ground and excited states of the NOSI molecule and thus enable us to determine the nature of the transformations which occur there. In this way we have been able to gain a great deal of understanding about the different processes that are involved in the reactions that occur on these surfaces. Even though several very different NOSI systems have been investigated using a wide range of experimental techniques it is now possible to draw together all of the results that were obtained. This overview of these results will give a better understanding of the processes involved in NOSI photochromic reactions and may thus allow predictions to be made concerning the behaviour of other NOSI systems which have not yet been researched.

6.2. The absorption spectra of NOSI systems.

6.2.1. The A-form absorption spectra.

A knowledge of the A-form spectra of the NOSI compounds to be investigated was required before further work could be carried out. Molar decadic absorption coefficients had to be determined for this form of the molecule before they could be found for the corresponding B-forms. The ϵ_A values determined at the peak maximum of the lowest energy transitions was generally around 10000 $dm^3.mol^{-1}.cm^{-1}$. These peaks were positioned at wavelengths above 270nm and were the absorption bands that would be excited in all of the work which followed in order to initiate the photochemical reactions of NOSI compounds. Very little solvatochromism was seen for these absorption bands, although as may be expected spectral broadening did occur upon changing from non-polar to polar solvents. In view of the size and behaviour of these transitions they have been assigned as $\Pi - \Pi^*$ in nature. It has been shown in this work that whilst the NOSI compounds are in their A-forms the oxazine and the indoline halves of the NOSI molecules may be acting independently of one another in terms of their contributions to the measured NOSI absorption spectrum. This effect has been convincingly demonstrated for several NPSI and BPSI compounds [1,2], but is only

implied to be the case for the NOSI compounds studied here, since model compounds for the oxazine ring have as yet not been synthesized. It has, however, been possible to identify some of the spectral bands expected from the indoline moiety under the NOSI1 absorption envelope. If the two halves of the NOSI1 molecule are isolated then photo-excitation above 315nm would specifically excite the oxazine half of the molecule whereas with excitation below 315nm both halves of the molecule can be excited. The relative excitation occurring on each half of the molecule is dependent upon the relative absorption that occurs on each of the two halves at the excitation wavelength. In support of this theory, Kholmanskii *et al* measured a lower value of Φ_A when irradiating NOSI1 in ethanol at 313nm than they did when irradiating the same solution at 366nm, a result which they put down to a poor energy transfer efficiency from the indoline ring across the spiro bond and too the oxazine C-O bond (3).

The basicity of the 6'-substituent greatly affects the A-form absorption spectrum. The spectra obtained were red shifted in the order NOSI4≥NOSI2>NOSI3>NOSI1. This does not simply follow the trends in the substituent basicity, the 6'-indoline on NOSI2, although not the most electron donating group, does extend the conjugation of the oxazine ring more than the 6'-piperidine group does on NOSI3 and the resulting NOSI2 spectrum is more red shifted. These 6'-substituent shifts tend to confirm the assignation of these A-form transitions as being $\Pi - \Pi^*$, since $n - \Pi^*$ transitions would be expected to blue shift upon the replacement of the 6'-hydrogen by a piperidine or an indoline. This would occur because the electrons from the hetero atoms on these rings raise the energy of the Π -bonding orbitals more than they do the antibonding orbitals, leaving the non bonding orbitals at the same energy.

Table 6.2. S_1->S_0 energies for indoline and NOSI1-4 A-forms.

Compound	Estimated position of 0->0 transition/nm	Estimated S_1->S_0 energy/kJ.mole^{-1}
Indoline	300	399
NOSI1	350	342
NOSI2	386	310
NOSI3	370	323
NOSI4	386	259

Note that no discernible solvent shifts were observed for the A-form spectra and therefore no solvent information has been given.

The lowest excited singlet state energies for indoline and NOSI1-4 can be estimated using the estimated positions of the peak maximum of the lowest energy transition this has been done and these energies are given in table 6.2. These are rough estimates because the spectra are sometimes broad and featureless and the 0->0 transitions are therefore very difficult to pin-point, this is especially true for NOSI2 and NOSI4.

6.2.2. The B-form absorption spectra.

The spectral properties of the B-form were investigated after the relevant values of ϵ_A had first been determined. Using these values of ϵ_A it was then possible to measure the values of ϵ_B for the corresponding NOSI B-forms. The spectral measurements that were made for the B-forms demonstrated that these compounds exhibited strong solvatochromism towards the red end of the spectrum as the solvent polarity was increased. Accompanying these red shifts was an increase in the measured values of ϵ_B. The value of ϵ_B determined for NOSI2 increased from 40000 to 58000 $dm^3.mol^{-1}.cm^{-1}$ upon changing the solvent from cyclohexane to methanol this increase occurred at the same time as the peak maximum shifted from 562 to 611nm. The solvent shifts seen for NOSI merocyanine type structures as the polarity changes have been explained in terms of the first excited singlet state of the B-form being a more charge separated species than the ground state [4]. For many merocyanine dyes, BPSI and NPSI, the solvent shifts are in the opposite direction to those occurring for NOSI B-forms a result which has been put down to the ground state being a more charge separated species than the first excited singlet state [1,5,6,7,8]. The reason why this difference in the charge separations of the two states occurs is explained in terms of the possible resonance structures in which the B-form isomers can exist. Merocyanine isomers are highly conjugated and are able exist as a resonance hybrid made up of contributions from a quinoidal resonance structure and contributions from a zwitterionic form. If the two ends of a NOSI merocyanine isomer have different basicities then the individual resonant structures will not be degenerate. However the ground state of the resonance hybrid will have a lower energy than either of the individual resonant structures due to resonance stabilisation energy.The solvent shifts that were observed here for all of the NOSI B-forms imply that of the two possible resonant forms which can contribute to the ground state of the B-form, it is the less charge separated quinoidal structure and not the zwitterionic form which is the major contributor. The zwitterionic character is therefore predominantly taken up by the first excited singlet state. An energy level diagram which shows the effects of solvent polarity upon the S_1->S_0 transition is shown for a typical NOSI compound in figure 6.2.

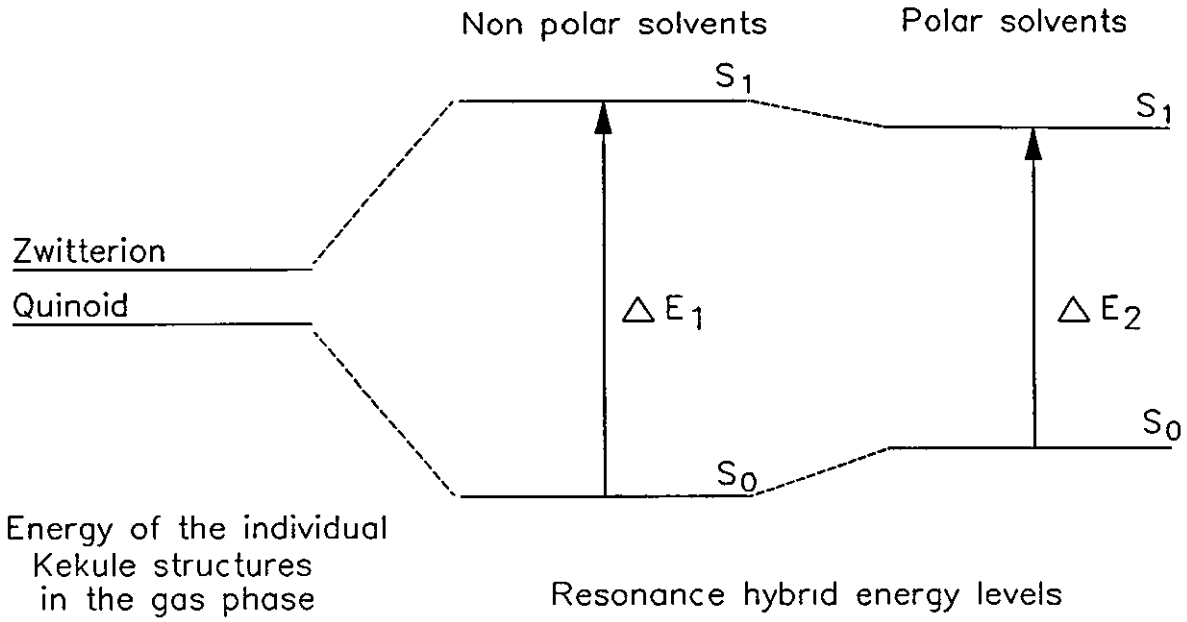

Figure 6.2. Diagram showing the effect of solvent polarity upon the $S_1 \rightarrow S_0$ transition for a NOSI resonance hybrid ground state which is predominantly quinoidal and a first excited singlet state which is polar.

One result which did not fit in with the explanation for the solvent shifts that is given above is that the B-form peak maximum that was measured for NOSI2 and n-iso-butyl NOSI2 in acetonitrile is closer to that observed in benzene solutions than that measured in methanol solutions. This result suggests that solvent polarity is not alone in determining the observed spectral shifts because acetonitrile and methanol have polarities more similar to one another than to benzene. If the relative contributions from the zwitterionic and the quinoidal structures to the ground state and first excited singlet state and the effects of solvent polarity upon these states, was the only factor governing the position of the peak maximum then the spectra of the n-alkyl NOSI2 compounds should be similar in acetonitrile and methanol and both of these should be different to that measured in benzene. Since this is not the case some other mechanism must be influencing this result.

As is the case for NPSI [9] the relative stabilisation of the four possible merocyanine isomers, that are trans about the central C-N bond and which make up the B-form, may also be a factor in determining the spectral positions in the different solvents. The possible merocyanine isomers that are trans about the C-N bond are given in figure 6.3 in their zwitterionic forms. The relative stability of the different isomers in the different solvents is qualitatively discussed below.

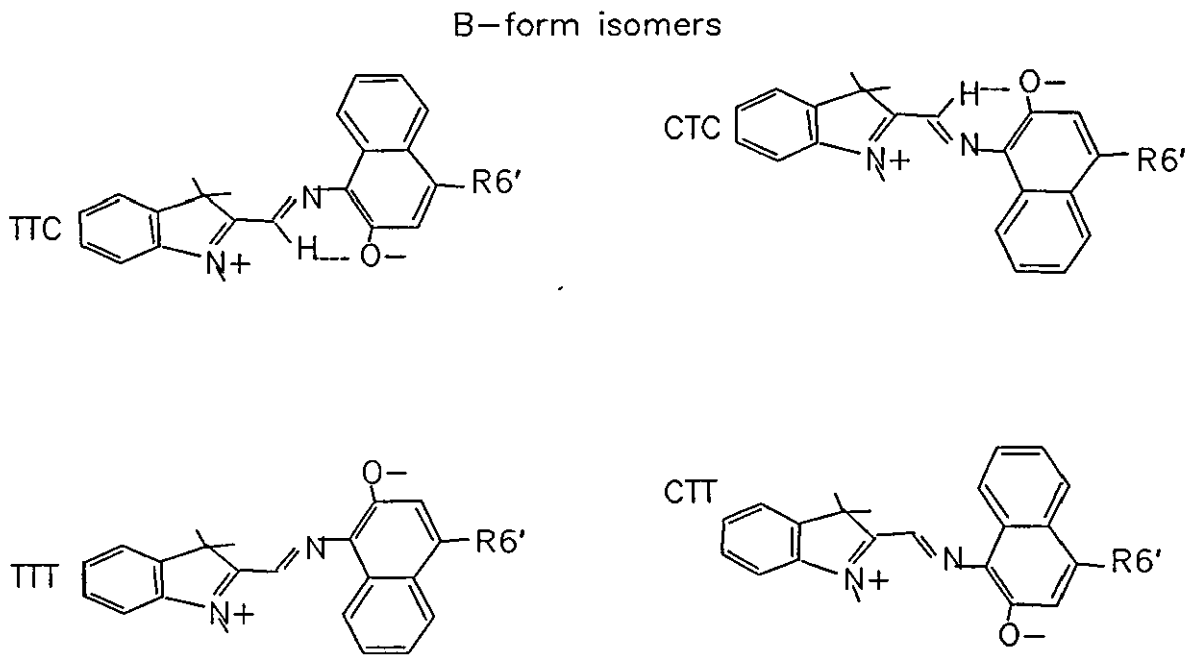

Figure 6.3. The merocyanine isomers which can contribute to give the B-form.

The TTC isomer is likely to be the most favoured in aliphatic hydrocarbon solvents since it is the least charge separated [10,11,12]. In the case of TTC the ability of the molecule to form efficient hydrogen bonds with the solvent is reduced because the hydrogens in the bridged region form intramolecular hydrogen bonds instead [10,11,12]. This effect will tend to stabilise this isomer even more in low polarity solvents. Another factor which has to be taken into account in the following arguments is the bridged region hydrogen interaction with the C_{10} hydrogen, which for TTC is minimal [10].

CTT has an unfavourable interaction occurring between the bridge hydrogens and the C_{10} hydrogen. This isomer will however be stabilised by hydrogen bonding solvents because intramolecular hydrogen bonding does not occur to the same extent as for TTC, further the charge separation for this structure is greater than that of the TTC isomer which means it will tend to be slightly less stable in aliphatic hydrocarbon solvents, but may be favoured in polar solvents [10,11,12].

CTC is poorly stabilised by hydrogen bonding solvents because the bridged region hydrogen interacts with the oxygen in the same way as for TTC [10,11,12]. The charge separation of this form is about the same as for CTT.

TTT is the most charge separated of the four isomers and will be least stable in non polar aliphatic solvents, however since it does not form intramolecular hydrogen bonds in the same manner as CTC or TTC it will be stabilised in hydrogen bonding solvents [10,11,12].

The effects mentioned above are summed up in the trends given below.

(a) The ability to hydrogen bond with the solvent decreases in the order: TTT~CTT>CTC~TTC.

(b) Intramolecular hydrogen bonding decreases in the order: TTC~CTC>CTT~TTT.

(c) Charge separation decreases in the order: TTT>CTT~CTC>TTC.

(d) Bridged region hydrogen interaction with the C_{10} oxygen decreases in the order: TTT=CTT>TTC=CTT.

(e) The overall steric hindrance is said to decreases in the order: CTC>TTC~CTT>TTT [10]. The bridged hydrogen interactions with either the oxygen or the C_{10} hydrogen is the main factor that needs to be taken into account in the placing of these isomers in this order.

From the above arguments the following contributions from each isomer may be expected to occur in the different solvent types:

In aliphatic non polar solvents TTC is expected to be the most stable with CTC also stabilised but to a lesser extent.

In polar solutions of BPSI and 6-nitro BPSI it has been suggested that the TTT isomer is too charge separated for stabilisation by solvent polarity alone to overcome the effects of the large electrostatic separation [10,11] and in fact it is the CTT and CTC isomers which are suggested to be the most stable forms in non-protic polar solvents. This may or may not be expected in the case of NOSI compounds, since these are presumed to be more quinoidal than zwitterionic and therefore in general less charge separated. Also where there is an electron donating 6'-substituent the overall charge separation is likely to be further reduced.

In hydrogen bonding solvents TTT and CTT are expected to be the major contributors to the observed spectral envelope [10,11,12].

From steric considerations the Π-electron overlap is likely to decrease in the order TTT>CTT~TTC>CTC. The steric interactions in the bridged region will tend to force the two halves of the molecule out of planarity which will lead to a decrease in the conjugation of the system and a corresponding increase in the energy of the $\Pi - \Pi^*$ transition. Thus the trend in the total steric interactions should follow the trend in the spectral shift for each isomer towards the blue. In other words TTT should absorb at longer wavelengths than CTT and TTC which will in turn absorb at longer wavelengths than CTC. In the polar hydrogen bonding solvents such as methanol the absorption spectra are shifted the furthest towards the red which is consistent with the largest contribution coming from the TTT isomer.

In non protic acetonitrile CTT and CTC are likely to be the major isomers since the

spectrum is not shifted as far to the red as in methanol. This suggests that there is a different isomeric distribution in the hydrogen bonded solvents to that which occurs in the non protic solvents even when the polarity is the same. This result suggests that as is the case for BPSI and NPSI B-forms [10,11] the TTT isomer is in fact too charge separated to be stabilised more than CTT and CTC in non protic polar solvents. In cyclohexane the B-form spectra of the NOSI compounds studied are the most blue shifted. This is consistent with a relatively large contribution to the spectral envelope from either the TTC or the CTC isomers.
It is possible to estimate the energy of the S_1->S_0 transition for the B-form spectra obtained in the same way as has already been done for the A-form spectra in table 6.2. The values are given in table 6.3.

Table 6.3. S_1->S_0 energies for NOSI1-4 B-forms estimated from the positions of the peak maxima in different solvent.

Compound	Estimated position of 0->0 transition/nm	S_1->S_0 energy/kJ.mole^{-1}
NOSI1	555 cyclohexane 592 toluene 612 ethanol	216 202 196
NOSI2	562 cyclohexane 583 toluene 611 methanol	213 205 196
NOSI3	560 toluene	214
NOSI4	588 toluene	204

Note that the values given in table 6.3 are quite possibly associated with the S_1->S_0 energy for the isomer which is contributing the most to the measured spectrum in each solvent. The energies given may therefore be for quite distinct conformations of the NOSI B-form.

In summary the shifts in the B-form spectra are probably determined to a large extent by the stability of the various B-form isomers in the different solvents as well as by the relative contributions from either the quinoidal or the zwitterionic forms to the B-form resonance hybrid.

6.3. The ground state potential energy surface.

There were two main results from the experiments designed to investigate the NOSI ground state potential energy surface. The first of these was that the rate of the thermal reverse reaction was retarded upon increasing the size of n-alkyl side chain. This effect is probably the result of a steric requirement that the n-alkyl group has to adopt a specific orientation with respect to the oxazine ring prior to isomerisation. This requirement shows up in the fact that the value of $\Delta S^{o\ddagger}$ becomes more negative as the n-alkyl group size is increased whereas the value of $\Delta H^{o\ddagger}$ remains constant. This result can be explained only if the oxazine half of the molecule passes on the same side of the molecule as the n-alkyl group during the isomerisation, then the n-alkyl group has to orientate itself out of the way of the oxazine ring before the isomerisation can proceed any further. This being so it is suggested that only a certain fraction of the NOSI molecules will possess this orientation and the entropy of activation is a more negative for the compounds with the bulkier groups. This means that the molecule must rotate through either a CCC or a CCT conformation during the isomerisation reaction occurring on the ground state potential energy surface. Of these two isomers it is the CCC isomer that is most likely intermediate since it is less sterically crowded than CCT. The CCT isomer has been proposed as an intermediate in the thermal fade reaction of BPSI [13], however this conformation is not likely to occur for NOSI compounds because the oxazine ring is much bigger than the bezopyran ring and the CCT isomer would be sterically crowded.

The second result of this work was that increasing the electron donating power of the 6'-substituent decreased the rate of the thermal reverse reaction. This effect is most probably caused by the stabilisation of the B-form isomers relative to some transition state. In this case the stability of the B-form is enhanced by its ability to exist in more resonant forms with either the oxygen or the NOSI indoline nitrogen resonant with the 6'-group. This stabilisation would not occur to the same extent for any species which is cis about the central C-N bond because such a conformation would be less effectively conjugated due to steric effects. If the CCC isomer is an intermediate in the thermal fade reaction then it would not be stabilised to the same extent as the B-form by the 6'-groups electron donating power and this would result in a net increase in the activation barrier for the thermal fade reaction.

6.4. The values of Φ_A and Φ_B/Φ_A determined for various NOSI solvent systems.

The ratio Φ_B/Φ_A was determined in several solvents for several NOSI molecules. The measured value was generally less than 0.06. In other words the forward photochemical reaction occurs with a much greater efficiency than the reverse reaction when the sample is irradiated with 352nm and 414nm light.

The value of Φ_A decreased as the solvent polarity increased for NOSI1, NOSI2 and n-iso-butyl NOSI2. This could indicate that there may be a transient that is present in the photochemical isomerisation reaction which is affected in some way by solvent polarity, for example the intermediate may be some charge separated species.

As the electron donating power of the 6'-group decreases the value of Φ_A decreases. This result could be caused either by a reduction in the spiro C-O bond order due to electron donation from the 6'-group or it could be due to an affect further on in the isomerisation reaction caused by the stabilisation or destabilisation of some intermediate state.

Interestingly there was no effect upon the value of Φ_A caused by increasing the length of the n-alkyl side chain from a methyl to an iso-butyl group.

The value of Φ_A was lower for n-iso-butyl NOSI2 in more rigid polyurethane matrices, however there was again no effect seen upon replacement of the n-iso-butyl group with an n-methyl group in these more rigid media. This result suggests that a harder more cross linked polyurethane matrix reduces the forward efficiency, possibly because the increased viscosity hinders the rotations that the molecule must undergo in order to form the B-form.

The fact that the photochemical isomerisation is unaffected by increasing the size of the n-alkyl group suggests that the forward photochemical mechanism is different to the thermal reverse reaction mechanism which is significantly retarded by increasing the size of the n-alkyl chain.

These results are consistent with a transient in the photoisomerisation which is charge separated and with the n-alkyl group positioned away from the oxazine ring during the subsequent bond rotations occurring as the B-form isomers are formed. The TCC or TCT isomers are possible candidates for such a transient.

6.5. The NOSI photoisomerisation via the triplet state.

The energy of the NOSI2 triplet state in toluene was measured and found to lie between 210 kJ.mol^{-1} and 193 kJ.mol^{-1}. The triplet energy of NOSI1 has been determined by other workers [14] to be 212 kJ.mol^{-1}. Since the two halves of the NOSI molecule are most probably held at right angles to each other, the two heterocyclic regions are likely to be electronically isolated from one another [1,3]. If this is true then the indoline half of the

molecule should have a triplet energy that is different to the triplet energy of the oxazine half of the molecule. If this is the case then the triplet energies given above are more than likely the energies for the triplet state of the oxazine half of the molecule. This is suggested because the triplet energy of the indoline ring should be closer to those measured for similar compounds such as indole and aniline which both have triplet energies of ~300 kJ.mol^{-1} [15]. In view of this, when para-methoxy acetophenone was used as the sensitizer it is quite possible that both the oxazine and the indoline halves of the molecule had triplet energy donated to them since the triplet energy of this donor is 300 kJ.mol^{-1} [16]. The fact that the B-form yield was still unity when using para-methoxy acetophenone as the triplet energy donor suggests that energy transfer across the spiro link is 100% efficient from the indoline in its triplet state. Remember that Kholmanskii *et al* found that direct excitation of the oxazine and indoline parts of the molecule with the 313nm light from a mercury lamp did not yield the B-form as efficiently as excitation solely onto the oxazine half of the molecule with 366nm light [3]. This suggests that under conditions of direct excitation the energy transfer across the spiro link may not be as efficient as it is via the triplet state and the reaction following direct excitation will probably proceed at least to some extent through an excited singlet state and not solely via a triplet state.

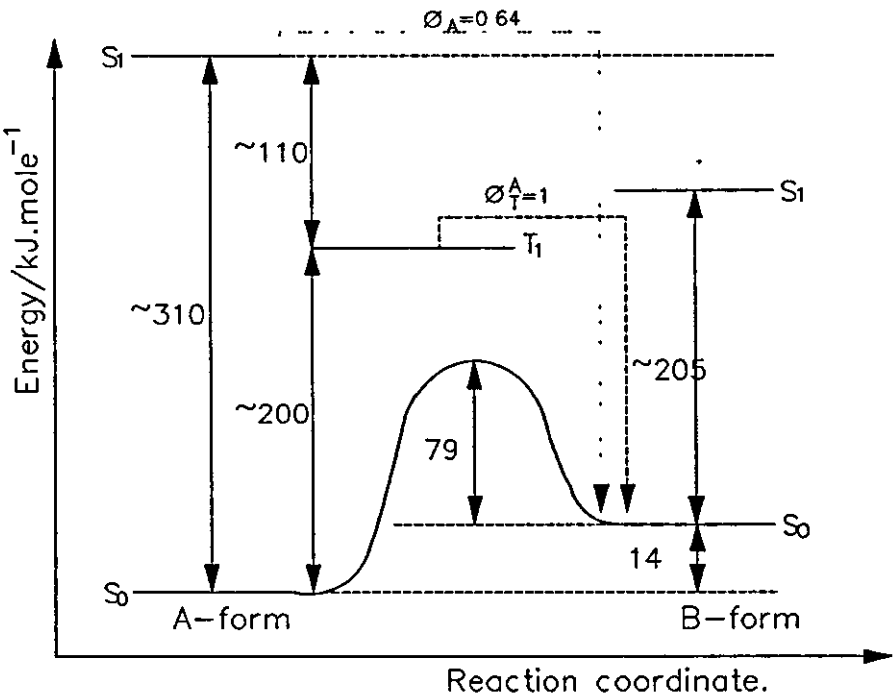

Figure 6.4. The energy level diagram for NOSI2 in toluene.

It is now possible to draw an energy level diagram for NOSI2 in toluene that includes the ground state potential energy surface, the energy of A-form and B-form $S_1 -> S_0$ transitions and the A-form triplet energy (probably the oxazine triplet) in toluene, from an amalgamation of the results described so far in this chapter. This has been done and is shown in figure 6.4.

6.6. Picosecond transient absorption (PTA) and picosecond time resolved resonance Raman (PTR^3) experiments.

The results obtained from the picosecond transient absorption (PTA) experiments have lead to the following reaction scheme being proposed:

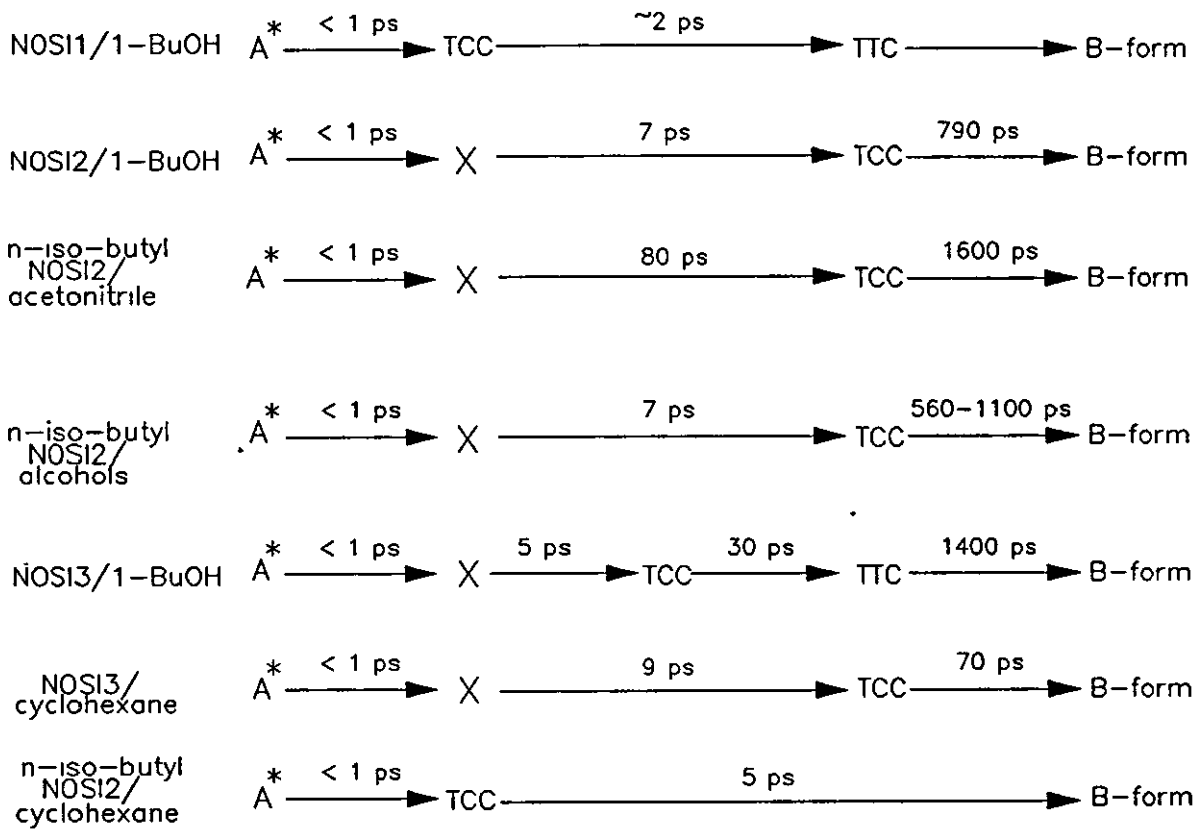

Figure 6.5. The proposed reaction scheme for the photochemical isomerisation from the A-form to the B-form isomers.

The arguments which have lead to the assignments in the scheme shown in figure 6.5 are described in detail chapter 5. The conformational changes that are proposed to occur with the lifetimes given in figure 6.5 are depicted in figure 6.6. This depiction of the conformational changes constitutes a general description which is proposed to occur for all of the NOSI systems studied, up until the formation of TTC. TTC is then proposed to

isomerise in the different solvents to form the final merocyanine isomer distribution. The compositon of this distribution and hence the conformational changes required to achieve it are dictated by the particular solvent requirements:

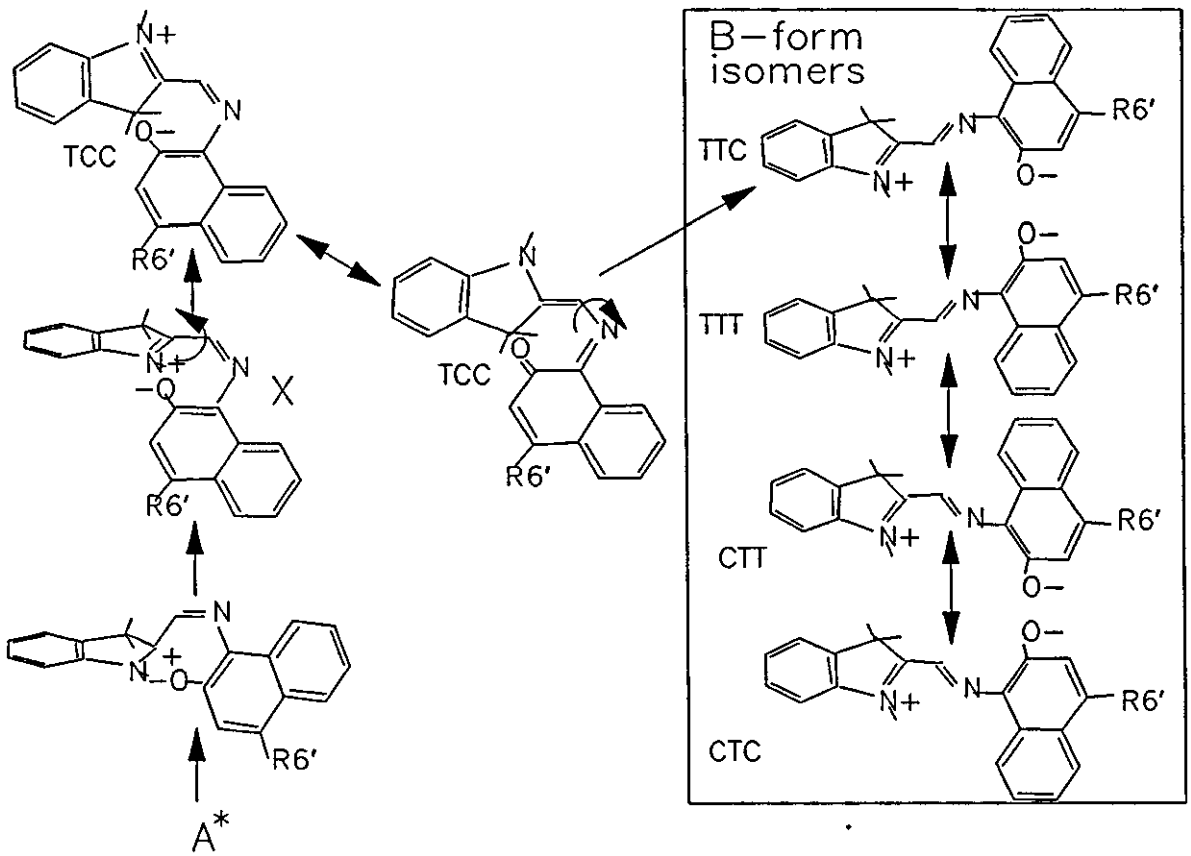

Figure 6.6. The structural changes which may occur during the photochemical formation of the B-form.

The first excited singlet state and a charge separated species referred to as X, which still retains some degree of the parent A-form geometry, are formed within the convoluted pump and probe pulse. The temporal resolution available with these pulses is ~800 femtoseconds. X then forms TCC which is again probably a charge separated intermediate. TCC then undergoes an isomerisation about its central C-N bond forming the TTC merocyanine isomer. TTC then forms the most stable merocyanine isomeric distribution for the particular solvent being used. It is suggested from the present results that in cyclohexane TTC is not required to undergo any further isomerisations once it is formed, since it is probably the most stable of the four possible merocyanine B-form isomers in this solvent.In alcoholic n-alkyl NOSI2 solutions it is likely that TTC is the first of the B-form merocyanine isomers that forms, this again occurs via the TCC isomer. TTC

would then be required to equilibrate with the TTT and the CTT isomers which have been proposed as the most stable structures in polar hydrogen bonding solvents such as the alcohols [10,11,12]. In acetonitrile it is most likely that TTC is again the first merocyanine isomer to form. TTC then equilibrates to form the CTC and CTT isomers which are predicted to be the most stable isomers in this solvent [10,11,12]. The isomeric distributions which are proposed here are thought to occur on the grounds of the B-form spectral shifts measured in the different solvent types as well as from the literature on NOSI, NPSI and BPSI isomeric stability and distribution [10,11,12]. These redistributions would in most cases be undiscernable at the 435nm probe wavelength used since the equilibrated B-form spectra in the different solvents, which are shown in chapter 2 figures 2.11 and 2.12, are in fact very similar to each other at this wavelength.

The picosecond time resolved resonance Raman (PTR^3) experiments were carried out in order to compliment the PTA results. The 580nm the probe wavelength used is only likely to probe the formation of those merocyanine isomers which are trans about the C-N bond and which make up the B-form. The PTR^3 results obtained for NOSI3 in cyclohexane have lead to the suggestion that a single isomer is formed which is stable in this solvent and is therefore not required to undergo any further transformations. This single species is proposed because the time resolved spectra obtained show no evolution in the shape of the spectral envelope. It has been suggested that the TTC isomer is the most stable merocyanine in cyclohexane [10,11,12], which fits in well with the assignment of TCC as the conformation through which the molecule must rotate prior the formation of any of the B-form structures, since TCC forms TTC directly after a single rotation about the C-N bond.

In 1-butanol solutions of NOSI3 the PTR^3 data suggests that there may be up to three different merocyanine species which are formed at different rates. TTC is again suggested to be a common merocyanine isomer from which the equilibrated B-form isomers are formed, because the peaks that form most rapidly in 1-butanol have spectral positions which are very close to the peaks which have already been assigned to TTC for the NOSI3 spectra measured in cyclohexane and which are described above. Another one or maybe even two sets of peaks are also seen to grow with longer time constants in 1-butanol. These are positioned on either side of the TTC peaks. In 1-butanol the time taken for the peaks assigned to TTC to fully grow in was around 100 picoseconds which is not inconsistent with the 30 picosecond mean lifetime transient absorption decay that was measured in the PTA work carried out on NOSI3 in 1-butanol. The transformation occurring with this lifetime in the PTA work is therefore assignable to the isomerisation from TCC to TTC and the

subsequent absorption changes are then probably due to isomeric redistributions. These smaller absorption changes are only seen here because TCC forms TTC rapidly allowing the smaller absorption changes caused by this equilibration to be observed.
From the PTR[3] experiments it is not clear whether the spectral development seen in 1-butanol is due to different merocyanine isomers that each form directly from a common intermediate which is not detected by the 580nm probe (probably TCC), or if the peaks that form more slowly than the TTC peaks are due to isomers which form as TTC equilibrates in the hydrogen bonding solvent. These other species are expected to be the TTT and CTT isomers [10,11,12].

6.7. A summary of the general NOSI photocolouration and thermal fade cycle.

The examination and amalgamation of all of the data collected during this study on NOSI compounds and presented in this thesis has lead to the proposal of the reaction scheme which is shown in figure 6.7. This scheme accounts for the observations made during the investigation of both the photochemical and the thermal reactions of the A-form and the B-form merocyanine isomers.

This scheme is also represented in figure 6.8 as a potential energy diagram. This diagram shows that the photochemical isomerisation is thought to proceed via the first excited singlet state passing through an intermediate X which is similar in geometry to A^*. X then forms the more stable TCC isomer which directly forms the first of the B-form merocyanine isomers, TTC. TTC then equilibrates itself to form the isomers which are the most stable under the reaction conditions. The B-form then thermally converts back to the A-form probably via the CTC B-form isomer and then finally through the non planar CCC conformation.

6.8. Suggestions for future work.

From the present work it is suggested that a correlation may exist between the lifetimes of the transformation assigned to TCC isomerising to TTC and the values of Φ_A. These Φ_A values showed certain dependencies upon solvent polarity and upon matrix effects just as the TCC isomer lifetime did, and further the size of the n-alkyl side chain affected neither of these results. The TCC lifetime may then influence Φ_A. Unfortunately the solvents used in each study were not the same. This potential correlation would be an interesting area for further investigation.
Another experiment which is a progression from the present studies and which could give

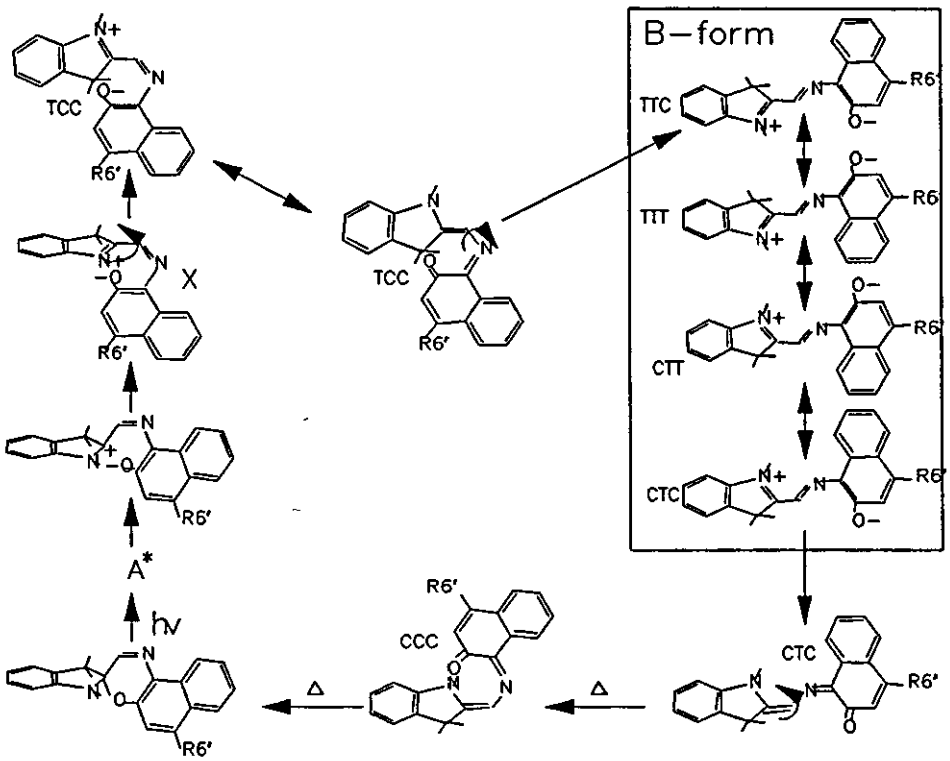

Figure 6.7. The proposed structural changes that occur during photochemical formation of the NOSI B-form and the thermal reformation of the NOSI A-form.

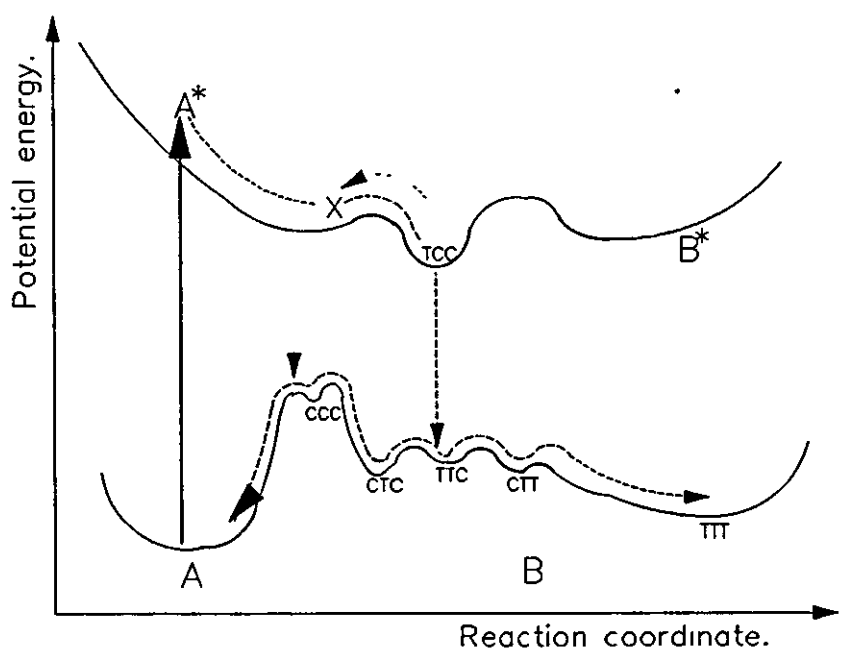

Figure 6.8. The proposed singlet state potential energy surfaces involved in the photochemical isomerisation to the B-form and the thermal reformation of the A-form in a hydrogen bonding solvent such as 1-butanol.

some valuable information, is the determination of the indoline triplet energy. If this value were known then it would be possible to establish the efficiency of energy transfer across the spiro linkage via the triplet state and thus establish whether the transfer has a different efficiency following direct excitation. Some initial quenching experiments have suggested that the indoline triplet state is sensitized by para-methoxy acetophenone with $k_q = 8.5 \times 10^9$ $dm^3.mol^{-1}.s^{-1}$. This implies that both the oxazine and indoline rings would have both of their individual triplet states sensitized by the para-methoxy acetophenone triplet.

Transient species were identified in the present work using both PTA and PTR^3 methods. The PTA results gave good kinetic information about the photochemical isomerisation reaction, however the kinetics of the growth of the PTR^3 peaks needs to be established in order to correlate this data with the PTA data.

One prediction of the present work is that substituting the 2'-hydrogen with a methyl group should affect the formation of the TTC isomer which is suggested to form directly from the TCC intermediate. This is because the methyl sterically crowds the bridged region and the CTC and TCC isomers will be most susceptible to this, hence the photoproducts resulting from the 2'-methyl NOSI1 may be different to those forming from the unsubstituted NOSI1. The results of Bohne *et al* [17] confirm that the photoproducts of these two compounds are different. One valuable way to investigate these differences would be using the PTR^3 and PTA methods described in chapter 5 especially since the transient observed by Bohne *et al* absorbs at 580nm which is a wavelength easily produced using the PTR^3 apparatus described in chapter 5.

The present work has highlighted the fact that different B-form isomer distributions may be present in different types of solvent. It has been shown that the shape of NPSI spectra change as the temperature is reduced until ~110K [9]. At temperatures below this further cooling does not result in further spectral changes. It was suggested that these observations were due to the existence of a thermal equilibrium between the possible B-form isomers for which the isomeric distribution is frozen below ~110K. Hence the different isomers will no longer be able to thermally interchange with one another whereas above 110K they can. In the same piece of work it was reported that at temperatures below 110K irradiation of the NPSI A-form resulted in the formation of species having a spectrum quite distinct from any of the B-form spectra formed after irradiation above this temperature. If this same solution was then heated to above 110K the normal B-form spectrum for that temperature formed, however recooling the solution to below 110K did not lead to the reformation of the initial spectrum which resulting from the photolysis below 110K. It was proposed that photolysis carried out at temperatures below 110K resulted in the formation of a species that is an intermediate in the NOSI photochemical isomerisation, but the

formation of the B-form from this species is frozen out. In the same series of experiments it was observed that below 110K the B-form spectrum could be bleached out at a particular wavelength with a corresponding increase in the absorption in a different region of the B-form spectrum, but with no reformation of the A-form spectrum. These results suggests that the B-form isomers can be made to photochemically interconvert but at these temperatures the interconversion between the A-form and the B-form is frozen out. In a similar way it may be possible to thermally block some of the transformations which are shown in figure 6.7 by cooling a solution of a NOSI compound in a solvent which forms a glass at low temperature. This may allow the contribution to the absorption envelope form the various B-form isomers to be bleached out selectivity by irradiation with a suitable excitation wavelength. It may also be possible to isolate transient states in the isomerisation reactions by thermally retarding a particular step in the reaction.

Chapter 6 References.

1.D.A. Reeves, F. Wilkinson, J. Chem. Soc. Faraday Trans. 2, 69, 1381.

2.R.S. Becker, N.W. Tyer, Jr, J. Am. Chem. Soc. 1970, 92, 1289.

3. A.S. Kholmanskii and K.M. Dyumaev, Dokl. Akad. Nauk. SSSR, 1988, 303.

4. C.B. McArdle, Applied Photochromic Polymer Systems, Blackie, USA: Chapman and Hall, New York, 39.

5. L.G.S. Brooker, G.H. Keyes, J. Am. Chem. 1951, 156.

6. L.G.S. Brooker, J. Am. Chem. 1951, 73, 5332.

7. L.G.S. Brooker, G.H. Keyes, D.W. Heseltine J. Am. Chem. 1951, 73, 5350.

8. P. Sappan, J. Chem. Soc. A, 1968, 3125.

9. R. Heligman-Rim, Y. Hirshberg, E.Fischer, J. Am. Chem. soc. Dec. 1962, 66, 2465.

10. H. Takahashi, K. Yoda, H. Isaka, T. Ohzecki, Y. Sakaino, Chem. Phys. Lett. 18 Sept. 1987, 90.

11. H. Takahashi, H. Murakawa, Y. Sakaino, T. Ohzecki, J. Abe, O. Yamada, J.Photochem. Photobiol. A: Chem., 45, 1988, 233.

12. S. Schneider, A. Mindl and G. Elfinger, Ber. Bunsenges. Phys. Chem. 91, 1987, 1225.

13. N. P. Ernsting and Arthen-Engeland, Pure and App. Chem. 1990, 62, 8, 1483.

14. D. Eloy, P. Escaffre, R. Gautron, P. Jardon, J. Chim. Phys, 1992, 89, 897.

15. J. C. Scaiano, Handbook of Organic Photochemistry, C.R.C. Press, Cleveland, 1989. ISBN. 0-8493-2953-1. 376.

16. S.L. Murov, I. Carmichael, G.L. Hug, Handbook of Photochemistry, 2nd Ed. Marcel Dekker, ISBN-0-8247-7911-8, 1993, 207.

17. C. Bohne, M.G. Fan, Z.J. Liang, J. Lusztyk, J.C. Scaiano, J. Potochem. Photobiol. A. Chem, 66, 1992, 79.